

**A New Treatment Strategy for Pulmonary
Fibrosis Targeting the Bone Morphogenetic Protein
Pathway, and the Importance of Radiological
Pattern for Selecting Candidates for Receiving a
New Treatment for Pulmonary Fibrosis**

by

Jun Fukihara

A thesis submitted to the University of Adelaide in fulfilment of the requirements
for the degree of Doctor of Philosophy

Nagoya-Adelaide Joint Degree Program
Department of Respiratory Medicine,
Nagoya University Graduate School of Medicine (JAPAN) /
School of Medicine, Faculty of Health and Medical Sciences,
The University of Adelaide

February 2022

Table of Contents

Table of Contents.....	2
Abstract.....	7
Declaration	9
Acknowledgements.....	10
I. Introduction	12
1. Interstitial lung disease	13
1.1 Overview.....	13
1.2 Causes of ILD.....	13
1.3 Classification and diagnosis of IIPs	13
2. Definition of idiopathic pulmonary fibrosis (IPF)	15
2.1 Overview.....	15
2.2 Current guideline for diagnosis of IPF.....	15
2.2.1 Clinical context.....	15
2.2.2 Radiological criteria.....	15
2.2.3 Histopathological criteria.....	17
2.2.4 Diagnostic criteria for IPF.....	17
2.3 Eligibility for clinical trials.....	18
3. The role of transforming growth factor (TGF)- β in the pathogenesis of IPF	20
3.1 Overview.....	20
3.2 TGF- β signalling.....	20
3.3 ECM deposition and fibrogenesis by fibroblasts/myofibroblasts	21
3.4 Reaction of alveolar epithelial cells (AECs) to microinjuries	23
3.5 Migration and differentiation of fibrocytes into myofibroblasts	24
3.6 Transdifferentiation of endothelial cells into mesenchymal cells.....	25
4. Bone morphogenetic protein (BMP) pathway and pulmonary fibrosis.....	26
4.1 Overview.....	26
4.2 BMP signalling.....	26
4.3 TGF- β and BMP crosstalk in fibrosis	28
4.4 BMP pathway and pulmonary fibrosis.....	29
4.4.1 Role of BMPs against pulmonary fibrosis.....	29
4.4.2 Endogenous BMP inhibitors in pulmonary fibrosis	30
4.4.3 BMPR2 in pulmonary fibrosis.....	31
5. Endothelial colony forming cells (ECFCs).....	32
5.1 Overview and definition of endothelial colony forming cell (ECFC)	32

5.2	Utilisation of EPCs/ECFCs as therapeutic agents.....	33
5.3	Treatment of PH using gene-modified EPCs.....	35
5.4	ECFCs and pulmonary fibrosis.....	35
6.	Treatment of IPF.....	37
6.1	Overview.....	37
6.2	Anti-fibrotic agents.....	37
6.2.1	Pirfenidone.....	37
6.2.2	Nintedanib.....	38
6.3	Cell therapy for pulmonary fibrosis.....	38
6.4	Research questions.....	41
II. Overexpression of BMPR2 suppresses transforming growth factor β-induced profibrotic responses in lung fibroblasts		43
	Statement of Authorship.....	44
	Abstract.....	47
	Introduction.....	48
	Materials and methods.....	48
	Animals and creation of bleomycin-induced pulmonary fibrosis model.....	48
	Cell lines and provided primary cells.....	48
	Rat lung fibroblast isolation.....	49
	Viral construction and BMPR2 transduction.....	49
	Induction of profibrotic changes and transduction of BMPR2 in HLFs/RLFs....	49
	Hematoxylin-Eosin staining and Masson's Trichrome staining.....	49
	Immunohistochemical analysis.....	49
	Western Blot.....	50
	RNA extraction and qRT-PCR.....	50
	Statistical analysis.....	51
	Results.....	51
	BMPR2 expression was decreased in fibrotic lungs and lung fibroblasts stimulated with TGF- β	51
	The sensitivity to TGF- β and BMPs did not differ between HLFs from healthy controls and IPF patients.....	53
	Stimulation with BMPs could not suppress TGF- β -induced profibrotic changes in lung fibroblasts.....	55
	BMPR2 transduction using adenovirus suppressed the TGF- β -induced phosphorylation of Smad2/3 in lung fibroblasts.....	55

BMPR2 transduction plus stimulation with BMP7, but not BMP4, suppressed the TGF- β -induced production of fibronectin in lung fibroblasts	55
BMPR2 transduction showed trends for reducing phosphorylation of p38 MAPK in lung fibroblasts.....	58
Discussion.....	58
References.....	62
Supplementary Figures	64
III. Transduction of BMPR2 to human and rat lung fibroblasts using exosomes secreted by BMPR2-transduced ECFCs	74
1. Overview.....	75
2. Methods	77
2.1 Human and rat samples	77
2.2 Cell lines and provided primary cells	77
2.3 RLF isolation from lung.....	77
2.4 Isolation of ECFCs from human peripheral blood	78
2.5 Isolation of EPCs from rat bone marrow.....	78
2.6 Viral construction.....	78
2.7 Adenoviral transduction of BMPR2 to human ECFCs/rat EPCs and purification of exosomes in their conditioned media	78
2.8 BMPR2 transduction to HLFs/RLFs and treatment with TGF- β /BMPs.....	79
2.9 Western Blot.....	79
2.10 Statistical analysis.....	80
3. Results	81
3.1 Lung fibroblasts treated with exosomes from BMPR2-transduced human ECFCs/rat EPCs showed elevation of BMPR2.....	81
3.2 BMPR2 transduced by exosomes reduced fibronectin production in lung fibroblasts.....	81
IV. Treatment of rats with bleomycin-induced pulmonary fibrosis using BMPR2-transduced rat EPCs	85
1. Overview.....	86
2. Methods	87
2.1 Preparation of BMPR2-transduced rat EPCs for intravenous injection	87
2.2 Creation of rat bleomycin-induced pulmonary fibrosis model and treatment with BMPR2-transduced rat EPCs.....	87
2.3 Hematoxylin-Eosin staining.....	88

2.4	Modified Achcroft's score.....	88
2.5	Collagen assay.....	88
2.6	Western Blot.....	88
2.7	Quantitative real time polymerase chain reaction (qRT-PCR).....	89
2.8	Statistical analysis.....	89
3.	Results.....	91
3.1	Optimisation of bleomycin dosage and the protocols for intratracheal administration and monitoring.....	91
3.2	Intravenously injected EPCs accumulated in the lungs of rats with bleomycin-induced pulmonary fibrosis shortly after injections.....	94
3.3	BMPR2-transduced EPC treatment might reduce collagen production in pulmonary fibrosis, though further validation is warranted.....	96
V.	Probable UIP pattern on chest CT is insufficient for making a definitive diagnosis of IPF	100
	Statement of Authorship.....	101
	Abstract.....	105
	Introduction.....	106
	Patients and Methods.....	106
	Study design and population.....	106
	Data collection.....	106
	Definition of AE.....	107
	Radiological and histopathological evaluation.....	107
	Final diagnosis of ILDs.....	107
	Statistical analysis.....	107
	Results.....	108
	Patient characteristics.....	108
	Prognosis: UIP pattern versus probable UIP pattern.....	109
	Prognosis of IPF: UIP pattern versus probable UIP pattern.....	109
	Prognosis of probable UIP pattern: final diagnosis of IPF versus non-IPF.....	110
	Discussion.....	111
	References.....	112
	Supplementary results.....	114
	Validation of sample size.....	114
	Validation of the diagnostic approach.....	114
	Annual rate of change in forced vital capacity.....	114

References	115
Supplemental tables	116
VI. Discussion	118
1. Summary of the studies and achievements.....	119
2. Impact of BMPR2 overexpression on the TGF- β -induced profibrotic responses in lung fibroblasts	120
3. Exosome-mediated BMPR2 transmission and its effect on the TGF- β -induced profibrotic responses in lung fibroblasts.....	121
4. Creation of bleomycin-induced pulmonary fibrosis model and accumulation of intravenous BMPR2-transduced rat EPCs in rat lungs	123
5. Importance of radiological pattern for diagnosing homogeneous IPF.....	125
6. Conclusions.....	126
VII. Bibliography	127

Abstract

Background

Idiopathic pulmonary fibrosis (IPF) is a progressive disease with a poor prognosis. As the efficacy of currently available medicines is limited, development of new therapy is warranted. Transforming growth factor (TGF)- β plays a central role in the pathogenesis of IPF through such mechanisms as promoting extracellular matrix production by fibroblasts. Conversely, bone morphogenetic protein (BMP)4 and 7 bind to BMP receptor type 2 (BMPR2) and counterbalance TGF- β signalling. However, the impact of BMPR2 overexpression for modulating the imbalance of the TGF- β /BMP axis has never been studied in pulmonary fibrosis.

How to select patients for new treatments is another concern, as IPF can be difficult to distinguished from other idiopathic interstitial pneumonias (IIPs). Although a “usual interstitial pneumonia (UIP) pattern” on chest computed tomography (CT) is necessary for diagnosing IPF in IIP patients without undergoing lung biopsy in the current guideline, recent studies have suggested that a “probable UIP pattern” is also sufficient for diagnosing IPF without histopathology. However, this “broader IPF diagnosis” has never been validated outside clinical trials by long-term outcomes such as survival.

Methods

For investigating the effect of BMPR2 overexpression, I have transduced BMPR2 into lung fibroblasts or the lungs of rats with bleomycin-induced pulmonary fibrosis, using adenovirus, BMPR2-overexpressing endothelial progenitor cells (EPCs) or exosomes from them. Suppression of Smad2/3 phosphorylation and fibronectin production were used as surrogates for treatment effect.

For validating the “broader IPF diagnosis”, I have conducted a retrospective cohort study to compare probability of non-IPF diagnosis between patients with a UIP pattern and those with a probable UIP pattern on chest CT. As IPF has poorer prognosis than other interstitial pneumonias, survival time and time to first acute exacerbation (AE) were also compared.

Results

BMPR2 was downregulated in rat lungs with fibrosis and in human/rat lung fibroblasts stimulated with TGF- β . Although BMP7 did not reduce TGF- β -induced p-Smad2/3 and fibronectin in lung fibroblasts, adenoviral BMPR2 transduction has

reduced p-Smad2/3 by itself and, when given with BMP7, reduced fibronectin. The studies for treatment of rats with pulmonary fibrosis using BMPR2-transduced EPCs and fibroblasts using BMPR2-carrying exosomes could not be completed due to some technical problems.

In another study, 402 IIP patients' data were reviewed. Among patients with a "probable" UIP pattern, the probability of IPF was only 66%, while it was 81% in those with a UIP pattern. Probable UIP pattern was independently associated with longer survival and time to first AE. In IPF patients only, CT pattern was not associated with prognosis.

Conclusions

BMPR2 was reduced in fibrotic lungs and lung fibroblasts stimulated with TGF- β . Adenoviral BMPR2 transduction showed effects on suppressing TGF- β -induced profibrotic markers in lung fibroblasts. Further study is needed to elucidate the clinical effectiveness of BMPR2 overexpression.

Patients with a probable UIP pattern had a higher probability of non-IPF diagnoses and better prognosis than those with a UIP pattern. Although the "broader IPF diagnosis" may be valid when IPF is strongly suspected, prudent clinical evaluation and care for not misdiagnosing other interstitial pneumonias with better prognosis as IPF are important.

(500 words)

Declaration

I certify that this work contains no material which has been accepted for the award of any other degree or diploma in my name, in any university or other tertiary institution and, to the best of my knowledge and belief, contains no material previously published or written by another person, except where due reference has been made in the text. In addition, I certify that no part of this work will, in the future, be used in a submission in my name, for any other degree or diploma in any university or other tertiary institution without the prior approval of the University of Adelaide and where applicable, any partner institution responsible for the joint-award of this degree.

I acknowledge that copyright of published works contained within this thesis resides with the copyright holder(s) of those works.

I also give permission for the digital version of my thesis to be made available on the web, via the University's digital research repository, the Library Search and also through web search engines, unless permission has been granted by the University to restrict access for a period of time.

Jun Fukihara

Date: 01. 12. 2021

Acknowledgements

There have been many people who have contributed to the success of this work, of whom I am grateful and would like to, particularly mention.

Firstly, I express my sincere thanks to my supervisor Prof. Paul Reynolds for inviting me to your lab in Adelaide. Despite I have been a quite immature PhD student with a significant language barrier, I could complete my mission with your polite guidance and encouragement. I'm really grateful to your patience and to seeking with me a good way to overcome the time and financial limitations. Though it is a pity that I could not achieve a great scientific success during my short-duration of stay in Adelaide, the way of scientific thinking and everything else I have learned from you will be a treasure for me in my future career as a doctor involved in medical research. I also really appreciate to both you and Debra's public and private support have helped me and my family to settle in and spend wonderful time in Adelaide.

I would also like to show my appreciation to Dr. Naozumi Hashimoto, my Japanese supervisor. Not only before departing to Australia, but you have given me a lot of important advice also via online meetings during my stay in Adelaide. I have learned the fundamental way of scientific thinking from zero from you, which was essential for me to make progress in my studies. Your support throughout my PhD was considerably helpful to maximise the impact of my achievements and to successfully complete the newly-established Joint Degree Program.

Prof. Yoshinori Hasegawa and Prof. Hideki Kasuya, thank you so much for giving me such a wonderful opportunity to study abroad. It was not an easy mission to do things as I have originally expected, however, through this Joint Degree Program, I have been able to have many irreplaceable encounters and experiences. And I would also like to show my appreciation to the staff of Nagoya University Office of International Affairs for your supports throughout my PhD carrier.

Suzie, I can't thank you enough for your kindness during I was in Adelaide. Not only teaching me lab rules and study protocols, but you have given me a lot of important advice for trouble shooting in my experiments and practically helped my experiments even on weekends and holidays. If you were not a member of our group, I would not be able to achieve the results presented in this thesis. Jess and Jemma, it was my pleasure to work with you in the same group. The term we could spend together was not very long, but I will never forget your kindness that helped

me very much. Jess, I'm also grateful to your support in running extra experiments and paper draft editing even after my coming back to Japan.

And finally, I would like to express my heartfelt gratitude to my wife, Sayuri, and my son, Daichi. I think it was never easy to adapt to life in Australia where the language, culture and customs are considerably different from those in Japan. Nevertheless, you have broadened your community and given me chances to get to know with people who I would never see if I was alone in Adelaide. I think our spending time together has made each our everyday experience in Australia memorable and impressive. I'm really pleased to have been able to share our wonderful, brilliant experiences through our 2-year journey.

Part I

Introduction

1. Interstitial lung disease

1.1 Overview

Interstitial lung disease (ILD) is a group of heterogeneous pulmonary diseases affecting the lung interstitium (the tissue and space around the alveoli). Damaged interstitium thickened with infiltration of inflammatory cells and/or fibrosis reduces oxygen diffusion to the bloodstream and lung elasticity, resulting in dyspnoea and respiratory failure. The treatment strategies and prognoses vary depending on the causes and types of ILD, so it is important to make a correct diagnosis.

1.2 Causes of ILD

The most common identifiable causes of ILD are exposure to occupational and environmental agents (e.g., asbestosis, pneumoconiosis, berylliosis, or hypersensitivity pneumonitis, such as farmer's lung, bird fancier's disease and summer-type hypersensitivity pneumonitis), drug-induced lung diseases, and radiation-induced pneumonitis.

ILD is a common complication of most of the connective tissue diseases (CTDs), such as scleroderma, rheumatoid arthritis, polymyositis/dermatomyositis, Sjögren syndrome, systemic lupus erythematosus and mixed connective tissue disease. Vasculitis associated with anti-neutrophil cytoplasmic antibody can also be complicated with ILD. Furthermore, ILD is often associated with a variety of pulmonary infections such as *Pneumocystis jirovecii* pneumonia, atypical bacterial pneumonias and viral pneumonias, and lymphoproliferative disorders including sarcoidosis, multicentric Castleman's disease, IgG4-related disease, and malignant lymphoma.

Other ILDs without identifiable causes are classified as idiopathic interstitial pneumonias (IIPs).

1.3 Classification and diagnosis of IIPs

In the latest international statement for the classification of IIPs, IIPs are at first classified into major, minor, and unclassifiable (1). Major IIPs are further subdivided into chronic fibrosing, smoking-related and acute/subacute (1), as summarised in Table 1-1.

Although the diagnosis of IIPs needs exclusion of ILDs with identifiable causes, that is generally difficult. In addition to history taking and physical examination, a broad spectrum of blood tests including specific antibodies for CTDs,

Table 1-1. Classification of IIPs (1)

Classification	Diagnosis
Major IIPs	
Chronic fibrosing IP	Idiopathic pulmonary fibrosis (IPF) Idiopathic nonspecific interstitial pneumonia (NSIP)
Smoking-related IP	Desquamative interstitial pneumonia (DIP) Respiratory bronchiolitis-ILD (RB-ILD)
Acute/subacute IP	Cryptogenic organising pneumonia (COP) Acute interstitial pneumonia (AIP)
Minor IIPs	Idiopathic lymphoid interstitial pneumonia (LIP) Idiopathic pleuroparenchymal fibroelastosis (PPFE)
Unclassifiable IIPs	

IIP: idiopathic interstitial pneumonia; IP: interstitial pneumonia; ILD: interstitial lung disease.

highly specialised interpretation of high-resolution computed tomography (HRCT), and surgical lung biopsy (SLB) are often required. Despite these efforts, it is not rare to be unable to make a definitive diagnosis, resulting in the final diagnosis of “unclassifiable IIP”. Causes of this include inadequate clinical, radiological, or histopathological data and major discordance between clinical, radiological, and histopathological findings due to the alteration of radiological or histopathological findings by previous therapy, a new entity or unusual variant of a recognized entity, not adequately characterized by the current classification, and coexisting multiple HRCT and/or histopathology patterns (1).

2. Definition of idiopathic pulmonary fibrosis (IPF)

2.1 Overview

Idiopathic pulmonary fibrosis (IPF) is a chronic, progressive, and fibrosing ILD of unknown cause with a poor prognosis. The median survival time after diagnosis is 3-5 years (2). This is the most common type of IIP associated with a “usual interstitial pneumonia (UIP) pattern” on HRCT and histopathology on SLB. However, many patients with a histopathological UIP pattern lack some typical features necessary for UIP pattern on HRCT and/or have histories/findings suggestive of other ILDs with specific causes, such as CTDs or dust exposure. Moreover, histopathological UIP pattern is defined by a combination of multiple findings (3) which is sometimes difficult to be distinguished from findings suggestive of other diseases. Therefore, consensus made through multidisciplinary discussion with expert clinician, radiologist and pathologist is required to make a definitive diagnosis of IPF in the diagnosis guideline (1, 3).

2.2 Current guideline for diagnosis of IPF

2.2.1 Clinical context

IPF occurs primarily in older adults (typically older than 60 years old). The majority of patients are male and current- or ex-smokers. Chronic exertional dyspnoea, dry cough, and bibasilar inspiratory crackles are the typical clinical traits of IPF. Common comorbidities of IPF include emphysema, lung cancer, pulmonary hypertension (PH), and coronary artery disease (4). Although all those features are not specific to IPF, detailed clinical history and precise physical examination are important to exclude other possible identifiable causes of the ILD and increase the pre-test probability of IPF prior to SLB.

Some patients with IPF may manifest acute exacerbation, which is frequently a fatal event showing an unexplained worsening of dyspnoea over a few weeks and new ground-glass opacities on HRCT superimposed on a background of lower lobe fibrotic shadows, causing acute respiratory failure (5). A recent review of the definition of acute exacerbation means that identifiable infections are now not excluded from the definition. As these exacerbations may respond to specific anti-microbial treatment, the overall mortality of acute exacerbations as a group may improve.

2.2.2 Radiological criteria

The most typical HRCT features seen in IPF are honeycombing and traction bronchiectasis. Honeycombing is clustered cystic airspaces of diameter of 3-10 mm with thick, well-defined walls. Traction bronchiectasis is formed by bronchial dilatation due to the contraction of surrounding fibrotic lung tissue and ranges from subtle irregularity and non-tapering of the bronchial wall to marked airway distortion. Those findings are predominant in peripheral/subpleural areas of IPF lungs and often coexist. As it is generally difficult to distinguish honeycombing from traction bronchiectasis or subpleural cysts, agreement for honeycombing is often not achieved even among expert radiologists.

In the latest 2018 guideline for diagnosis of IPF, four diagnostic categories (a “UIP pattern”, “probable UIP pattern”, “indeterminate for UIP pattern” and “alternative diagnosis”) are suggested (3). The UIP pattern is the hallmark radiological pattern of IPF. Honeycombing must be present, and the reticular abnormalities are predominantly distributed in the subpleural and basal lung areas, though upper lobe involvement is also not rare. Positive predictive value of a UIP pattern on HRCT for a histopathological UIP pattern is reported to be more than 90% (6-8); however, it has also been reported that there is a significant minority of patients with a histopathological UIP pattern and a non-UIP HRCT pattern (6, 7). Ground-glass opacities superimposed on a reticular shadow may be present but are not dominant in the UIP pattern. Probable UIP pattern is characterised by the similar distribution of reticular abnormalities to that of UIP pattern, which must be accompanied by peripheral traction bronchiectasis but is in the absence of true honeycombing. In the previous 2011 guideline, reticular abnormalities distributed predominantly in subpleural and basal lung areas without honeycombing were defined as a “possible UIP pattern” regardless of presence or absence of traction bronchiectasis (4). Afterward, several studies have reported that a possible UIP pattern accompanied by traction bronchiectasis on HRCT in the clinical setting consistent with IPF was likely associated with a histopathological UIP pattern on SLB (9-11). Therefore, a new HRCT pattern of “probable UIP” has been defined by addition of traction bronchiectasis to the original possible UIP pattern. Indeterminate for UIP pattern does not fulfill the criteria for UIP or probable UIP patterns, except for subpleural and basal distribution of reticular abnormalities, and does not explicitly suggest any specific aetiology. This includes subtle reticulation with or without ground-glass opacities that may represent “early IPF”.

2.2.3 Histopathological criteria

The histopathological hallmark of UIP pattern is a patchy dense fibrosis that causes remodelling of lung architecture and often results in honeycombing, and alternates with normal or less affected parenchyma. Those findings are predominant in the subpleural and paraseptal areas (3). Foci composed mainly of proliferating fibroblasts and deposited collagen (so-called fibroblastic foci) are scattered in the subepithelial areas of the fibrotic lesions. Honeycombing is characterized by cystic airspaces with alveolar walls thickened by dense fibrosis. All the above features other than honeycombing are necessary for making a diagnosis of histopathological UIP pattern. Mild inflammation caused by an interstitial lymphocytosis and plasmacytosis associated with hyperplasia of type 2 alveolar epithelial cells (AECs) can be observed.

Histopathological patterns are categorised into “UIP,” “probable UIP,” “indeterminate for UIP” and “alternative diagnosis” in the current IPF guidelines in a similar way to the radiological patterns (3). Diagnosis of histopathological pattern of probable UIP can be made when some features of UIP are present but insufficient to make a definitive diagnosis of UIP. Indeterminate for UIP pattern also needs to show evidence of fibrosis but does not meet the criteria for a histopathological UIP pattern or any other fibrotic interstitial pneumonia.

2.2.4 Diagnostic criteria for IPF

A definitive diagnosis of IPF requires that IPF is clinically suspected, other identifiable causes of ILD are excluded, and either the presence of a UIP pattern on HRCT or, in patients who underwent SLB, specific combinations of HRCT and histopathological patterns as specified in Table 1-2. In other words, if an HRCT pattern is not UIP, patients need to undergo SLB to make a definitive diagnosis of IPF (3).

On the other hand, because SLB is highly invasive as a mere diagnostic method, transbronchial lung cryobiopsy (TBLC) using bronchoscopy has become an alternative to SLB. Although the lung samples collected by TBLC are not as large as that by SLB, it has been reported that if diagnoses made after TBLC were highly confident, they were consistent with those made after SLB. Conversely, if confidence of diagnoses made after TBLC were low, half of them were altered after SLB (12). Therefore, in some selected patients, TBLC may be useful for omitting SLB. However, it should be noted that some TBLC-specific complications can occur, such as airway bleeding and pneumothorax. The frequency and severity of

procedure-related complications are not significantly lower than those with SLB, and some patients need to undergo both biopsies if TBLC precedes SLB. For the moment, SLB is still a gold-standard for taking lung samples for making a histopathological diagnosis.

Table 1-2. Diagnosis of IPF based on HRCT and histopathological patterns (3)

		Histopathological pattern			
		UIP	Probable UIP	Indeterminate for UIP	Alternative diagnosis
HRCT pattern	UIP	IPF	IPF	IPF	Non-IPF
	Probable UIP	IPF	IPF	IPF (likely)	Non-IPF
	Indeterminate for UIP	IPF	IPF (likely)	Indeterminate for IPF	Non-IPF
	Alternative diagnosis	IPF (likely) /non-IPF	Non-IPF	Non-IPF	Non-IPF

IPF: idiopathic pulmonary fibrosis; UIP: usual interstitial pneumonia; HRCT: high-resolution computed tomography.

2.3 Eligibility for clinical trials

Since IPF has a poorer prognosis and is more frequent than other chronic fibrosing IIPs, it has been the main target for development of new treatment agents with anti-fibrotic effect. In the past clinical trials for IPF, participants have needed to have a diagnosis of guideline-defined IPF (13-16). However, a significant number of patients in the real world do not get a definitive diagnosis because of not undergoing SLB for various reasons, such as refusal or excessive perioperative risks.

On the other hand, in some recent clinical trials, IIP patients with a probable UIP pattern on HRCT were also eligible even if they had not undergone SLB (17). This approach is supported by some reports demonstrating a high positive predictive value of a probable UIP pattern for a histopathological UIP pattern (9-11) or significant correlation of traction bronchiectasis on HRCT and a poor prognosis in patients with fibrotic IIP (18, 19), allowing more people to be eligible for the clinical trials while avoiding the risk of SLB for making a diagnosis of IPF. The INPULSIS trials, which evaluated the safety and efficacy of nintedanib (an anti-fibrotic agent) as a treatment of IPF, were the first clinical trials using this

diagnostic criterion (17). In the *post-hoc* analysis of the INPULSIS trials, patients with a probable UIP pattern on HRCT who had not undergone SLB showed similar disease progression and treatment responsiveness to subjects with guideline-defined IPF (11), supporting that the trial diagnostic approach has correctly selected patients with IPF.

However, this new diagnostic approach has the potential to misdiagnose non-IPF ILDs as IPF. The *post-hoc* analysis of the INPULSIS trials has focused on disease progression for just a short-term (1 year) and not evaluated the impact on long-term outcome, such as survival (11), but if the prevalence of non-IPF in the cohort is significant, the prognosis of the cohort may become better than that of pure guideline-defined IPF. Additionally, we should also notice that the participants of clinical trials are clinically suspected to have IPF by ILD expert-physicians, which may make the probability of a histopathological UIP pattern and a final diagnosis of IPF in patients with a probable UIP pattern on HRCT higher than that in a real-world setting. Studies evaluating the impact of contamination of non-IPF ILDs in the diagnostic criteria applied in the recent clinical trials on short- and long-term prognosis in the real-world are warranted.

3. The role of transforming growth factor (TGF)- β in the pathogenesis of IPF

3.1 Overview

The proteins of the transforming growth factor (TGF)- β superfamily include some growth factors that are involved in a variety of processes such as embryogenesis, cellular development and differentiation, inflammatory response and wound repair (20). In the lungs, TGF- β is produced by various types of cells, including alveolar macrophages, neutrophils, AECs, endothelial cells, fibroblasts and myofibroblasts.

IPF is induced by repetitive microinjuries to alveolar epithelium and subsequent epithelial hyperplasia. Injured epithelium and accumulated inflammatory cells release more profibrotic mediators, in particular TGF- β , than usual (21-23). Among three major isoforms (TGF- β 1, -2 and -3), TGF- β 1 plays central roles in the development of IPF, causing accumulation of mesenchymal cells in the lung interstitium, the activation/proliferation of fibroblasts and their differentiation into myofibroblasts, and deposition of extracellular matrix (ECM) composed mainly of collagens and fibronectin. In the early pathological stage of IPF, fibrotic lesions are formed by accumulated fibroblasts and ECM, which is then followed by basal membrane disruption, fibrin formation, abnormal wound repair, and angiogenesis. The origins of the fibroblasts are considered to be multiple, such as the proliferation of resident fibroblasts, the recruitment of circulating bone marrow-derived progenitor cells such as fibrocytes, and the transdifferentiation of AECs, endothelial cells and other types of cells through the mesenchymal transition.

3.2 TGF- β signalling

TGF- β is a cytokine secreted in a homodimeric inactive form attached to a latency-associated peptide (LAP) and a latent TGF- β binding protein. The cleavage of the LAP/latent TGF- β -binding protein complex to release the activated form of TGF- β from it is mediated by matrix metalloproteinase (MMP)2 and 9 (24, 25), lowered pH (26), reactive oxygen species (ROS) (27), thrombospondin 1 (28), increasing ECM stiffness by myofibroblast contraction (29), and integrin $\alpha\beta$ 6 (30). Active TGF- β initially binds to a serine/threonine transmembrane receptor kinase known as TGF- β receptor type 2 (T β R2), which then recruits and phosphorylates TGF- β receptor type 1 (T β R1), also termed activin receptor-like kinase (ALK) (Figure 1-1). ALK5 is expressed on almost all cell types, while ALK1 is mainly

expressed on endothelial cells and transmits TGF- β signalling which antagonises TGF- β /ALK5 signalling (31).

Signalling from the TGF- β receptor complex is mediated by both Smad and non-Smad pathways and transmitted to the nucleus. Smad proteins are categorised into the following three groups based on their functions: the receptor activated Smads (R-Smads, Smad2/3 and Smad1/5/8), the common mediator Smad (Co-Smad, Smad4) and the inhibitory Smads (I-Smads, Smad6/7). Among R-Smads, Smad2/3 are mainly activated through TGF- β pathways, while Smad1/5/8 are activated through the bone morphogenetic protein (BMP) pathways (see the next chapter). After R-Smads are phosphorylated by T β R1, they form complexes with Smad4 and move into the nucleus. Then, the Smad complex modulates the target gene expressions in cooperation with various transcription factors, co-activators, and co-repressors (20, 32, 33). I-Smads are also produced through this process and inhibit the phosphorylation of R-Smads and compete with the formation of activated R-Smads/Smad4 complex (Figure 1-1).

On the other hand, non-Smad pathways are activated or suppressed depending on the specific cell types and context. For example, TGF- β activates phosphoinositide 3-kinase (PI3K), which then activates two profibrotic pathways: p21-activated kinase (PAK2)/c-Abelson kinase (c-Abl) and Akt (34). Mitogen-activated protein kinase (MAPK) pathways, such as the extracellular signal-regulated kinase (ERK), p38 and c-Jun-N-terminal kinase (JNK), are also profibrotic pathways activated by TGF- β and regulate myofibroblast formation and ECM production (35-38). Furthermore, the interaction of TGF- β signalling with other profibrotic pathways including Wnt, Notch, connective tissue growth factor (CTGF), platelet-derived growth factor (PDGF), and epidermal growth factor, has also been reported (20, 39) (Figure 1-1).

3.3 ECM deposition and fibrogenesis by fibroblasts/myofibroblasts

Fibroblasts are distributed all over the lung structures and play a main role in controlling turnover of ECM proteins through the production of MMPs, which degrade ECM, and tissue inhibitors of metalloproteinases (TIMPs), which inhibit MMPs. Activation, proliferation, and migration of fibroblasts into the injured site and deposition of ECM are induced by fibrogenic mediators, such as TGF- β . Those mediators also induce differentiation of fibroblasts into myofibroblasts, which have features of both mesenchymal cells, such as production of ECM proteins, and smooth muscle cells, such as being contractile and expressing α -smooth muscle

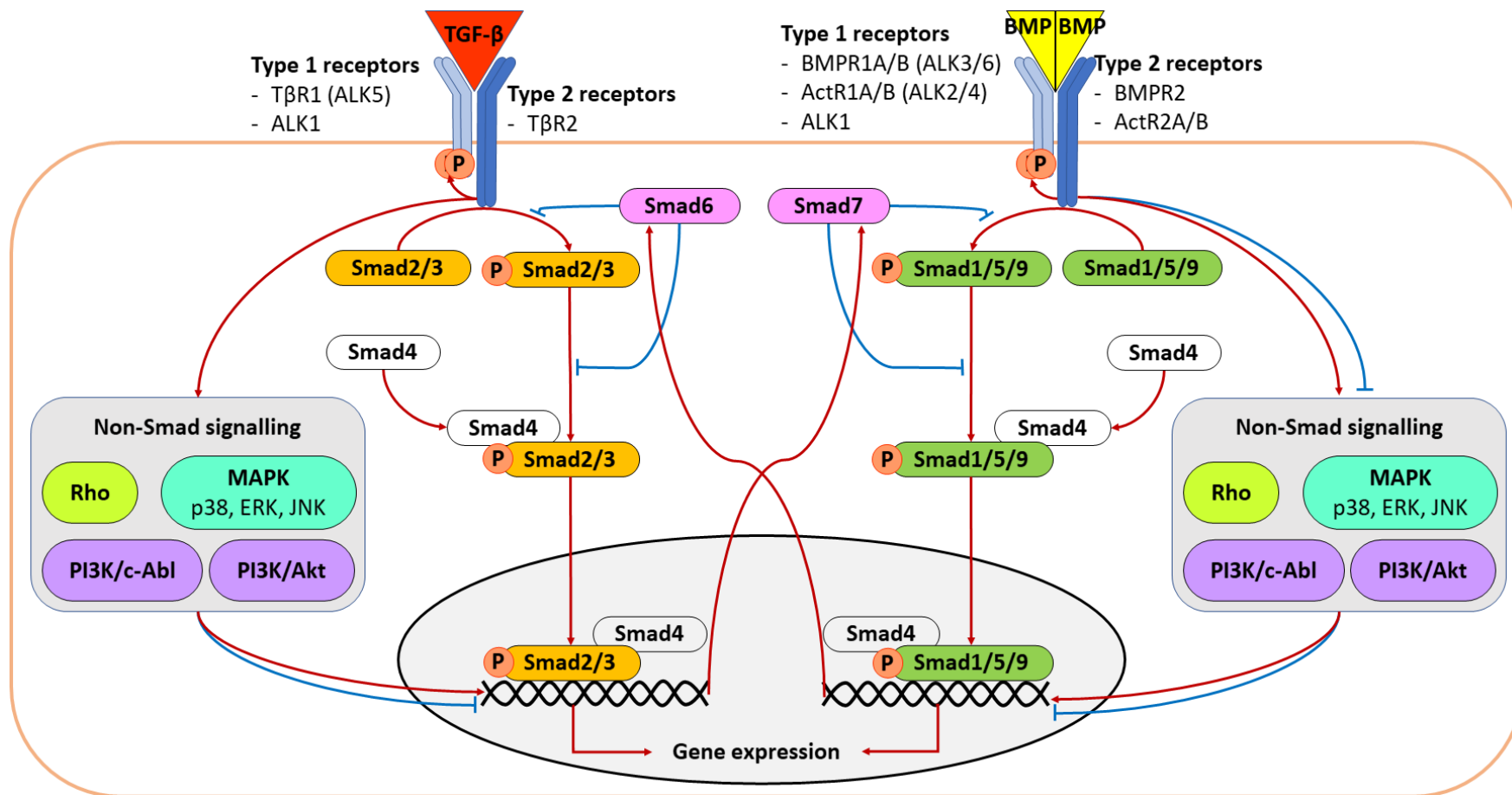


Figure 1-1. TGF- β and BMP signalling pathways. TGF- β , transforming growth factor- β ; T β R1/2, TGF- β receptor type 1/2; ALK, activin receptor-like kinase; BMPR1/2, bone morphogenetic protein receptor type 1/2; ActR1/2, activin A receptor type 1/2; BMP, bone morphogenetic protein; MAPK, mitogen-activated protein kinase; ERK, extracellular-signal regulated kinase; JNK, c-Jun-N terminal kinase; PI3K, phosphoinositide 3-kinase; c-Abl, c-Abelson kinase.

actin (α -SMA), resulting in the regulation of ECM remodelling. In particular, the main source of the increased deposition of ECM proteins and excessive TIMPs found in IPF is thought to be the activated fibroblasts and myofibroblasts in fibroblastic foci, the histopathological hallmarks of the disease, which locate adjacent to hyperplastic or apoptotic type 2 AECs.

Fibroblasts become resistant to apoptosis in IPF. The PI3K/Akt signalling was aberrantly activated while the activity of phosphatase and tensin homologue (PTEN), an inhibitor of PI3K/Akt signalling, was lower in lung fibroblasts from IPF (40-42). Akt inactivates the function of forkhead box (Fox)O3a, one of the inhibitors of apoptosis (43, 44), which may confer a phenotype of resistance to apoptosis to IPF fibroblasts.

The Wnt/ β -catenin pathway is known to be associated with activation of lung fibroblasts and the dysregulation of wound repair (45). Canonical Wnt signalling promotes translocation of β -catenin into the nucleus and its regulation of target gene expression by inhibiting the degradation of it. Moreover, Wnt signalling is induced during TGF- β -mediated differentiation of fibroblasts into myofibroblasts, and in turn TGF- β requires activation of Wnt for induction of fibrosis (46). The activation of focal adhesion kinase (FAK), one of the downstream proteins of the vascular endothelial growth factor (VEGF) pathway, and inhibition of FAK-related non kinase (FRNK) has also been demonstrated to be related to the migration of fibroblasts and their differentiation into myofibroblasts (47, 48).

The source of TGF- β and other mediators activating fibroblasts during early stages of IPF development are still not well understood. Various cells in the fibrotic lesion, such as inflammatory cells and injured AECs, may possibly produce the signals inducing differentiation and activation of fibroblasts, and generated myofibroblasts can also be a source of TGF- β , which induces apoptosis of AECs, making the aberrant wound healing process continue indefinitely.

3.4 Reaction of alveolar epithelial cells (AECs) to microinjuries

Repetitive alveolar epithelial injury is considered to be an important trigger of IPF. When type 1 AECs, which constitute the majority of the alveolar epithelium, are damaged, type 2 AECs proliferate to cover the injured basement membranes. The excessive hyperplastic type 2 AECs spread and differentiate into type 1 AECs and the remaining cells undergo apoptosis. Based on the evidence that targeted deletion of type 2 AECs results in fibrosis (49), loss of viable type 2 AECs via injury may be a key instigator of pulmonary fibrosis.

The transdifferentiation of injured AECs into fibroblasts through epithelial-mesenchymal transition (EMT) is hypothesised to be one of the processes linking the microinjury to alveolar epithelium and lung fibrosis. Through EMT, AECs lose apical-basal polarity and the expression of cell adhesion molecules such as E-cadherin, while producing mesenchymal molecules such as α -SMA, fibronectin and N-cadherin and becoming migratory. Although the importance of EMT in IPF is still controversial (50, 51), it has been reported that AECs can differentiate into myofibroblasts (52-54). TGF- β 1 signalling mediated by phosphorylation of Smad2/3 is a major inducer of EMT and finally regulates the transcription of CTGF, α -SMA, collagen and plasminogen activator inhibitor (PAI)-1. PAI-1 inhibits plasminogen activation and in turn upregulation of prostaglandin (PG) E2 secretion, which represents an anti-fibrotic signal in AECs (55). On the other hand, activation of TGF- β /non-Smad signalling such as ERK and JNK MAPK, PI3K/Akt, and Wnt pathways are also related with induction and development of EMT (56-59). Integrin α 3 β 1 and α v β 6 have been reported to be required for α -SMA upregulation, differentiation of fibroblasts, and EMT via alteration of Smad and β -catenin signalling (53, 54).

The loss of control of the dead type 2 AECs over the fibroblasts, resulting in their excessive proliferation and production of ECM, may also be a mechanism for inducing fibrosis. PGE2 has been reported not only to suppress EMT, but also to control proliferation and differentiation of fibroblasts. In IPF, excessive epithelial apoptosis causes downregulation of PGE2 levels which lead to the loss of control of profibrotic phenotypes in fibroblasts (60). Although the mechanisms causing AEC death are not sufficiently elucidated, it is known that TGF- β induces apoptosis in AECs through modulation of Fas-mediated apoptosis by activating caspase-3 and downregulating p21 (61). Oxidative stress, which is shown to be increased in IPF, is considered to be another cause of AEC damage. ROS alters the balance between MMPs and TIMPs and activates TGF- β , while TGF- β induces ROS production (62). It has been shown that AECs were the main cell type undergoing endoplasmic reticulum stress resulting in apoptosis (63).

3.5 Migration and differentiation of fibrocytes into myofibroblasts

Fibrocytes are a group of bone marrow-derived fibroblast progenitor cells, characterised by the co-expression of the stem cell marker CD34, the leukocyte common antigen CD45 and fibroblast markers (collagen-1, -3 and fibronectin), which may be another source of lung fibroblasts in IPF (64). Like fibroblasts and

AECs, fibrocytes also differentiate into myofibroblasts through the activation of TGF- β -induced Smad2/3 and SAPK/JNK MAPK pathways (65).

Inhibition of the CC chemokine receptor type 2 (CCR2) mediated fibrocyte recruitment and differentiation has been reported to suppress the development of lung fibrosis in vivo (66, 67). Fibrocytes also express the CXC chemokine receptor type 4 (CXCR4), which is involved in the migration of these cells when stimulated with its ligand, stromal cell-derived factor 1 (CXCL12) (68), released from various cells including injured AECs. CXCR4 and CXCL12 are highly increased in IPF lung tissue (64), which may be another therapeutic target.

3.6 Transdifferentiation of endothelial cells into mesenchymal cells

IPF is associated with increased vascular density in alveolar walls in the early stages, decreased vascular density in fibrotic lesions and abnormal vascular remodelling/angiogenesis close to fibrotic areas (69, 70). The endothelial dysfunction is regarded as one of the potential inducers of IPF. Endothelial cells from mice with bleomycin (BLM)-induced pulmonary fibrosis have been reported to promote collagen-1 production by fibroblasts and their transition to myofibroblasts (71). Repetitive lung injury has been shown to activate pulmonary capillary endothelial cells, which inhibits normal alveolar repair and promotes fibrosis (72).

In several studies, TGF- β has been demonstrated to promote the generation of myofibroblasts through endothelial-mesenchymal transition (EndMT) via both Smad and non-Smad pathways. Moreover, a major vasoactive peptide endothelin 1 (ET-1) has been found to promote TGF- β -induced EndMT (73, 74). Notch and TGF- β signalling have been reported to induce EndMT synergistically (75, 76). Loss of cell-cell junctions-related and other endothelial markers, such as platelet endothelial cell adhesion molecule (PECAM-1/CD31), VE-cadherin, vascular endothelial growth factor receptor (VEGFR) and the angiopoietin receptor Tie-2, increased expression of α -SMA, fibronectin and vimentin, and increased migratory potential, have been demonstrated in TGF- β -induced EndMT. Although it has not been completely clarified whether EndMT occurs in the pathogenesis of human lung fibrosis, Hashimoto et al. have shown that lung endothelial cells may be sources of fibroblasts in the lungs of mice with BLM-induced pulmonary fibrosis (77).

4. Bone morphogenetic protein (BMP) pathway and pulmonary fibrosis

4.1 Overview

The bone morphogenetic proteins (BMPs) are members of the TGF- β superfamily of growth factors, which includes TGF- β s and activins. The BMPs were originally known for inducing de novo bone tissue formation, however, a variety of other important biological activities of BMPs have also been broadly elucidated, such as regulation of morphogenesis, differentiation, proliferation, and apoptosis of a variety of cells. Although BMPs are broadly expressed in various tissues during embryogenesis, some of them becomes restrictedly expressed in some specific organs/tissues after birth. For instance, BMP7 is abundantly expressed in kidney, whereas BMP3-6 is high in lung in adult mice (78). BMP3 is highly expressed by osteoblasts and osteocytes in bone matrix of mice (79). BMP9 is secreted by hepatocytes and released into plasma (80), which suggests that BMPs can work not only locally but also systemically.

It has been shown that some BMPs may play a role in the pathogenesis of fibrosis. In contrast to the TGF- β s, some of the BMPs have anti-fibrotic potentials and are thought to counterbalance the profibrotic phenotypes induced by the TGF- β s.

4.2 BMP signalling

BMPs are synthesized as inactive large precursor proteins. Each unprocessed BMP contains an N-terminal signal peptide, a bioactive BMP at the C-terminus and a pro-domain connecting those two regions. Following signal peptide cleavage by a pro-protein convertase such as furin, the precursor protein undergoes glycosylation and either homo- or heterodimerization. The pro-domain is cleaved when the mature dimeric BMP is secreted (81).

In common with other TGF- β superfamily cytokines, BMPs bind to their specific type 2 receptors. Dimeric BMPs bind to specific sets of two type 2 receptors, which then induce formation of heteromeric complexes with two type 1 receptors and phosphorylation of them. While BMP receptor type 2 (BMPR2) is selective for BMPs, activin receptors type 2 (ActR2) A and B are shared by BMPs and activins. On the other hand, there are four type 1 receptors: ALK1, ALK2 (also termed activin A receptor type IA; ActR1A), ALK3 (also termed BMP receptor type IA; BMPR1A), and ALK6 (also termed BMP receptor type 1B; BMPR1B). ALK2 and 3 are expressed in various types of cells, while ALK6 expression is more restricted

Table 1-3. Specific combinations of the BMPs, their receptors and downstream R-Smad proteins.

Ligand	Type 2 receptor	Type 1 receptor	R-Smad
BMP2, 4	BMPR2	ALK3 (BMPR1A) ALK6 (BMPR1B)	Smad1, 5, 8
BMP5-8		ALK2 (ActR1A) ALK3 (BMPR1A) ALK6 (BMPR1B)	
BMP9, 10		ALK1 ALK2 (ActR1A)	
BMP12-14		ALK6 (BMPR1B)	
BMP3		ALK4 (ActR1B)	
BMP11, 15, GDF9		ALK5 (T β R1)	

Modified from (82). BMP: bone morphogenetic protein; BMPR2: BMP receptor type 2; ActR2: activin receptor type 2; ALK: activin receptor-like kinase; BMPR1: BMP receptor type 1; ActR1: activin A receptor type 1.

and ALK1 is expressed only in endothelial cells and certain other cells. Each BMP has high affinity to specific type 1 receptors, as summarised in Table 1-3 and shown in Figure 1-1.

Phosphorylation of type 1 receptors mediated by a majority of BMPs induces phosphorylation of BMP-dependent R-Smads (Smad1/5/8). Like TGF- β -dependent Smad2/3, those phosphorylated R-Smads form complexes with Co-Smad4 and translocate into the nucleus and regulate the transcription of the specific target genes, such as the inhibitors of DNA binding 1-4 (Id1-4), GATA2 and Tob. In addition to the Smad pathway, BMPs also induce non-Smad signalling, such as ERK, p38 and JNK MAPKs, PI3K/Akt and small GTPases such as Rho and Rac (36). These non-Smad pathways regulate various cellular responses independently from or in cooperation with Smad pathways (Figure 1-1). On the other hand, BMP3, 11, 15 and GDF9 bind to ALK4 (also termed activin A receptor type 1B; ActR1B) or ALK5, leading to activation of "TGF- β -dependent" R-Smads (Smad2/3) pathway (Table 1-3) (83, 84) that have potential to suppress the role of other BMPs.

BMP signalling is regulated by various factors. The extracellular BMP antagonists, such as noggin, chordin, gremlin, follistatin and follistatin-like 1 (FSTL1) directly bind to BMPs and prevent them from binding to their receptors. Oppositely, Kielin/chordin-like protein (KCP) binds to BMPs and promotes binding

of BMPs to type 1 receptors (85). BMP and activin membrane-bound inhibitor (BAMBI) is the cell membrane pseudoreceptor which lacks the intracellular kinase domain and negatively regulates both TGF- β and BMP signalling (86). Besides, there are some type 3 receptors such as betaglycan and endoglin, which are co-receptors of TGF- β superfamily members and regulate signalling both positively and negatively (87, 88). I-Smad6/7 and the E3 ubiquitin ligases Smurf1/2 are intracellular regulators of BMP signalling. Smad6/7 suppresses activation of the TGF- β /BMP receptors and transcription of the target genes. Transcriptional co-repressors, such as c-Ski, SnoN, and Tob, regulate transcription of the target genes in the nucleus (89, 90). On the other hand, BMP1, which is not classified as a member of BMPs, is a metalloproteinase. BMP1 activates BMP signalling through cleaving chordin in BMP-chordin complexes and releasing active BMPs from it (91, 92).

4.3 TGF- β and BMP crosstalk in fibrosis

The crosstalk between TGF- β and BMPs in the pathogenesis of fibrosis has been mainly studied in the organs frequently affected by fibrosis, including kidneys, liver, lungs, and heart. In this context, fibrosis is defined by the excessive accumulation of ECM produced by activated myofibroblasts. TGF- β plays a main role in the progression of fibrosis, and the inhibition of TGF- β has been shown to suppress the fibrogenesis. Due to the common signal transduction modality, BMPs are involved in fibrogenesis interactively with TGF- β through either reciprocally promoting or suppressing each other.

In the pathogenesis of renal fibrosis, the BMPs are known to antagonize the profibrotic effects of TGF- β . BMP7 has been shown to antagonize the TGF- β -induced secretion of PAI-1 via Smad5 and its downstream Smad6 in cultured mesangial cells. The BMP7-induced reduction of PAI-1 promotes MMP2 activity, which degrades ECM (93). Hence, BMP7 is reported to suppress TGF- β 1-induced EMT (94) and has shown a therapeutic potency in the mouse chronic renal fibrosis model (95, 96).

When it comes to liver fibrosis, TGF- β promotes proliferation and migration of hepatic stellate cells (HSCs) and their differentiation into myofibroblasts. Administration of BMP7 can decrease expression of TGF- β 1, phosphorylated (p-) Smad2, α -SMA and collagen and improve liver fibrosis in vivo (97, 98) and the expression of collagen 1 and 3 by primary HSCs through inhibition of the nuclear translocation of Smad2/3 (98). Moreover, TGF- β diminishes the expression and

release of BMP2 by HSCs, and oppositely, BMP2 downregulates the expression of TGF- β and its own receptors (99). However, there is also a report demonstrating increased proliferation and ECM production in HSCs treated with BMP7 (100).

BMP2 has proven to antagonise the profibrotic effects of TGF- β 1 in cardiac fibrosis. In cardiomyocytes, BMP2 promotes the formation of the Smad6/Smurf1 complex, which promotes the degradation of TGF- β receptors and inhibits activation of Smad3 (101). BMP7 may also ameliorate myocardial fibrosis by limiting the TGF- β 1-dependent upregulation of collagen 1 and α -SMA in myocardial fibroblasts (102) and by suppression of EndMT (103).

4.4 BMP pathway and pulmonary fibrosis

4.4.1 Role of BMPs against pulmonary fibrosis

BMP4 and 7 are the most studied BMP ligands in the field of pulmonary fibrosis. BMP4 has been reported to inhibit proliferation of human lung fibroblasts and promotes their differentiation into myofibroblasts via the Smad1 and JNK pathways (104). Pegorier et al have demonstrated that BMP4 (but not BMP7) can suppress the TGF- β -induced proliferation and production of ECM proteins in human lung fibroblasts, while BMP7 inhibits the activity of MMP2 and reverts the TGF- β -induced myofibroblast-like phenotype. Both BMP4 and 7 can reduce the activity of MMP13 (105). BMP7 was also reported to ameliorate the silica-induced pro-fibrotic phenotypes in rat AECs by suppressing the TGF- β /Smad signalling and activating the BMP7/Smad signalling, which eventually inhibited cell migration and ECM protein production (106). In another article, BMP7 overexpression by adenovirus inhibited TGF- β -induced collagen 1 and TIMP2 production from mouse lung myofibroblasts (107). On the other hand, there is an article denying the anti-fibrotic effect of BMP7 on ECM production and α -SMA expression in lung fibroblasts and suppression of EMT in AECs (108).

Regarding in vivo models, administration of BMP7 to rats with silica-induced pulmonary fibrosis reduced the expression of TGF- β and subsequent elevation of p-Smad2/3 in the lungs, resulting in the reduction of collagen deposition and fibrosis (109). Intravenous injection of BMP7-overexpressing bone-marrow stem cells could reduce ECM deposition and TGF- β 1 expression and preserve epithelial markers in the silica-induced rat pulmonary fibrosis model compared with injection of control cells (110). Moreover, Leppäranta et al has recently found an inducer of BMP2 and 7 in AECs called tilorone. In a silica-induced mouse pulmonary fibrosis model, p-Smad1 was decreased and p-Smad2 was increased in

AECs. Tilorone could revert this imbalance and ameliorate fibrosis in the lungs (111). However, again an article demonstrated that BMP7 did not show any anti-fibrotic effect on a BLM-induced mouse pulmonary fibrosis model (108).

Although BMP3 is recognised as an antagonist against BMP signalling by activating Smad2/3 pathway (83), there are some reports demonstrating that BMP3 can also ameliorate pulmonary fibrosis. BMP3 and 4 have been reported to inhibit TGF- β 1-induced cell migration, while they promote collagen gel contraction in fetal lung fibroblasts (112). The expression of BMP3 was reduced in the lungs of IPF patients, as well as those from a BLM-induced mouse pulmonary fibrosis model, and administration of BMP3 could attenuate pulmonary fibrosis in those mice. In lung fibroblasts isolated from the mouse model, BMP3 suppressed proliferation and reverted α -SMA expression. BMP3 also attenuates TGF- β -induced reduction of p-Smad1/5/8 in lung fibroblasts (113), however, the reason for the discrepancy between past reports has not been elucidated.

4.4.2 Endogenous BMP inhibitors in pulmonary fibrosis

Murphy et al have recently reported that mRNA expression of BMP-binding antagonists gremlin 1, noggin, follistatin, and FSTL1 are significantly increased, while that of other BMP antagonists chordin, nephroblastoma overexpressed gene, BAMBI, and a BMP enhancer KCP are decreased in the lungs of the mice with BLM-induced pulmonary fibrosis. In particular, regarding noggin, BAMBI, and FSTL1, their protein levels were also increased together with the significant decrease of BMP2. They were also increased in the lungs of IPF patients. In addition, TGF- β increased noggin, BAMBI, and FSTL1 expression in human AECs (114). In another article, BLM-induced pulmonary fibrosis was milder in noggin haploinsufficient mice than in normal mice. Those mice showed elevated expression of BMP2, 4 and 6 and I-Smad6/7 in the lungs, and preserved p-Smad1/5/8 expression, decreased proliferation and apoptosis of AECs (115). Similarly, FSTL1 haploinsufficient mice showed milder pulmonary fibrosis with decreased ECM deposition and myofibroblast accumulation than normal mice when taking BLM or silica administration, or radiation exposure (116-118). Administration of FSTL1 neutralising antibody had the same effect on suppression of fibrosis (116, 117). FSTL1 was demonstrated to enhance TGF- β -induced Smad2/3 signalling in mouse AECs and fibroblasts, as well as to suppress BMP-induced Smad1/5 signalling in AECs, resulting in induction of EMT and differentiation of fibroblasts into myofibroblasts (116, 117, 119). Moreover, FSTL1 can also enhance the ERK, p38

and JNK signalling in mouse lung fibroblasts, resulting in proliferation, migration, and differentiation into myofibroblasts (119).

The expression of gremlin was high in the lungs from IPF patients and in lung fibroblasts isolated from them, which are associated with impaired responsiveness to BMP4. AECs with TGF- β -induced EMT also showed elevated expression of gremlin. Additionally, overexpression of gremlin makes AECs more susceptible to TGF- β -induced EMT (120). In the lungs from mice with asbestos-induced pulmonary fibrosis, gremlin mRNA levels were elevated, which were mediated by the TGF- β and the MAPK kinase/ERK pathways in AECs. Supplementation of BMP7 significantly reduced collagen deposition in their lungs. (121). In another study, transient gremlin overexpression using adenovirus induced pulmonary fibrosis in rats, reduced p-Smad1/5/8 expression, and promoted proliferation and apoptosis in AECs close to the fibroblastic foci (122).

4.4.3 BMPR2 in pulmonary fibrosis

Chen et al has demonstrated that BMPR2 and p-Smad1/5/8 or ID1 were reduced and p-Smad2/3 was elevated in the lungs from IPF patients and BLM-induced pulmonary fibrosis mice. Inhibition of interleukin (IL)-6 attenuated fibrosis with elevated BMPR2 expression and reduction of some miRs which can cause dysfunction of BMPR2. Reduced BMPR2 was particularly observed in bone-marrow derived macrophages in IPF lungs (123). In another study, though BMPR2 reduction in BLM-treated mice was also demonstrated, fibrosis was not deteriorated in BMPR2 tet-on mutation mice, while worsening of associated secondary PH was observed. Mutant BMPR2 was correlated with increased hypoxia-inducible factor (HIF) 1- α stabilization in lungs and increased HIF1- α and ROS production in cultured pulmonary microvascular endothelial cells (124).

On the other hand, BMPR2 mRNA expression was increased by 24-hour TGF- β stimulation in lung fibroblasts, which could be reversed by BMP4 and 7 (105). In AECs, BMPR2 expression levels were not affected by TGF- β or BMP7 treatment (108).

Some of the apparent inconsistencies in studies may be due to the different times points and contexts investigated. To date, the impact of modulating BMPR2 expression level on pulmonary fibrosis has not been studied.

5. Endothelial colony forming cells (ECFCs)

5.1 Overview and definition of endothelial colony forming cell (ECFC)

Angiogenesis is a process of originating blood vessels from pre-existing vasculature through proliferation and migration of endothelial cells existing in it. On the other hand, de novo blood vessel formation from stem or progenitor cells that differentiate into endothelial cells and incorporate into the tissue is termed vasculogenesis. Both of those processes for blood vessel formation may play a role in revascularization cooperatively, which are important for the homeostasis of peripheral blood vessels. Vasculogenesis has originally been regarded as a part of embryogenic processes, however, the accumulating knowledge of endothelial colony forming cells (ECFCs) has proven that vasculogenesis occurs throughout life.

In 1997, Asahara et al discovered CD34⁺ hematopoietic precursor cells, which were isolated from peripheral blood-derived mononuclear cells and are able to differentiate into endothelial cells ex vivo (125). These cells expressed both hematopoietic and endothelial markers, could home specifically to sites of active angiogenesis such as areas of ischemia (125), differentiate, proliferate, and incorporate into pre-existing blood vessels under various circumstances including ischemia (126). These cells were named “endothelial progenitor cells (EPCs)”.

Through more than two decades of the accumulation of evidence, currently the term “EPC” encompasses two different cell types (127, 128). ECFCs (also termed outgrowth endothelial cells (OECs) or late EPCs) are cobblestone shaped cells forming colonies on collagen coated plates following at least 1 week of culture. They express markers of mature endothelial cells (CD31, CD146, VE-cadherin, Tie-2, von Willebrand factor (vWF) and VEGFR2) as well as mature (CD34) or immature (CD133) hematopoietic stem cell markers and have a high proliferation capacity and longer survival up to 12 weeks. They can differentiate into endothelial cells and form vessels (129, 130). In contrast, early EPCs (also termed circulating angiogenic cells (CACs) or myeloid angiogenic cells (MACs)) are spindle shaped cells forming colonies on fibronectin-coated plates following 4-7 days of culture, are less proliferative, and survive up to only 4 weeks in culture. They express haematopoietic markers as well as inflammatory markers (128), and contribute to angiogenesis through secreting cytokines such as VEGF (129, 130), but are not the direct source of mature endothelial cells. Therefore, an early EPC is actually not an “endothelial progenitor” and does not fulfill the original concept of EPC. In the recent consensus statement for nomenclature of EPCs it is suggested that the term

“ECFC” should be used for “true” EPCs to avoid discrepancies between the literatures and distinguish them from early EPCs (127).

ECFCs have attracted significant attention due to their vasculogenic property and targeted delivery of therapeutic agents, as they have characteristics of homing to the sites of vascular injury, occlusion, or hypoxia. This homing is mediated by multiple molecules such as VEGF, CXCL12 or erythropoietin (EPO) released from endothelial cells and/or platelets, which is induced by production of ROS, activation of P-selectin or HIF-1 α (131-134). A number of experimental and even clinical studies have suggested the feasibility, safety, and efficacy of EPC-based therapy in multiple diseases including ischemic heart disease, pulmonary arterial hypertension (PAH), and liver cirrhosis.

Accumulating evidence has suggested that ECFCs play an important role in various diseases. Circulating ECFCs are decreased in patients with chronic diseases, such as chronic heart failure (135), stroke (136), diabetes (137, 138), rheumatoid arthritis (139), chronic renal failure (140, 141), PH (142, 143) and pulmonary fibrosis (142, 144), perhaps due to progressive exhaustion of repair capabilities. On the contrary, acute ischemia is known to mobilise ECFCs, as reported in patients with acute myocardial infarction (145, 146). It is also known that low plasma levels of ECFCs correlate with increase of cardiovascular risk factors (147-149).

5.2 Utilisation of EPCs/ECFCs as therapeutic agents

EPCs (in particular, ECFCs) have been trailed as a therapy for various diseases mainly related to ischemic conditions or vascular damage. Several mechanisms of action of ECFCs at those sites have been suggested, such as direct incorporation of ECFCs to damaged vasculature and promotion of vasculogenesis (150, 151), paracrine effect, i.e. secretion of pro-angiogenic growth factors or extracellular vesicles (EVs) (152, 153), support for vascular repair by other cells, such as mesenchymal progenitor cells (154, 155) or adipose stromal cells (156).

There are a growing number of experimental reports demonstrating the efficacy of ECFCs predominantly on ischemic diseases such as hindlimb ischemia (151, 157), myocardial infarction (158) and ischemic retinopathy (159) mainly through direct incorporation of ECFCs and/or paracrine effects. Ischemic stroke (160) and traumatic brain injury (161) can also be treated with ECFCs mainly through the paracrine effect rather than the direct incorporation. Furthermore, ECFC treatment was also attempted for other conditions such as PAH and bronchopulmonary

dysplasia (BPD). In rat BPD models, intravenous injection of ECFCs or ECFC-derived conditioned media was effective for preserving the alveolar and lung vascular growth, and attenuated PH, which might be due to a paracrine effect (152, 162). ECFCs can also attenuate the severity of disease and preserve vascular function in animal models of acute kidney injury through paracrine effects (153, 163).

Regarding human clinical trials, "EPCs" have been tested as treatments for peripheral arterial disease, coronary artery disease and PAH. However, the cells used for clinical studies are significantly heterogeneous regarding methods of cell isolation and the markers on cell surface used for phenotyping. Hence, the cells used in those trials may not be pure ECFCs, but mixture of other kinds of cells such as early EPCs, circulating endothelial cells or other kinds of precursor cells.

Intramuscular administration of EPCs have been demonstrated to be safe and effective for tissue perfusion and pain relief in patients with critical limb ischemia (CLI) (164) and diabetic feet (165). Liotta et al demonstrated significant improvement in pain-free walking distance and quality of life, and reduction of mortality rate and major amputations in patients with CLI (166).

On the other hand, Wang et al demonstrated the safety, feasibility, and significant improvements of exercise capacity and pulmonary hemodynamics in adult idiopathic PAH patients treated with intravenous injection of EPCs (167). Likewise, positive effects were also observed in children with idiopathic PAH (168). They also demonstrated the efficacy of thymosin β 1 pre-treated EPCs for exercise capacity and left ventricular function in patients with ST segment elevated myocardial infarction (169). In another study, eNOS modified EPCs showed effectiveness for reducing pulmonary vascular resistance in PAH patients (170).

ECFCs have also been used as cellular vehicles for gene therapy. Comparing with other types of cells, ECFCs can be isolated non-invasively from peripheral blood, are genomically stable and easy to manipulate genetically. For instance, ECFCs have been used for gene therapy in canine models of haemophilia A. Subcutaneous or omental implantation of Factor VIII-transduced ECFCs kept the Factor VIII in therapeutic levels over a long period of time (171, 172). Subcutaneous implantation of genetically modified ECFCs expressing EPO controlled by a tetracycline-regulated system to mice resulted in formation of vascular networks reversibly releasing EPO into bloodstream (173), which can be expected to be used for treating EPO-dependent renal anaemia. In the field of cancer therapy, ECFCs have been used for directly delivering inhibitors of angiogenesis or other suicide

genes to the tumour endothelium. Administration of ECFCs carrying fms-like tyrosine kinase-1 or angiostatin-endostatin fusion protein could reduce the volume of tumour and extended survival in mice cancer models (174, 175).

5.3 Treatment of PH using gene-modified EPCs

PAH is a lethal disease characterized by increased pulmonary vascular resistance due to remodelling. Mutations of *BMPR2* are present in up to 80% of familial and 11-40% of idiopathic PAH (176), leading to the imbalance of TGF- β /BMP axis and resulting in profibrotic phenotype. *BMPR2* expression is also reduced in other forms of PH, as well as in animal models (124, 177). To date our group has attempted to treat PAH animal models using *BMPR2* gene therapy. Intravenous injection of adenovirus encoding *BMPR2* (Ad*BMPR2*) targeting pulmonary endothelium (178, 179) could attenuate PAH in the monocrotaline and hypoxia rat models as well as in a *BMPR2*-transgenic mouse model (180-183).

Most recently, we have demonstrated that intravenous injection of rat bone marrow-derived EPCs (they were not pure ECFCs as the cell-surface marker profile was not sufficiently definitive of ECFCs) transduced with adenovirus encoding *BMPR2* can increase the expression of *BMPR2* in the lungs and attenuate monocrotaline-induced rat PAH model both hemodynamically and histologically (184). The biodistribution study evaluated using EPCs transduced with luciferase reporter adenovirus revealed that though more than 99% of EPCs accumulated in the lungs 1-6 hours after injection, vast majority were lost by 24 hours. In view of this short retention time, the mechanism for the effects of this cell therapy may be due to paracrine effect via EVs.

5.4 ECFCs and pulmonary fibrosis

Several studies have demonstrated the altered levels of ECFCs in IPF patients. Fadini et al reported reduced ECFCs in patients with restrictive lung disease, in particular in those with reduced lung volumes and impaired alveolo-arterial diffusion capacity. The rate of apoptosis of ECFCs was high in patients with diffuse lung disease (185). They have also showed depleted ECFCs in IPF patients, which was more severe when associated with PH (142), which is one of the major complications of IPF typically associated with reduced diffusing capacity of the lung for carbon monoxide (D_LCO). On the contrary, ECFCs isolated from IPF patients with significantly impaired D_LCO and those from patients with history of acute exacerbation showed increased proliferative potential *ex vivo* (144). This

data is supported by a report demonstrating that EPCs cultured under hypoxic circumstance were shown to have higher capability of proliferation and differentiation (186).

There is evidence that ECFCs have profibrotic potential in IPF patients. ECFCs isolated from IPF patients release more EVs, in particular from those with a low DLCO, than controls. These EVs promote plasminogen activation and fibroblast migration, at least in part by an increased plasmin generation (187), suggesting a role of ECFC-derived EVs to the pathogenesis of IPF. In another report, ECFCs from IPF patients showed high senescent and apoptotic states and increased secretion of IL-8, which induced migration of neutrophils, and increased IL-8 in peripheral blood was associated with a poor prognosis in IPF patients (188). In addition, ECFCs are also considered to cooperate with fibrocytes to promote the abnormal vascular remodelling and vasculogenesis close to fibrotic areas mediated by CXCR4 (189).

Transdifferentiation of ECFCs into mesenchymal cells like EndMT may also contribute to the pathogenesis of IPF. Díez et al reported that co-culture of ECFCs with smooth muscle cells resulted in the reduction of endothelial markers and the increase of mesenchymal markers, which was mediated by the TGF- β pathway (190, 191). Those transdifferentiated ECFCs demonstrated pro-angiogenic properties mediated by fibroblast growth factor (FGF)-2 and angiopoietin-1 through a paracrine manner (191).

Regarding the application to treatment, ECFCs have not been successfully used for treating pulmonary fibrosis. In a report by Blandinières et al., ECFCs could not modulate fibrosis or vascular density before or after the completion of fibrogenesis in BLM-induced pulmonary fibrosis mouse model (192). This may possibly be due to the above-mentioned profibrotic characteristics of ECFCs. However, the information available so far regarding therapeutic potential of ECFCs against pulmonary fibrosis is insufficient. Given that ECFCs have shown positive therapeutic effect in PAH patients (167-170), and that rat PAH treated with gene-modified EPCs showed reduced vascular remodelling in our previous study (184), and no significant profibrotic adverse effects were observed in those studies, further investigation of the effect of ECFCs on pulmonary fibrosis is warranted.

6. Treatment of IPF

6.1 Overview

Despite the high medical need, recommended treatment options in the 2011 international IPF guidelines were limited to oxygen supplementation and lung transplantation (4). IPF patients had been treated with corticosteroids +/- azathioprine or cyclophosphamide for decades. Subsequently, N-acetylcysteine (a precursor of glutathione, an antioxidant) combined with prednisone and azathioprine had become the standard therapy of IPF (193). However, this triple therapy had later been proven to be harmful based on the results of the PANTHER-IPF trial (14). Other clinical trials for etanercept (tumor necrosis factor (TNF)- α antagonist) (194), interferon gamma (195), imatinib (196), warfarin (13), endothelin receptor antagonists (15, 197-199), N-acetylcysteine monotherapy (200), and tralokinumab (anti-IL13 monoclonal antibody) (201) also demonstrated disappointing results.

In 2014, large scale international phase 3 randomised controlled trials (RCTs) of 2 antifibrotics, pirfenidone (16) and nintedanib (17), finally showed positive results. Given this evidence, in the 2016 update of the IPF guideline, these drugs are conditionally recommended for the treatment of IPF (202). Nevertheless, both drugs have major side effects and their effects are limited to only slowing down the disease progression and improve survival rate just slightly. Therefore, alternative therapeutic options are still necessary to be sought.

6.2 Anti-fibrotic agents

6.2.1 Pirfenidone

Pirfenidone is an antifibrotic drug with various effects. It regulates the levels of TGF- β and TNF- α in vitro (203) and reduces proliferation of fibroblasts and production of collagen in animal models of lung fibrosis (204-206). One relatively small RCT of pirfenidone for mild to moderate IPF carried out in Japan was stopped early due to a potential benefit for reducing the frequency of acute exacerbation, a secondary outcome (207). Additionally, pirfenidone was also effective to preserve FVC over time and the oxygen saturation during 6-minute-walk test. Although a highly selected patients were enrolled and the primary endpoint was altered during the study in the second Japanese trial, it also demonstrated a benefit of pirfenidone regarding a reduction in the rate of decline in FVC and improved progression-free survival (208). In the phase 3 replicate CAPACITY trials

(CAPACITY 004 and 006) (209), pirfenidone showed a reduction in decline of FVC at week 72 only in one of the trials. Subsequently, in the ASCEND trial, applying stricter selection criteria (16), pirfenidone significantly reduced the rate of patients whose annual rate of decline in FVC was more than 10%, and extended 6-minute-walk distance and progression-free survival. Mortality or dyspnoea scores did not differ. Pooled results from these trials suggested reduction in mortality and the rate of FVC decline with pirfenidone, though the effect on mortality is limited (3.2% reduction of 1-year all-cause mortality and 2.4% of IPF-related mortality) (210).

6.2.2 Nintedanib

Nintedanib is an inhibitor of receptor tyrosine kinases of multiple growth factors, including VEGF, FGF, and PDGF. In the phase 3 replicate INPULSIS trials (INPULSIS-1 and -2) for nintedanib in IPF patients, nintedanib showed significant effect on the reduction of the rate of decline in FVC over 52 weeks compared with placebo (17). Additionally, a meta-analysis of one phase 2 (TOMORROW) and two INPULSIS trials revealed that the odds ratio for a greater than 10% absolute decline in FVC was significantly lower in the nintedanib group at week 52 (211). The time to the first acute exacerbation was significantly longer in the nintedanib group only in one of the two INPULSIS trials (17). On the other hand, in a pooled analysis of the two INPULSIS trials, the use of nintedanib was significantly correlated with longer time to the first acute exacerbation and lower rate of acute exacerbation (17). In terms of mortality, none of above-mentioned trials was powered to show a benefit of nintedanib.

The benefit of nintedanib has recently been revealed also in patients with non-IPF progressive fibrosing ILDs in a RCT (212). The annual rate of decline in FVC was significantly reduced by using nintedanib. Based on this evidence, now nintedanib is prescribed for patients with non-IPF fibrosing ILDs being progressive in spite of appropriate management such as anti-inflammatory therapies.

6.3 Cell therapy for pulmonary fibrosis

The potential of cell therapy has been extensively investigated in pulmonary fibrosis. The efficacy of cell therapy is expected to be achieved mainly by promoting the correct re-epithelialization of the alveoli with regenerated cells and/or the paracrine properties of the administered cells.

In the alveolar epithelium, type 2 AECs can self-replicate and differentiate into type 1 AECs as normal turnover or when type 1 AECs are reduced by injury. A study

showed that intratracheal administration of freshly isolated type 2 AECs can reverse fibrogenesis in a BLM-induced pulmonary fibrosis model (213). Type 2 AECs derived from pluripotent or embryonic stem cells could also reduce collagen deposition in a BLM-induced pulmonary fibrosis model (214, 215). Furthermore, since the process for isolating or generating type 2 AECs is complicated, it was considered to be easier, faster and more efficient to use mixed lung epithelial cells alternatively. The intratracheal administration of mixed lung epithelial cells was shown to attenuate fibrosis in a BLM-induced pulmonary fibrosis model (216).

Mesenchymal stem cells (MSCs) are usually isolated from adult bone marrow, umbilical cord blood, adipose tissue, or placenta. The therapeutic effect of MSCs is not mainly related to their capability of differentiating into multilineage cells, but to their anti-proliferative, anti-apoptotic, anti-inflammatory, and immunomodulatory characteristics, and the capability of modulating microenvironment at the sites of engraftment. Most of these effects are expressed by the secretion of soluble factors and EVs. In BLM-induced pulmonary fibrosis models, bone marrow-derived MSCs can reverse the fibrosis through their engraftment and differentiation into lung cells, and reduction in inflammatory cytokines (217-219). Similarly, umbilical cord- and placenta-derived MSCs were also demonstrated to have efficacy through inhibition of lung inflammation by suppressing the profibrotic cytokine expression (220) and the infiltration of neutrophils (221). On the other hand, some subpopulations of MSCs may contribute to fibrogenesis. As MSCs expressed a myofibroblast marker when delivered to the lesions of established irradiation-induced pneumonitis in a mouse model (222), the phenotype of MSCs may be guided by the microenvironment of injured lungs.

Adipose tissue contains pluripotent cells (adipose derived stromal cells; ADSCs) which can also differentiate into various cell lineages. ADSCs can be isolated from adipose tissue of obesity patients who undergo liposuction and produce many bioactive factors. The ADSC therapy resulted in a suppression of the hyperplasia and apoptosis of AECs, alveolar septal thickening, alveolar enlargement, infiltrations of inflammatory cells, and TGF- β levels in the lungs of a BLM-induced pulmonary fibrosis model (223).

Other than above-mentioned cell types, intravenous injection of human amnion epithelial cells has also been proved to prevent, and moreover, treat BLM-induced pulmonary fibrosis by reducing production of pro-inflammatory and profibrotic cytokines, and collagen deposition (224). They can be used through intraperitoneal

injection as well for treating pulmonary fibrosis, which is suspected to work via paracrine effects (225).

In the clinical field, Tzouveleakis et al conducted a study for the safety and feasibility of endobronchial administration of ADSCs in 14 IPF patients. No significant adverse event was observed, and pulmonary function parameters and 6-minute walk distance were unchanged over 12 months (226). In the follow-up study, a significant decline of pulmonary function at 24 months was observed (227), which was at the same level as that observed in the placebo arm of large phase III RCTs of antifibrotics (16, 17). Subsequently, Chambers et al conducted a dose-escalation phase 1b study on the intravenous placenta-derived MSCs in 8 moderately severe IPF patients. Each dose was well tolerated with only minor and transient acute adverse effects. There was no decline in FVC at 6 months (228). Most recently, Averyanov et al conducted a placebo-controlled trial including 10 IPF patients for intravenous injection of bone marrow-derived MSCs in IPF patients with rapid pulmonary function decline (229). MSC therapy resulted in significantly longer 6-minute walk distance and better pulmonary function compared with placebo without any adverse events, though it did not improve mortality rate or HRCT fibrosis score.

Combination of cell and gene therapy may also be a new treatment strategy for IPF. Aguilar et al demonstrated a therapeutic effect of keratinocyte growth factor-transduced bone marrow stem cells in an animal model with BLM-induced pulmonary fibrosis (230). Genetically modified stem cells have the property of accumulating specifically in the injured sites of the lungs and delivering certain genes to those sites. Further research is warranted to identify the appropriate stem cell type for gene therapy in the lung, and the safe gene vector that can sustain expression of a specific gene.

6.4 Research questions

As described in the previous sections, the currently available therapeutic agents for IPF have limited efficacy and significant side effects, and further research for new treatment strategies is warranted. The treatment strategies attempted to date have mainly focused on the suppression of profibrotic factors such as TGF- β and other growth factors, TNF- α , IL-13 and ROS (14, 16, 17, 194, 201). On the other hand, the upregulation of anti-fibrotic pathway such as the BMP pathway has not been well studied in clinical field. In the field of experimental studies, administration of BMPs or suppression of intrinsic BMP inhibitors have shown positive effects on the treatment of pulmonary fibrosis models (106-108, 115-117, 121), while the manipulation of BMP receptors has never been attempted. As there are a few reports describing the reduction of BMPR2 in a BLM-induced mouse pulmonary fibrosis model (123, 124), the upregulation of BMPR2 seems to be a reasonable strategy for modulating the balance of TGF- β /BMP axis. Moreover, the treatment using BMPR2-expressing EPCs for transducing BMPR2, which was established by our group (184), may be an effective method for achieving this strategy.

Once a new treatment is established, how to select the candidates for the treatment is another concern. As IPF can be difficult to distinguished from other chronic fibrosing ILDs, the definition of disease may be modified based on the purpose for the diagnosis. In particular, either an radiological or a histopathological UIP pattern is required for a definitive diagnosis of IPF in the guideline (3), while there are some clinical trials being able to enrol patients without histopathological information as long as showing a probable UIP pattern on HRCT (17, 231), which allows more patients to be eligible for the trials. However, this diagnostic approach involves a risk for overdiagnosis of IPF in patients with other ILDs with better prognoses. Although the validity of this approach has been confirmed in the post-hoc analysis of the RCTs (11), the participants in the clinical trials are generally highly suspected to be “true” IPF by expert physicians of ILDs and do not reflect the usual ILD population in the real world. Furthermore, the evidence for the validity is based on the short-term outcome such as the annual rate of the decline in FVC and time to the first acute exacerbation in the first year, so there is a lack of the long-term data including survival time.

According to the above-mentioned matters, I have established the following two research questions and planned studies to answer them.

Question 1: Can the BMPR2 transduction ameliorate pulmonary fibrosis?

To evaluate the efficacy of BMPR2 transduction on pulmonary fibrosis, at first, I have planned to use primary lung fibroblasts from healthy controls and IPF patients to compare the TGF- β /BMP signalling and the profibrotic reaction to TGF- β . Those cells would then be used for evaluating the effect of the BMPR2 transduction on the TGF- β -induced profibrotic phenotypes. Moreover, our original techniques for the BMPR2 transduction using gene-modified EPCs expressing BMPR2 were going to be utilised to treat the BLM-induced rat pulmonary fibrosis model.

Question 2: Is a probable UIP pattern on HRCT sufficient for making a diagnosis of IPF?

To evaluate the validity of the approach for diagnosing IPF in patients with a probable UIP pattern on HRCT but without histopathological information, I have planned to collect the data of IIP patients from clinical charts retrospectively and to compare long term survival and the time to the first acute exacerbation between those with a UIP pattern versus those with a probable UIP pattern on HRCT. I would also investigate the prevalence of a final diagnosis of IPF made through multidisciplinary discussion in patients with a probable UIP pattern on HRCT for evaluating the extent of heterogeneity.

Part II

**Overexpression of BMPR2 suppresses
transforming growth factor β -induced profibrotic
responses in lung fibroblasts**

Statement of Authorship

Title of Paper	Overexpression of bone morphogenetic protein type 2 suppresses transforming growth factor β -induced profibrotic responses in lung fibroblasts		
Publication Status	<input type="checkbox"/> Published	<input checked="" type="checkbox"/> Accepted for Publication	<input type="checkbox"/> Published and Unsubmitted work written in script style
Publication Details	Fukihara J, Maiolo S, Kovac JF, Sakamoto K, Wakahara K, Hashimoto N, Reynolds PN. Overexpression of bone morphogenetic protein type 2 suppresses transforming growth factor β -induced profibrotic responses in lung fibroblasts.		

Principal Author

Name of Principal Author (Candidate)	Jun Fukihara		
Contribution to the Paper	Designed the study, collected the data, performed statistical analysis, interpreted the results, drafted, and revised the manuscript.		
Overall percentage (%)	80%		
Certification:	This paper reports on original research I conducted during the period of my Higher Degree by Research candidature and is not subject to any obligations or contractual agreements with a third party. I am the primary author of this paper.		
Signature		Date	//2021

Co-Author Contributions

By signing the Statement of Authorship, each author certifies that:

- the candidate's stated contribution to the publication is accurate (as detailed above);
- permission is granted for the candidate to include the publication in the thesis; and
- the sum of all co-author contributions is equal to 100% less the candidate's stated contribution.

Name of Co-Author	Suzanne Maiolo		
Contribution to the Paper	Collected the data and supported the experiments.		
Signature		Date	

Name of Co-Author	Jessica F Kovac		
Contribution to the Paper	Collected the data, supported the experiments, and edited the manuscript.		
Signature		Date	

Please cut and paste additional co-author panels here as required.

Name of Co-Author	Koji Sakamoto		
Contribution to the Paper	Supported animal model creation and edited the manuscript.		
Signature		Date	

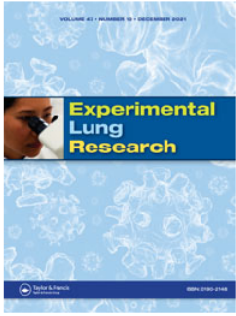
Name of Co-Author	Keiko Wakahara		
Contribution to the Paper	Interpreted the results and edited the manuscript.		
Signature		Date	

Name of Co-Author	Naozumi Hashimoto		
Contribution to the Paper	Supported study designation, interpreted the results, and edited the manuscript.		
Signature		Date	

Name of Co-Author	Paul N Reynolds		
Contribution to the Paper	Got the grant for this study, designed the study, interpreted the results, and edited the manuscript.		
Signature		Date	

Name of Co-Author			
Contribution to the Paper			
Signature		Date	

Name of Co-Author			
Contribution to the Paper			
Signature		Date	




Overexpression of bone morphogenetic protein receptor type 2 suppresses transforming growth factor β -induced profibrotic responses in lung fibroblasts

Jun Fukihara, Suzanne Maiolo, Jessica Kovac, Koji Sakamoto, Keiko Wakahara, Naozumi Hashimoto & Paul N. Reynolds

To cite this article: Jun Fukihara, Suzanne Maiolo, Jessica Kovac, Koji Sakamoto, Keiko Wakahara, Naozumi Hashimoto & Paul N. Reynolds (2022): Overexpression of bone morphogenetic protein receptor type 2 suppresses transforming growth factor β -induced profibrotic responses in lung fibroblasts, *Experimental Lung Research*, DOI: [10.1080/01902148.2021.2024301](https://doi.org/10.1080/01902148.2021.2024301)

To link to this article: <https://doi.org/10.1080/01902148.2021.2024301>

 View supplementary material [↗](#)

 Published online: 17 Jan 2022.

 Submit your article to this journal [↗](#)

 View related articles [↗](#)

 View Crossmark data [↗](#)



Overexpression of bone morphogenetic protein receptor type 2 suppresses transforming growth factor β -induced profibrotic responses in lung fibroblasts

Jun Fukihara^{a,b}, Suzanne Maiolo^b, Jessica Kovac^b, Koji Sakamoto^a, Keiko Wakahara^a, Naozumi Hashimoto^a and Paul N. Reynolds^{b,c}

^aDepartment of Respiratory Medicine, Nagoya University Graduate School of Medicine, Nagoya, Aichi, Japan; ^bAdelaide Medical School, University of Adelaide, Adelaide, South Australia, Australia; ^cDepartment of Thoracic Medicine, Royal Adelaide Hospital, Adelaide, South Australia, Australia

ABSTRACT

Purpose of the study: Idiopathic pulmonary fibrosis (IPF) is a progressive disease with a poor prognosis. As the efficacy of currently available antifibrotics is limited, development of new therapies is warranted. Transforming growth factor (TGF)- β plays a central role in the pathogenesis of IPF through mechanisms such as promoting the production of extracellular matrix by fibroblasts. Conversely, bone morphogenetic proteins (BMPs) are known to be antifibrotic and may counterbalance TGF- β signaling via BMP receptor type 2 (BMPR2). However, little is known about the expression status of BMPR2 and its function in pulmonary fibrosis, and manipulation of BMPR2 expression has never been attempted. In this study, we aimed at evaluating the effectiveness of BMPR2 upregulation for modulating the imbalance of the TGF- β /BMP axis and reduce the profibrotic changes in lung fibroblasts.

Materials and Methods: We investigated BMPR2 expression in pulmonary fibrosis and TGF- β /BMP signaling in lung fibroblasts. Then we evaluated the impact of BMPR2 upregulation using adenoviral transduction on TGF- β -induced Smad2/3 phosphorylation and fibronectin production in lung fibroblasts.

Results: BMPR2 was distributed in airway epithelium and alveolar walls in rat lungs. BMPR2 expression was decreased in fibrotic lesions in the lungs of rats with bleomycin-induced pulmonary fibrosis and in human lung fibroblasts (HLFs) stimulated with TGF- β . Although Smad2/3 phosphorylation and fibronectin production were not suppressed solely by BMPs, phosphorylated Smad2/3 was decreased in BMPR2-transduced cells even without BMP stimulation. Fibronectin was decreased only when BMPR2-transduced HLFs were stimulated with BMP7 (but not BMP4). Similar results were also observed in IPF patient HLFs and rat lung fibroblasts.

Conclusions: BMPR2 expression was reduced in fibrotic lungs and lung fibroblasts stimulated with TGF- β . BMPR2 transduction to lung fibroblasts reduced Smad2/3 phosphorylation, and reduced fibronectin production when treated with BMP7. Upregulation of BMPR2 may be a possible strategy for treating pulmonary fibrosis.



Abbreviations: AdBMPR2: AdCMVBMPR2myc (adenovirus encoding BMPR2 gene); AdTrack: control adenovirus (adenovirus encoding green fluorescent protein and luciferase gene); AEC: airway epithelial cell; ANOVA: analysis of variance; BMP: bone morphogenetic protein; BMPR2: bone morphogenetic protein receptor type 2; Ctrl: control; DMEM: Dulbecco's Modified Eagle's Medium; ECM: extracellular matrix; ERK: extracellular signal-regulated kinase; FCS: fetal calf serum; HLF: human lung fibroblast; IPF: idiopathic pulmonary fibrosis; MAPK: mitogen-activated protein kinase p-phosphorylated; PBS: phosphate-buffered saline; qRT-PCR: quantitative real time polymerase chain reaction; RLF: rat lung fibroblast; TGF- β : transforming growth factor- β


ARTICLE HISTORY

Received 9 November 2021
Accepted 27 December 2021

KEYWORDS

Bone morphogenetic protein; bone morphogenetic protein receptor type 2; fibroblasts; pulmonary fibrosis; transforming growth factor- β

CONTACT Paul N. Reynolds  paul.reynolds@adelaide.edu.au  Lung Research Laboratory, Adelaide Health and Medical Sciences North Terrace, Adelaide, South Australia 5000, Australia.

 Supplemental data for this article can be accessed online at <http://dx.doi.org/10.1080/01902148.2021.2024301>

© 2022 Taylor & Francis Group, LLC

Introduction

Idiopathic pulmonary fibrosis (IPF) is a chronic and fibrotic pulmonary disease with a median survival time of 3–5 years.¹ Diffuse fibrosis in alveolar walls causes lung stiffness and reduced oxygen diffusion into pulmonary blood vessels. In 2014, phase 3 randomized controlled trials of two antifibrotics, pirfenidone and nintedanib,^{2,3} showed positive effects on the suppression of pulmonary function decline, however, both drugs cause major adverse events and only slow down disease progression, with limited effect on prognosis. Though these drugs are recommended in the guidelines for treatment of IPF,⁴ given the high medical need, more effective therapeutic options are still needed.

Transforming growth factor- β (TGF- β) plays a central profibrotic role in the pathogenesis of pulmonary fibrosis. It promotes migration of fibrocytes to the injured lung tissue, transdifferentiation of epithelial or endothelial cells into mesenchymal cells, proliferation of fibroblasts and their differentiation into myofibroblasts and generation and accumulation of extracellular matrix (ECM), such as fibronectin, by lung fibroblasts.^{5,6} These profibrotic effects are mainly mediated by activation of the Smad2/3 signaling pathway, where TGF- β binds to its membrane bound receptors to signal the upregulation of phosphorylated (p-)Smad2/3.⁷ Some Smad-independent (non-Smad) pathways such as the mitogen-activated protein kinase (MAPK) pathway also play important roles in regulating profibrotic changes.^{8–11} On the contrary, the bone morphogenetic proteins (BMPs) have been demonstrated to have antifibrotic effects. BMPs (including BMP-7 and -4) signal the phosphorylation of Smad1/5/9 by binding to a key membrane bound receptor, BMP receptor type 2 (BMPR2). P-Smad1/5/9 promotes antifibrotic effects by inhibiting fibrogenic gene expression and counterbalancing TGF- β mediated Smad2/3 phosphorylation. Imbalances in profibrotic and antifibrotic phenotypes induced by TGF- β /BMPs have been reported in some fibrotic diseases, such as pulmonary arterial hypertension,¹² renal fibrosis,^{13,14} and liver cirrhosis.^{15,16}

Regarding pulmonary fibrosis, administration of BMPs or suppression of intrinsic BMP inhibitors could attenuate fibrosis in animal

models,^{17–23} but little is known about the role of BMPR2. The expression status of BMPR2 and its function in pulmonary fibrosis require further investigation,^{24,25} and manipulation of BMPR2 expression has never been attempted for treatment of pulmonary fibrosis. Regardless of the baseline expression levels, BMPR2 upregulation may modulate the imbalance of the TGF- β /BMP axis and attenuate fibrosis.

In this study, we hypothesized that upregulation of BMPR2 can suppress TGF- β -induced ECM production from lung fibroblasts by modulating the imbalance of the TGF- β /BMP axis. We have evaluated BMPR2 expression status in a rat model of pulmonary fibrosis and in lung fibroblasts from rats and humans, and the responsiveness of lung fibroblasts to TGF- β /BMP stimuli. We then assessed the effect of BMPR2 upregulation using a BMPR2-encoding adenovirus on the TGF- β -induced profibrotic changes in lung fibroblasts.

Materials and methods

Animals and creation of bleomycin-induced pulmonary fibrosis model

Male Fischer 344 rats were used for all animal experiments throughout this study. The protocols for animal experiments were approved by the University of South Australia Animal Ethics Committee (U18-19) and undertaken as per the guidelines established by the “Australian Code of Practice for the Care and Use of Animals for Scientific Purposes”. Animals were housed in the University of South Australia Core Animal Facility (Adelaide, SA, Australia).

To create the bleomycin-induced pulmonary fibrosis model, rats at 8–10 weeks were administered bleomycin sulfate (Cayman Chemical, Ann Arbor, MI, USA) intratracheally (1.5 mg/kg in a total volume of 2 mL/kg saline), or the same volume of saline on day 0 and were held in normal circumstance. Their lungs were harvested on day 14 for further analysis.

Cell lines and provided primary cells

HEK-293 cells were used for adenovirus amplification and transduction studies. These cells were

grown in Dulbecco's Modified Eagle's Medium (DMEM) with HEPES buffer with Ham's F12 Nutrient Mixture (50:50) (Gibco, Grand Island, NY, USA), 10% fetal calf serum (FCS) (Lonza, Basel, Switzerland), L-glutamine (2 mM) (Cosmo Bio, Tokyo, Japan), sodium pyruvate (1 mM) (Gibco), penicillin (62.5 µg/ml) and streptomycin (100 µg/mL) (Gibco, Grand Island, NY, USA). Human lung fibroblasts (HLFs) isolated from healthy people (n=8) and IPF patients (n=4) were provided by Dr. D. Knight (University of Newcastle, Callaghan, NSW, Australia) and Dr. M. Rojas (University of Pittsburgh, Pittsburgh, PA, USA). HLFs were grown in DMEM with 10% FCS. All cells were grown in a 5% CO₂-atmosphere at 37°C.

Rat lung fibroblast isolation

Rat lung fibroblasts (RLFs) were isolated from male Fischer 344 rats that were humanely killed using CO₂ asphyxiation. Their lungs were collected into DMEM and immediately stored on ice. They were then minced into very small pieces and incubated at 37°C with collagenase type III (30 mg) and DNase type I (750 µg) (Worthington Biochemical, Lakewood, NJ, USA) in a volume of 30 mL media for 60–80 min with gentle shaking. The cell suspension was filtered through a 70-µm cell strainer. Cells were then incubated in red cell lysis buffer (150 mM NH₄Cl, 10 mM KHCO₃, 0.1 mM Na-EDTA, pH 7.2) for 5 min. After pelleting, cells were then resuspended and seeded in DMEM with 15% FCS. After 4 days, the media was changed to DMEM with 10% FCS. After 2 weeks, cells were passaged and used for further experiments at passage 1–4.

Viral construction and BMPR2 transduction

AdCMVBMPR2myc (adenovirus encoding BMPR2; AdBMPR2 henceforth), a replication-incompetent serotype 5 adenoviral vector, and control adenovirus (AdTrack) containing the cytomegalovirus promoter driving expression of reporter genes luciferase and green fluorescent protein were prepared as previously described.²⁶ Viral titer was determined by 50% tissue culture infectious dose assay using HEK-293 cells and particle titer by optical density at 260 nm.

Induction of profibrotic changes and transduction of BMPR2 in HLFs/RLFs

When HLFs/RLFs reached 70–80% confluency, the culture media was replaced with media containing 2 ng/mL of recombinant human TGF-β1 (Pepro Tech, Rocky Hill, NJ, USA) and/or 200 ng/mL of recombinant human BMP4 (Pepro Tech) or 300 ng/mL of recombinant human BMP7 (Pepro Tech). The dosages of BMPs were determined through dose-setting studies in order to maximize the levels of p-Smad1/5/9 induced in lung fibroblasts (Figure S2A, B). For evaluating production of ECM proteins, after 3 days of incubation with growth factors, cells were harvested and processed for Western blot and quantitative real time polymerase chain reaction (qRT-PCR). To evaluate phosphorylation of the Smad/non-Smad signaling proteins, serum starvation for 24 h was performed prior to the incubation with TGF-β and/or BMP7 or 4 at the same concentrations as above for 1 h. After the treatment, cells were harvested for Western blot.

For the adenoviral transduction, when cells had reached 70–80% confluency, culture media was replaced with transduction media containing 100 pfu/mL of either AdTrack or AdBMPR2. After incubation for 48 h, the transduction media was removed and cells were washed with phosphate-buffered saline (PBS). The cells were then incubated with TGF-β1 and/or BMP7 or 4 as described above.

Hematoxylin-eosin and Masson's trichrome staining

The left lung lobes taken from rats were fixed with 10% formalin for 24 h and submitted to the Adelaide Medical School Histology Services (Adelaide, SA, Australia) for routine histological examination. Sections of 5 µm were heat mounted (58°C for 1 h) on coated glass slides (InstrumeC, Sandringham, VIC, Australia), deparaffinised with xylene and stained.

Immunohistochemical analysis

Formalin-fixed paraffin embedded lung sections were created from human/rat lung specimens and deparaffinised. Sections were first placed in

preheated Target Retrieval Solution (Dako Denmark A/S, Glostrup, Denmark) at 97°C for 30 min. Once cooled, the slides were immersed in 3% H₂O₂ in PBS for endogenous peroxidase block, blocked with 5% horse serum (Vector Laboratories, Burlingame, CA, USA) for 1 h, and then incubated overnight at 4°C with mouse anti-BMP2 antibody (BD Biosciences, San Jose, CA, USA) diluted 1:200 in 1.5% horse serum. The following day, slides were washed and blocked with 5% horse serum for 1 h again followed by incubation with biotinylated secondary antibody (Vector Laboratories) for 5 min. After performing a second endogenous peroxidase block with 3% H₂O₂, the slides were treated using ready-to-use Streptavidin/Peroxidase complex (Vector Laboratories) for 30 min and diaminobenzidine color detection systems (Vector Laboratories) according to the manufacturer's protocol. Sections were counterstained with Hematoxylin QS (Vector Laboratories), dehydrated with 100% ethanol, cleared in xylene, and mounted with DePeX (BDH Laboratory Supplies, Poole, UK). The slides were scanned using a NanoZoomer high resolution, high speed slide scanner (Hamamatsu Photonics, Hamamatsu, Japan). A representative section from a rat with pulmonary fibrosis was analyzed using ImageJ.²⁷ The whole section was split into 20 subsections, and the extent of BMP2 staining in preserved lung areas and fibrotic lesions was evaluated in each subsection.

Western blot

For cell cultures, samples were lysed with ice cold PierceTM RIPA buffer (Thermo ScientificTM, Waltham, MA, USA) containing proteinase inhibitor (cOmpleteTM Mini, Sigma-Aldrich, St. Louis, MO, USA) and phosphatase inhibitor cocktail (HaltTM, Thermo ScientificTM). Long's lysis buffer was used instead of RIPA buffer for detection of baseline non-transduced BMP2,²⁸ as baseline BMP2 was difficult to detect in samples lysed with RIPA buffer (data not shown). For rat lung protein extraction, after CO₂ asphyxiation the right lung lobes were collected and snap frozen. Lung samples were homogenized and lysed with Long's lysis buffer containing proteinase inhibitor and phosphatase

inhibitor as described above. Protein quantification was performed using the DC protein assay kit (Bio-Rad Laboratories, Hercules, CA, USA). Protein samples (15–30 µg) were loaded on 10% polyacrylamide/SDS gels for electrophoresis and transferred to a 0.2 µm Nitrocellulose membrane (Bio-Rad Laboratories) using the Trans-Blot Turbo Transfer System (Bio-Rad Laboratories). Membranes were blocked with Odyssey Blocking Buffer (LI-COR Biosciences, Lincoln, NE, USA) for 1 h at room temperature. The membranes were then incubated overnight at 4°C with primary antibodies in Odyssey Blocking Buffer: rabbit anti-p-Smad1/5/9, p-Smad2/3, extracellular signal-regulated kinase (ERK), p-ERK, p38 MAPK, p-p38 MAPK, Akt and p-Akt (1:1000); rabbit anti-β-actin (1:2000) (Cell Signaling Technology, Danvers, MA, USA); rabbit anti-fibronectin (1:250) (Proteintech, Rosemont, IL, USA) and mouse anti-BMP2 (1:250) (BD Biosciences). The secondary antibodies used were goat anti-rabbit, donkey anti-rabbit and goat anti-mouse (1:20000) (LI-COR Biosciences) and incubated for 1 h at room temperature. Membrane scanning was performed on the Odyssey Imaging System (LI-COR Biosciences) and data analysis was carried out using Image Studio Lite version 5.2 (LI-COR Biosciences). Values of each sample were calculated as the integrated intensity counts, which reflect the relative fluorescence of each band, using the intensity of β-actin as a reference.

RNA extraction and qRT-PCR

RNA was isolated from cultured cells or lung homogenates using mirVanaTM miRNA Isolation Kit (InvitrogenTM) according to the manufacturer's instructions. The purity and quantity of RNA were assessed using the NanoDropTM One/One^C UV-VS Spectrophotometer (Thermo ScientificTM). The GoTaqTM 1-Step RT-qPCR System (Promega, Madison, WI, USA) was used for preparation of cDNA and qRT-PCR reaction. Each reaction contained 50 ng of total RNA in a volume of 14 µL. Reactions were performed on the CFX Connect Real Time PCR Detection System (Bio-Rad Laboratories) with the following conditions:

reverse transcription at 45 °C for 15 min, reverse transcript inactivation and hot-start activation at 95 °C for 10 min, followed by quantitative PCR of 40 cycles of 95 °C for 10 s and 60 °C for 30 s. All assays were run in duplicate. The C_q is defined as the PCR cycle at which the fluorescent signal of the reporter dye crosses an arbitrarily placed threshold in the exponential phase. The sample with a C_q value over 40 or with a melt curve with a different peak from that of other samples treated with the same primer was considered as invalid and was not useful for further analysis. The sequences of the primer pairs are summarized in Table 1. Values of each sample were expressed as $2^{-\Delta\Delta C_q}$ using 18S as a house-keeping gene and the ΔC_q value of one of the control samples as a reference.

Statistical analysis

Data are expressed as mean \pm standard error. For the experiments using samples from multiple individuals, results are expressed as the relative values using the average value of control samples as a reference. For replicated experiments using samples from a specific cell line, treatment results are expressed as relative values to normalized control samples in each experiment (i.e., there are no error bars for control data as the normalized value is 1). One-way analysis of variance (ANOVA) or student's *t*-test was used for inter-group analysis. When the *F* value indicated significance, the Sidak's test was carried out for multiple comparisons. A paired *t*-test was used to compare the rate of BMPR2 expression between preserved lung areas and fibrotic lesions. A value of $p < 0.05$ was considered to be statistically significant. All statistical analyses were conducted

using GraphPad Prism ver.9 (GraphPad Software, San Diego, CA, USA).

Results

BMPR2 expression was decreased in fibrotic lungs and lung fibroblasts stimulated with TGF- β

First, we have evaluated BMPR2 expression status *in vivo* using a rat model of pulmonary fibrosis. Lung sections from rats with bleomycin-induced pulmonary fibrosis developed fibrotic lesions. The lesions consisted of proliferated fibroblasts that disrupted normal lung structures, mainly in the area surrounding the airways (Figure 1A). Immunohistochemistry for healthy control rat lung sections showed that BMPR2 was distributed mainly in airway epithelial cells (AECs), and also all through the alveolar interstitium, mainly composed by microvascular endothelial cells (Figure 1B). Conversely, in lung sections with bleomycin-induced pulmonary fibrosis, BMPR2 staining was light in the fibrotic lesions compared with the preserved lung areas (Figure 1B). Quantification of BMPR2 staining density demonstrated BMPR2 expression was low in fibrotic lesions compared to the preserved lung areas (Figure 1C). Furthermore, in protein and mRNA analysis, BMPR2 expression levels were significantly lower in the lungs from pulmonary fibrosis model rats than in the normal rat lungs (Figure 1D, E), suggesting that BMPR2 expression in RLFs forming fibrotic lesions is lower than in other lung structural cell types.

The expression levels of BMPR2 in lung fibroblasts were then studied and compared between control cells and cells stimulated with TGF- β , in view of the known role of TGF- β in driving fibrosis. In terms of HLFs, BMPR2 levels did not

Table 1. Quantitative real time polymerase chain reaction primer sequences.

Spece	Gene		Primer sequence (5'-3')	Product length (bp)
Human	BMPR2	F	CCCTCCTGATTCTTGGCTGG	125
		R	AGCCGTCTTGATTCTGCGA	
	COL1A1	F	AAGGGACACAGAGGTTCAGT	186
		R	ACCATCATTTCACAGCA	
	18S	F	CAGCCACCCGAGATTGAGCA	252
		R	TAGTAGCGACGGGCGGTGTG	
Rat	bmpr2	F	AGTTTGGGGAACCGAGGCAC	238
		R	AAGCAGGAGGGCAAAGAAAAGA	
	18s	F	GCAATATTCCCATGAACG	123
		R	GGCCTCACTAAACCATCCAA	

F: forward; R: reverse.

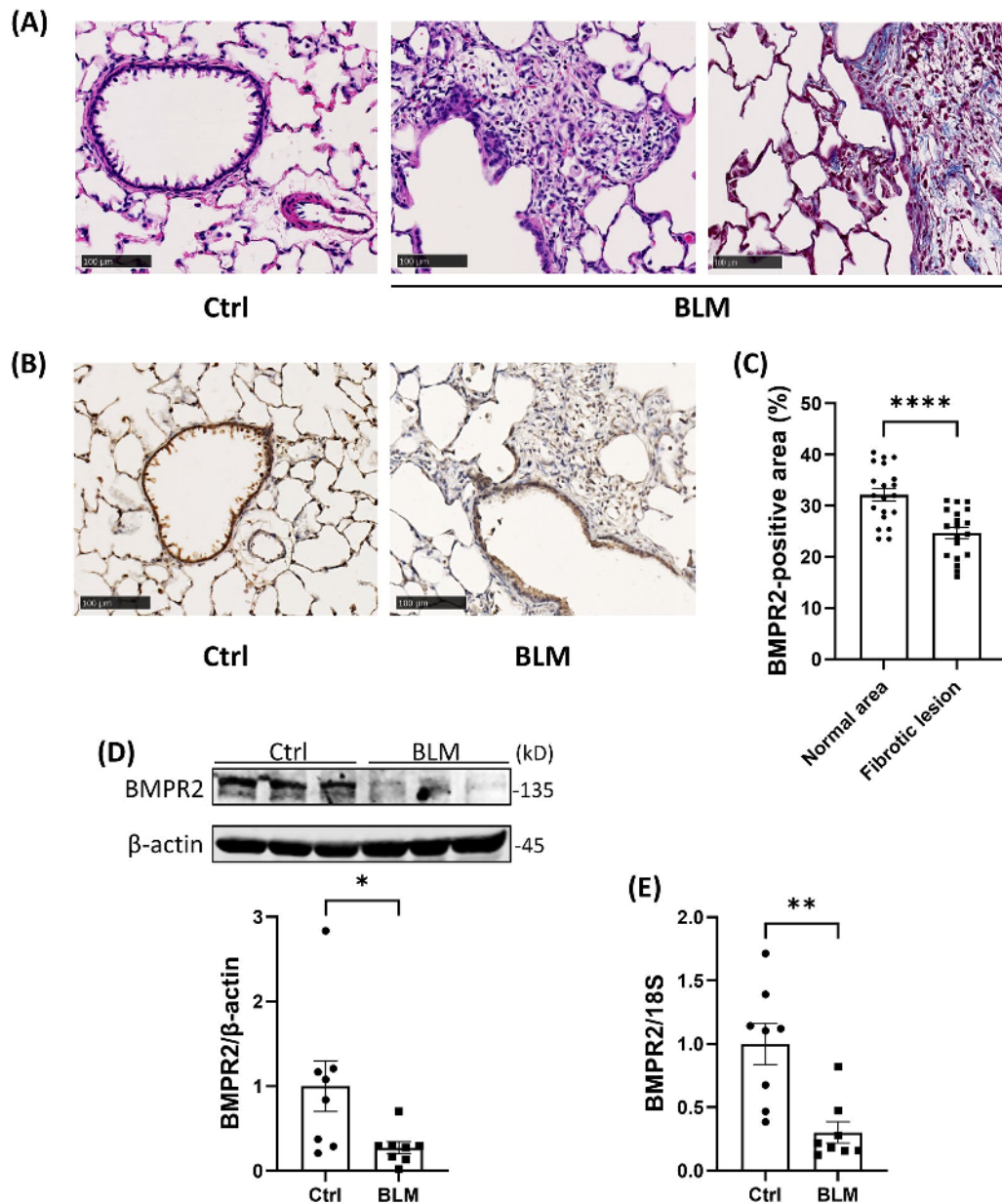


Figure 1. BMPR2 was decreased in rat lungs with bleomycin-induced pulmonary fibrosis. (A) Rat lungs with bleomycin-induced pulmonary fibrosis demonstrated fibrotic lesions in the surrounding areas of airways disrupting normal lung structures (Hematoxylin-Eosin (left and centre) and Masson's Trichrome (right)). (B) Immunohistochemistry of BMPR2 in control rat lungs showed localization of BMPR2 in airway epithelial cells and alveolar walls, whilst lungs from the bleomycin-induced pulmonary fibrosis model showed reduced expression of BMPR2. (C) BMPR2 signal quantification of the immunohistochemistry slide showed significantly decreased BMPR2 in fibrotic lesions compared with preserved lung areas. (D) BMPR2 was decreased in rat lungs from pulmonary fibrosis (n=8) compared with those from control rats (n=8) determined by Western blot, and (E) by qRT-PCR. Values are presented as mean ± SE and analysed by Student's t-test (C–E). BLM, bleomycin; Ctrl, control; * $p < 0.05$; ** $p < 0.01$; **** $p < 0.0001$.

differ *ex vivo* between healthy controls and IPF patients (Figure 2A, B). However, BMPR2 protein expression was significantly decreased by TGF- β stimulation in HLFs from both healthy control ($p < 0.001$) and IPF patients ($p < 0.05$) (Figure 2C), while mRNA levels of BMPR2 were not altered by TGF- β (Figure 2D). In RLFs, both protein and

mRNA of BMPR2 were significantly decreased when treated with TGF- β (Figure 2E, F). Western blot images of BMPR2 bands together with positive controls (BMPR2 transduced HLFs) are presented in Figure S1.

In summary, BMPR2 was decreased in fibrotic rat lungs, probably due to the destruction of

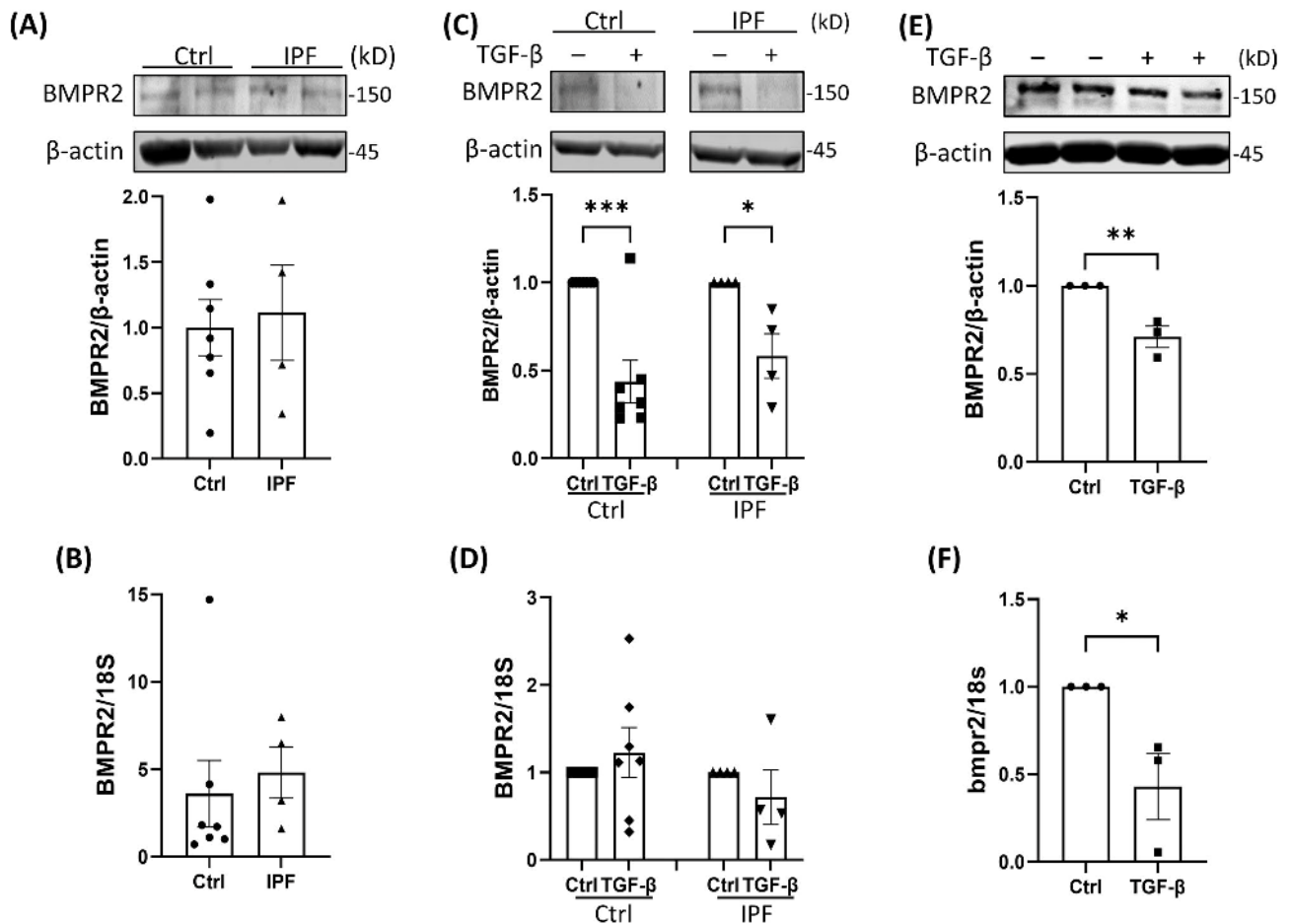


Figure 2. TGF- β reduced BMPR2 expression in lung fibroblasts. (A) BMPR2 expression was not different between HLFs from healthy controls (n=7) and IPF patients (n=4), determined by Western blot and (B) by qRT-PCR. (C) BMPR2 expression was significantly decreased by TGF- β stimulation in HLFs from both healthy controls (n=7) and IPF patients (n=4). (D) BMPR2 mRNA levels were not altered by TGF- β stimulation in HLFs, determined by qRT-PCR. (E) BMPR2 expression was significantly decreased by TGF- β stimulation in RLFs (n=3), determined by Western blot and (F) by qRT-PCR. Values are presented as mean \pm SE and analysed by Student's t-test (A, B, E, F) or one-way ANOVA followed by Sidak's multiple comparison test (C, D). Values of (C-F) indicate the ratios to the values of the cells without TGF- β stimulation. * $p < 0.05$; ** $p < 0.01$; *** $p < 0.001$.

BMPR2-expressing normal airway structure and proliferation of lung fibroblasts. Furthermore, BMPR2 was decreased by fibrogenic stimuli in lung fibroblasts.

The sensitivity to TGF- β and BMPs did not differ between HLFs from healthy controls and IPF patients

For elucidating the baseline sensitivity of lung fibroblasts to TGF- β and BMPs, we stimulated the cells with these growth factors. TGF- β sensitivity was assessed by the levels of p-Smad2/3 and fibronectin production and BMP reactivity was assessed by p-Smad1/5/9 production. Time course analyses showed phosphorylation of

Smad2/3 by TGF- β and Smad1/5/9 by BMPs were increased after incubation for 30–60 min (Figure 3A, B and S2C–F) and consequently the incubation period for all following Smad phosphorylation experiments was 1 h. TGF- β -induced phosphorylation of Smad2/3 in HLFs were compared to unstimulated HLFs. The extent of the responsiveness did not differ between the healthy control and IPF patient HLFs (Figure 3C). The extent of fibronectin production was not significantly different between HLFs from healthy controls and IPF patients at baseline or after TGF- β treatment (Figure 3D, E). When stimulated with BMP7 or 4, phosphorylation of Smad1/5/9 was significantly increased, while the extent of the responsiveness did not differ between HLFs from healthy controls and IPF patients (Figure 3F, G).

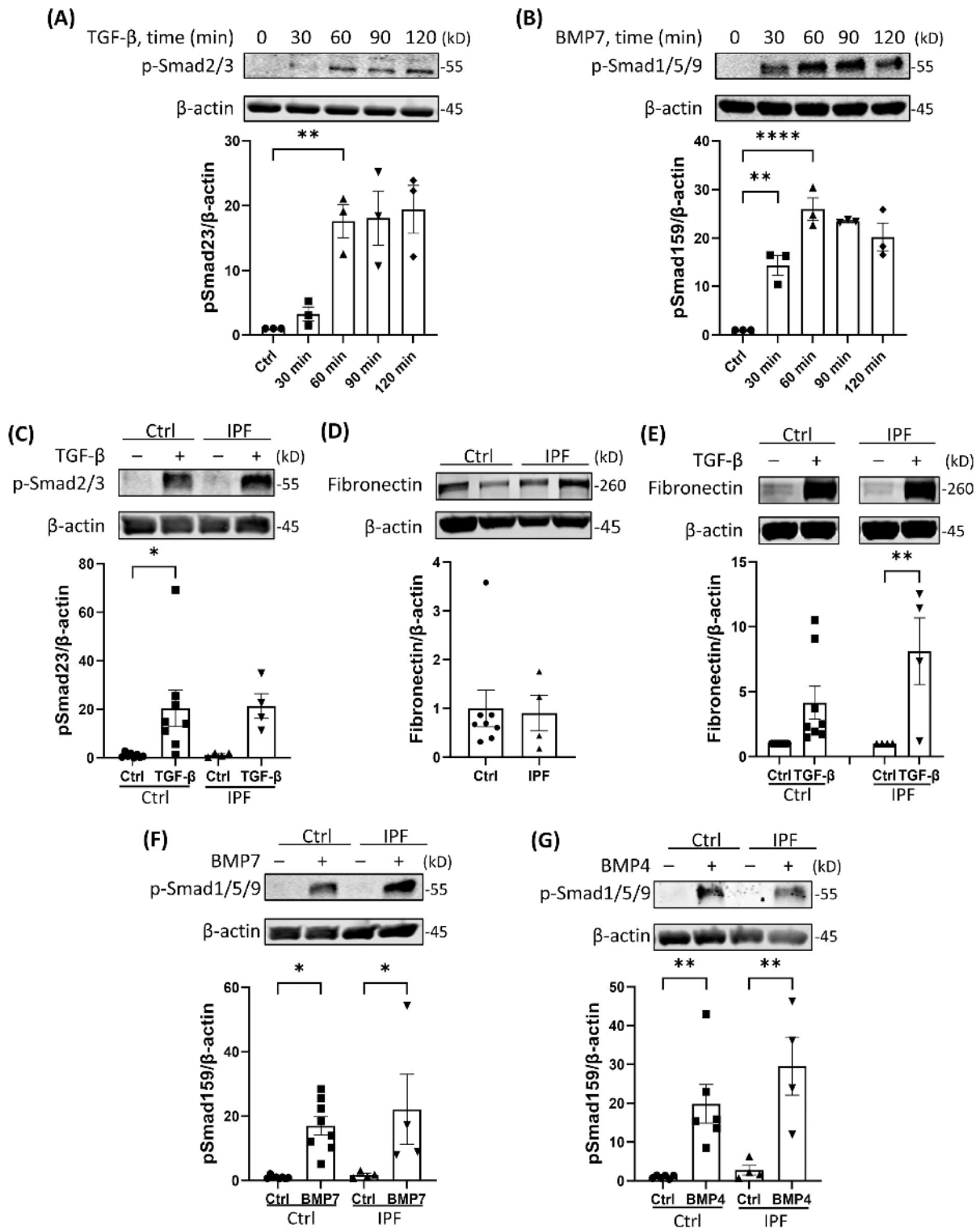


Figure 3. Reactions of HLFs to TGF- β or BMPs stimulation is not different between the cells from healthy controls and IPF patients. (A) Smad2/3 phosphorylation was induced by TGF- β stimulation for more than 60 min in HLFs, determined by Western blot (n=3). (B) Smad1/5/9 phosphorylation was induced by BMP7 stimulation for more than 30 min, determined by Western blot (n=3). (C) Smad2/3 phosphorylation was induced by TGF- β in HLFs from healthy controls and IPF patients, determined by Western blot. (D) Fibronectin expression at baseline was similar in HLFs from healthy controls and IPF patients. (E) Fibronectin was induced by TGF- β in HLFs from healthy controls and IPF patients. (F, G) Smad1/5/9 phosphorylation was induced by BMP7 and BMP4 in both HLFs from healthy controls and IPF patients. The samples from 8 healthy controls and 4 IPF patients were used for (C–F) and from 7 healthy controls and 4 IPF patients were for (G). Values are presented as mean \pm SE and analysed by one-way ANOVA followed by Sidak's multiple comparison test (A–C, E–G), or Student's t-test (D). Values of (A, B, E) indicate the ratios to the values of the cells not treated with TGF- β or BMPs. * $p < 0.05$; ** $p < 0.01$; **** $p < 0.0001$.

In summary, the sensitivity of HLFs to TGF- β and BMP stimuli was not significantly different between the cells from healthy controls and IPF patients, with upregulation of Smads and fibronectin observed as expected. This is consistent with previous reports showing that HLFs from healthy controls and IPF patients do not differ from each other in their responsiveness to TGF- β stimuli.^{29–31}

Stimulation with BMPs could not suppress TGF- β -induced profibrotic changes in lung fibroblasts

Next, we stimulated lung fibroblasts with both TGF- β and BMPs to evaluate whether BMPs may suppress the profibrotic changes induced by TGF- β . BMP7 stimulation of healthy control and IPF patient HLFs and RLFs did not reduce TGF- β -induced Smad2/3 phosphorylation, despite a concurrent increase of p-Smad1/5/9 (Figure 4A, B). Rather, though unexpectedly, BMP7 induced phosphorylation of Smad2/3. BMP7 stimulation also did not suppress the production of fibronectin and *COL1A1* mRNA induced by TGF- β (Figure 4C, D, S4A). Similarly, BMP4 stimulation did not reduce p-Smad2/3 and fibronectin despite an increase in p-Smad1/5/9 (Figure S3).

Therefore, unlike hypothesized, BMPs were not sufficient for suppressing profibrotic changes induced by TGF- β in lung fibroblasts. On the other hand, p-Smad2/3 was unexpectedly increased by BMP7 regardless of the origins of lung fibroblasts.

BMPR2 transduction using adenovirus suppressed the TGF- β -induced phosphorylation of Smad2/3 in lung fibroblasts

As BMPs could not suppress TGF- β -induced profibrotic changes in lung fibroblasts, we then transduced BMPR2 into the cells to enhance the antifibrotic role of BMPs. BMPR2 was strongly expressed both in HLFs (Figure 5A) and RLFs (Figure S5A) after infection with AdBMPR2. BMPR2 transduction of HLFs (Figure 5C) and RLFs (Figure S5E) that were stimulated with TGF- β suppressed phosphorylation of Smad2/3, even in the absence of supplemental BMP ligands

for activating the transduced receptor. On the other hand, the increase in phosphorylation of Smad1/5/9 with BMP7 or 4 was unaltered by BMPR2 transduction in HLFs (Figure 5B, S5C) and RLFs (Figure S5B, D).

Co-stimulation of BMPR2-transduced cells with TGF- β and BMP7 or 4 did not demonstrate additional efficacy for suppressing phosphorylation of Smad2/3 compared with the cells stimulated only with TGF- β , which was consistently observed in HLFs from healthy controls and IPF patients, and RLFs (Figure 5D–F, S6A–C).

In summary, BMPR2 transduction was effective for suppressing TGF- β -induced Smad2/3 phosphorylation, even when BMP ligands were not co-administered. Unexpectedly, p-Smad1/5/9 levels were unchanged by BMPR2 transduction, therefore, the suppression of p-Smad2/3 by BMPR2 might be induced independently from Smad1/5/9 phosphorylation (Table 2).

BMPR2 transduction plus stimulation with BMP7, but not BMP4, suppressed the TGF- β -induced production of fibronectin in lung fibroblasts

The effect of BMPR2 transduction on fibronectin production induced by TGF- β was then evaluated. BMP7 suppressed the TGF- β -induced production of fibronectin in lung fibroblasts transduced with BMPR2, which was consistently observed in HLFs from healthy controls and IPF patients, and RLFs (Figure 6A–C), while fibronectin production was not suppressed by BMPR2 transduction only. Though statistically insignificant, *COL1A1* mRNA also showed a similar trend in HLFs from healthy controls (Figure S4B). On the other hand, when stimulated with BMP4, the TGF- β -induced production of fibronectin was not suppressed, even in BMPR2-transduced cells (Figure 6D–F).

Therefore, despite a reduction in p-Smad2/3 seen in BMPR2-transduced cells without BMPs, BMP7 stimulus (but not BMP4) was necessary for suppressing TGF- β -induced fibronectin production. Given that the levels of p-Smad1/5/9 were not affected by BMPR2 transduction, fibronectin levels might be regulated independently of p-Smads (Table 2).

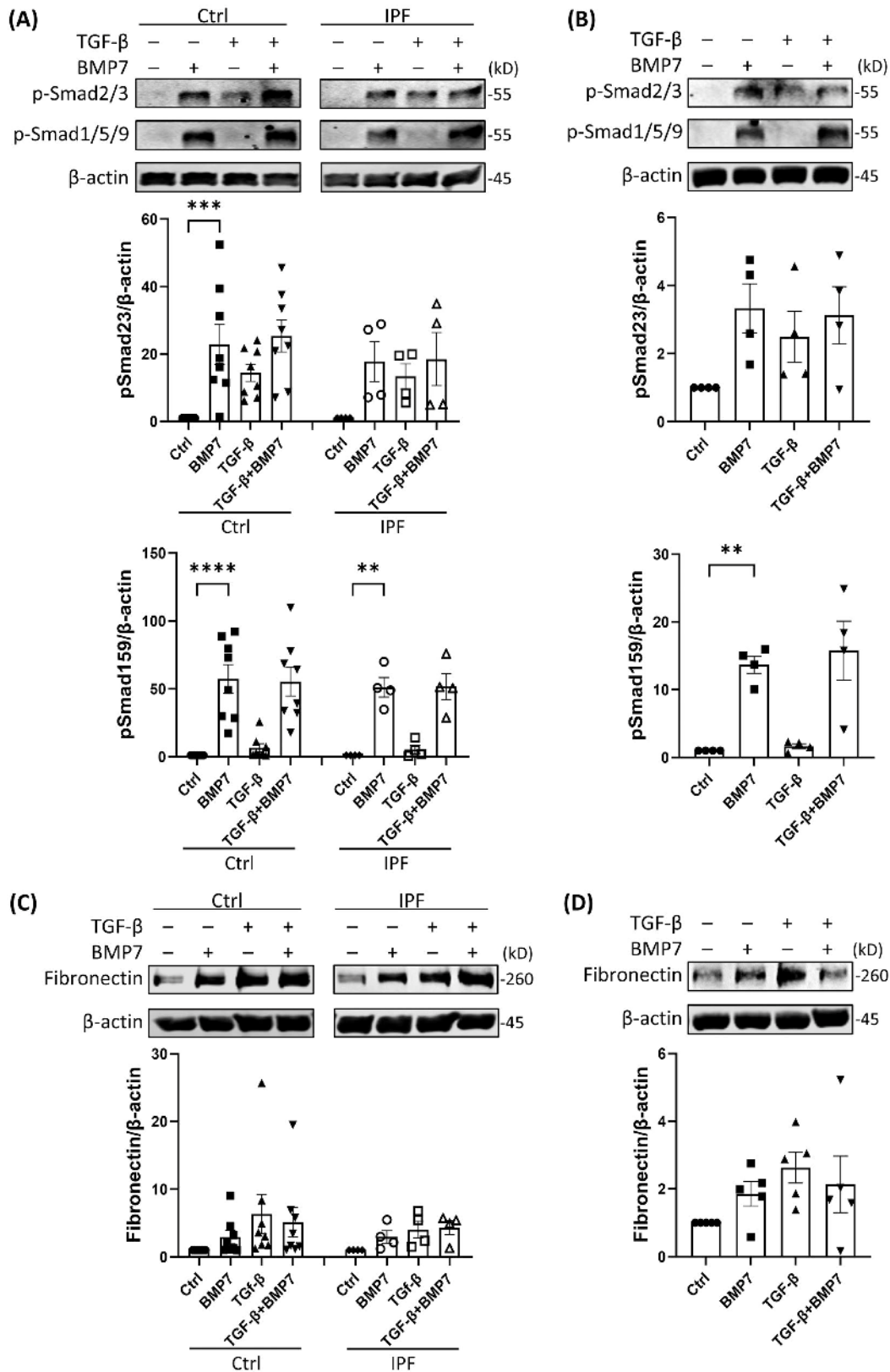


Figure 4. BMP7 did not suppress the TGF-β-induced changes in HLFs. (A, C) TGF-β-induced Smad2/3 phosphorylation and fibronectin production were not suppressed by BMP7 in HLFs from both healthy controls (n=8) and IPF patients (n=4), determined by Western blot. (B, D) TGF-β-induced Smad2/3 phosphorylation and fibronectin production were not suppressed by BMP7 in RLFs (n = 3). Values are presented as mean ± SE and analysed by one-way ANOVA followed by Sidak's multiple comparison test. Values indicate the ratios to the values of the cells not stimulated with TGF-β and/or BMPs. ** $p < 0.01$; *** $p < 0.001$; **** $p < 0.0001$.

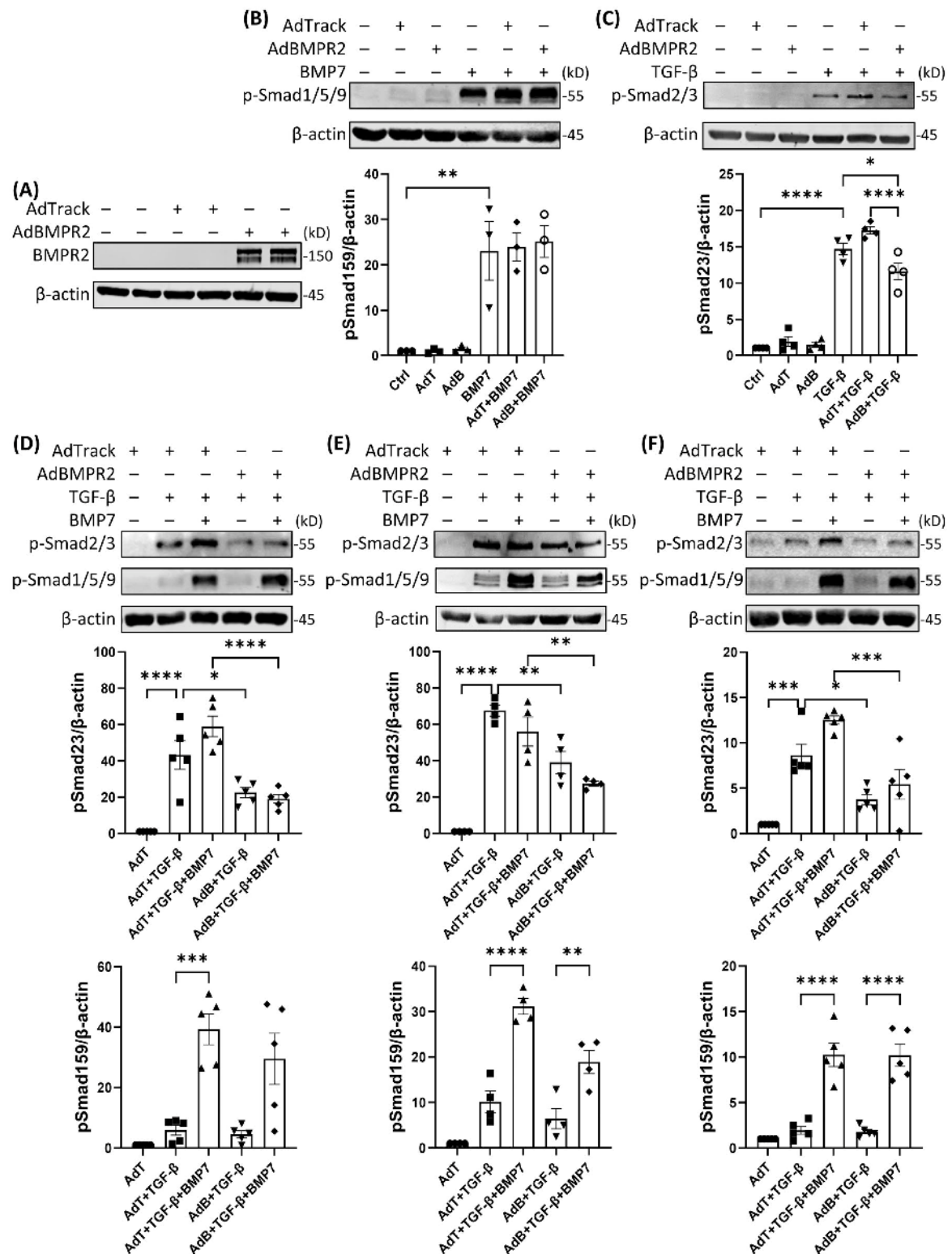


Figure 5. BMPR2 transduction using adenovirus suppressed TGF- β -induced Smad2/3 phosphorylation in lung fibroblasts. (A) BMPR2 was strongly expressed in HLFs from a healthy control infected with AdBMPR2. (B) BMPR2 transduction did not promote BMP7-induced Smad1/5/9 phosphorylation in HLFs from a healthy control, determined by Western blot ($n=3$). (C) BMPR2 transduction suppressed TGF- β -induced Smad2/3 phosphorylation even without stimulation with BMP ligands in HLFs from a healthy control ($n=4$). (D–F) BMPR2 transduction could suppress TGF- β -induced Smad2/3 phosphorylation regardless of the levels of p-Smad1/5/9 in (D) HLFs from a healthy control ($n=5$), (E) an IPF patient and (F) in RLFs ($n=5$). Values are presented as mean \pm SE and analysed by one-way ANOVA followed by Sidak's multiple comparison test. Values indicate the ratios to the values of the cells infected with AdTrack and not stimulated with TGF- β and/or BMPs. * $p < 0.05$; ** $p < 0.01$; *** $p < 0.005$; **** $p < 0.001$.

Table 2. Summary of findings and interpretations.

	p-Smad1/5/9	TGF- β -induced p-Smad2/3	TGF- β -induced Fibronectin	Interpretations
BMP7	Up	Unchanged (Up even without TGF- β)	Unchanged (slightly Up, though statistically insignificant)	p-Smad2/3 and fibronectin are regulated independently from p-Smad1/5/9
BMPR2 transduction	Unchanged	Down	Unchanged	p-Smad2/3 is regulated independently from p-Smad1/5/9. Fibronectin is regulated independently from p-Smad2/3.
BMPR2 + BMP7	Up (no significant additive effects of BMPR2)	Down (no significant additive effects of BMP7)	Down	
Interpretations	p-Smad1/5/9 is increased by BMP7, but BMPR2 transduction did not show an additive effect.	The direction of BMP7 effect changes depending on the amount of BMPR2. BMPR2 solely reduces p-Smad2/3, probably due to intrinsic BMPs or activins.	BMP7 shows antifibrotic effect only when BMPR2 is transduced.	BMPR2 transduction reduces p-Smad2/3, and BMPR2 + BMP7 reduces fibronectin, independently from p-Smads (probably via non-Smad pathways).

BMPR2 transduction showed trends for reducing phosphorylation of p38 MAPK in lung fibroblasts

Based on the results above, the antifibrotic effect of transduced BMPR2 was thought to be induced independently from Smad signaling (Table 2). So, we then evaluated the status of ERK, p38 MAPK and Akt signaling as some of the non-Smad pathways known to be related with fibrogenesis. The phosphorylation of p38 MAPK was decreased by BMPR2 transduction in HLFs and RLFs. This response was also observed with or without BMP stimulation (Figure S7), though this trend was not statistically significant. The reduced p-p38 MAPK patterns resembled the patterns observed for p-Smad2/3 in the BMPR2-transduced cells (Figure 5D–F, S6A–C). The phosphorylation of ERK and Akt did not show any correlations with the findings for p-Smad2/3 or fibronectin in the former experiments (data not shown).

Therefore, the p38 MAPK pathway may be associated with the suppression of Smad2/3 signaling observed in our BMPR2-transduction studies. However, as the trend is faint and statistically insignificant, we cannot make a firm conclusion from these results.

Discussion

In this study, we sought to investigate whether manipulation of BMPR2 signaling might counteract the profibrotic effects of TGF- β , as a potential target strategy for pulmonary fibrosis. We have

shown that BMPR2 expression was decreased in the lungs of rats with bleomycin-induced pulmonary fibrosis and in lung fibroblasts stimulated with TGF- β , highlighting the imbalance of profibrotic/antifibrotic regulation in the development of pulmonary fibrosis. Although BMP7 and 4 did not solely suppress TGF- β -induced Smad2/3 phosphorylation and fibronectin production in lung fibroblasts, BMPR2 overexpression could suppress Smad2/3 phosphorylation by itself and suppress fibronectin production in conjunction with BMP7 stimulation. The antifibrotic effects of BMPR2 overexpression may be acting via the BMPR2/non-Smad signaling pathways. To our knowledge, this is the first study attempting BMPR2 transduction of lung fibroblasts and evaluating its effect on TGF- β -induced profibrotic changes.

There are only a few studies to have evaluated the expression status and function of BMPR2 in pulmonary fibrosis or in profibrotic circumstances. Two reports have demonstrated that BMPR2 was decreased in the lungs from mice with bleomycin-induced pulmonary fibrosis and/or from IPF patients.^{24,25} Additionally Chen et al. revealed that BMPR2 was expressed broadly in the parenchyma of both lungs from IPF patients and a murine model, and decreased in fibrotic areas or remodeled pulmonary arterial walls.²⁴ Similarly to those reports, we have demonstrated that BMPR2 was decreased in the lungs from rats with bleomycin-induced pulmonary fibrosis, and was predominantly expressed in normal airway

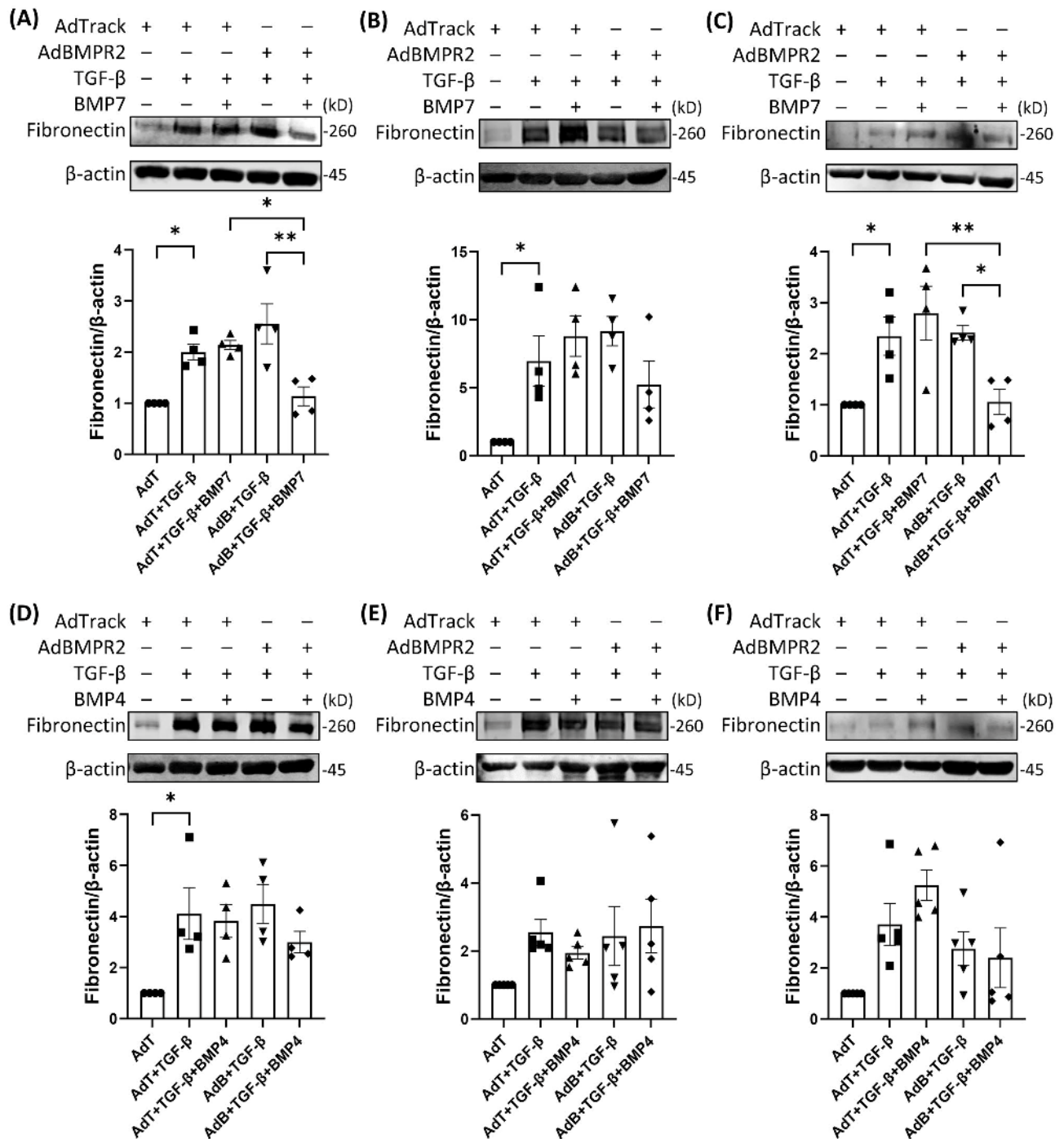


Figure 6. BMP7 stimulation after BMPR2 transduction suppressed TGF- β -induced fibronectin production in lung fibroblasts. (A–C) BMP7 stimulation was effective for suppressing TGF- β -induced fibronectin production only after BMPR2 transduction in HLFs from (A) healthy controls (n=4), (B) IPF patients (n=5), and (C) in RLFs (n=5). (D–F) BMP4 treatment was not effective for suppressing TGF- β -induced fibronectin production even after BMPR2 transduction in HLFs from (D) healthy controls (n=4), (E) IPF patients (n=5) and (F) in RLFs (n=5). Values are presented as mean \pm SE and analysed by one-way ANOVA followed by Sidak's multiple comparison test. Values indicate the ratios to the values of the cells infected with AdTrack and not treated with TGF- β and/or BMPs. * $p < 0.05$; ** $p < 0.01$.

epithelium and alveolar walls and scarcely expressed in fibrotic lesions. Moreover, we have newly confirmed that BMPR2 expression in lung fibroblasts is reduced by TGF- β stimulation, suggesting the

imbalance of TGF- β /BMP signaling in lung fibroblasts stimulated with TGF- β , and supporting the logic of modulating BMPR2 expression in lung fibroblasts under profibrotic circumstances.

BMP7 and 4 are the most studied BMP ligands in the field of pulmonary fibrosis, however, there have been inconsistent reports on their effects. In our study, neither BMP7 nor 4 reduced the effects of TGF- β on Smad2/3 phosphorylation or fibronectin production in BMPR2 non-transduced lung fibroblasts, despite BMP7 and 4 stimulation having increased phosphorylation of Smad1/5/9. Rather unexpectedly, p-Smad2/3 was increased by BMP7 stimulation. Some previous studies have shown antifibrotic effects of BMP7, where BMP7 has been shown to inhibit ECM degradation and revert the TGF- β -induced myofibroblast-like phenotype in HLFs,³² suppress the TGF- β -induced migration and ECM production of rat AECs or mouse lung fibroblasts.^{17,18} In *in vivo* models, BMP7 has also been shown to reduce the expression of TGF- β in the lungs from rats in silica-induced pulmonary fibrosis models, that reduced ECM deposition and fibrosis.^{33,34} BMP4 has also been reported to have antifibrotic effects by the inhibition of TGF- β -induced ECM production, proliferation and cell migration of HLFs,^{12,32,35} and promotes the differentiation of HLFs into myofibroblasts.^{12,35} The antifibrotic effects of other types of BMPs have also been demonstrated, for instance, BMP9 is reported to suppress pulmonary microvascular damage in the bleomycin-induced pulmonary fibrosis rat model, resulting in the improvement of perivascular fibrosis.³⁶ On the other hand, some studies have not shown antifibrotic effects of BMP7. Murray et al. did not find an effect of BMP7 on ECM production or muscularisation by lung fibroblasts, and any antifibrotic effect in bleomycin-induced mouse pulmonary fibrosis models.¹⁹ Pegorier et al. also reported that BMP7 did not suppress ECM production by HLFs.³²

It may also be possible for BMPs to have profibrotic potential in some specific conditions. There are some articles reporting the existence of BMP-induced Smad2/3 phosphorylation in some types of cells.^{37–39} Holtzhausen et al. evaluated p-Smad2/3 levels in 55 cell lines/primary cells treated with BMP2, where BMP2 induced Smad2/3 phosphorylation in 34 lines including 2 fibroblast lines.³⁸ Though little is known regarding the outcomes of the noncanonical Smad2/3 phosphorylation or the types of BMPs which can

induce such a noncanonical signaling, the increase of p-Smad2/3 in lung fibroblasts stimulated with BMP7 in our study may be reflecting a similar phenomenon. Given that BMP7 reduced fibronectin in BMPR2-transduced fibroblasts, the profibrotic and antifibrotic properties of BMP7 may be altered depending on the BMPR2 expression levels. As BMPs signal not only through BMPR2 but also through type 2 activin receptors and in combination with several type 1 receptors,⁴⁰ it is also possible that BMPR2 transduction might alter the proportion of each BMP receptor in the environment of the cell membrane, that might promote the antifibrotic effect of BMP7 more consistently. Our findings warrant further investigation regarding the unexpected profibrotic potential of BMP7 and the contexts altered by BMPR2 transduction in future studies to understand the mechanisms involved.

In terms of the downstream signaling in BMPR2-transduced cells, the antifibrotic phenotypes may be the result of noncanonical pathways. When lung fibroblasts were transduced with BMPR2, phosphorylation of Smad2/3 was suppressed even without supplementation of BMPs, despite no change to p-Smad1/5/9. The lack of response of p-Smad1/5/9 to BMPs in BMPR2-transduced cells may be because of the high dose of BMPs used for this study, where the maximum potential of the cells for phosphorylating Smad1/5/9 was already induced by the BMPs regardless of the levels of BMPR2. Additionally, suppression of fibronectin production was only observed in the BMPR2-transduced cells treated with BMP7. Hence, p-Smad2/3 was regulated by something other than p-Smad1/5/9, and fibronectin production was not suppressed solely by reducing p-Smad2/3. Therefore, there is likely involvement of BMPR2/non-Smad signaling in these antifibrotic pathways. Although it is generally thought that ECM production by fibroblasts is regulated through Smad2/3 signaling in various contexts, some articles insist that the non-Smad pathways can also regulate TGF- β -induced changes.^{8–11} Considering that there are some non-Smad pathways existing downstream of BMP/BMPR2,^{41–43} BMPR2 transduction in our study might have altered the regulation of some non-Smad signaling. Intrinsic BMPs, or

conceivably, given that BMPR2 is not just a receptor for BMPs but functions as a type 2 receptor for activins,⁴⁰ intrinsic activins auto-crined from lung fibroblasts, might be regulators of non-Smad signaling related to the antifibrotic effect of transduced BMPR2 in this study. Although we were limited in our investigations of non-Smad signaling pathways in this study, phosphorylation of p38 MAPK tended to be low in the cells transduced with BMPR2, which suggests the p38 MAPK pathway might be responsible for suppressing TGF- β -induced changes.

Some significant limitations in this study require mentioning. First, the baseline BMPR2 levels were not different between HLFs from healthy controls and IPF patients. This might be because the characteristics of fibroblasts from IPF lungs were “normalised” once isolated and cultured *ex vivo*. A similar thing can be said for the finding that the responsiveness to TGF- β was similar between control and IPF cells, as supported by some reports.^{29–31} Therefore, HLFs cultured from IPF patients might not reflect the phenomenon seen in situ in IPF lungs. On the other hand, BMPR2 was reduced in those cells by TGF- β stimulation, supporting our idea that BMPR2 is reduced under profibrotic circumstances.

Another concern is, unlike in RLFs, qRT-PCR for HLFs did not show reduction of *BMPR2* mRNA by TGF- β . Though BMPR2 protein levels were reduced, the mRNA results in the human subjects were far more variable, perhaps reflecting differing mechanisms and sensitivity between human subjects. It is known that the clinical progression of IPF can vary widely between patients and the reason for this variability is the subject of several large-scale clinical studies and registries. The numbers used in our study are clearly too small to adequately explore mechanisms distinguishing differing subtypes but nevertheless in our sample reduced BMPR2 did appear to be a “final common pathway”. BMPR2 levels might be differently regulated in HLFs and RLFs but also between different human subjects. Thus, the background mechanisms responsible for our findings require further study.

Although we have tried to evaluate some non-Smad pathways, as this study focused on

Smad pathways, the experiments were optimized only for Smad and fibronectin detection, and thus these protocols may not have been sufficient to detect changes in noncanonical pathways, such as the p38 MAPK pathway. Given that there are complicated interactions between TGF- β and BMP pathways and various possible combinations of ligand-receptor complexes,⁴⁰ further studies for evaluating the detail mechanism of antifibrotic property of BMPR2 transduction from various aspects need to be carried out.

In regard to markers of extracellular matrix production, we only found robust results with fibronectin protein and mRNA of collagen-1. Other markers such as the amount of collagen protein were explored, but technical factors with the assay precluded a clear conclusion. We did also attempt to look at α -smooth muscle actin, but it appeared that a nonspecific effect of the adenoviral vector increased this marker in both AdBMPR2 and AdTrack groups, precluding a conclusion to be drawn in regards to BMPR2.

The potential therapeutic application of BMPR2 transduction to the lungs *in vivo* is yet to be evaluated. Our group has previously established a method for transducing BMPR2 to the lungs by intravenous injection of pulmonary endothelium-targeting AdBMPR2,^{26,44} and more recently, by injection of BMPR2-transduced endothelial progenitor cells, possibly via the secretion of BMPR2-carrying exosomes,⁴⁵ both of which have shown positive treatment effects in rat pulmonary hypertension models. Although the background mechanism is still not elucidated in these studies, given the positive antifibrotic effect of BMPR2 transduction observed in this study, it may be worth investigating *in vivo* experiments applying those methods to transduce BMPR2 in the lungs of pulmonary fibrosis models. Unfortunately in our hands to date, the consistency of adequate fibrosis induction versus ethically unacceptable toxicity in the rat bleomycin model has hampered our progress in this area.

In conclusion, BMPR2 was reduced in fibrotic lungs and in lung fibroblasts stimulated with TGF- β . Although BMPs could not solely suppress profibrotic changes induced by TGF- β , adenovirus-mediated BMPR2 transduction alone

could suppress Smad2/3 phosphorylation, and could suppress fibronectin production when treated with BMP7. Further studies are warranted to elucidate the background molecular mechanism of these effects and the potential beneficial impact of BMPR2 transduction in pulmonary fibrosis.

Acknowledgements

This study was supported by the Royal Adelaide Hospital Research Committee under grant (number: HREC/18/CALHN/268) and National Health and Medical Research Council grant APP1147619. The funding source had no involvement in designing the study, in the collection, analysis and interpretation of data, in the writing of the report and in the decision to submit the article for publication.

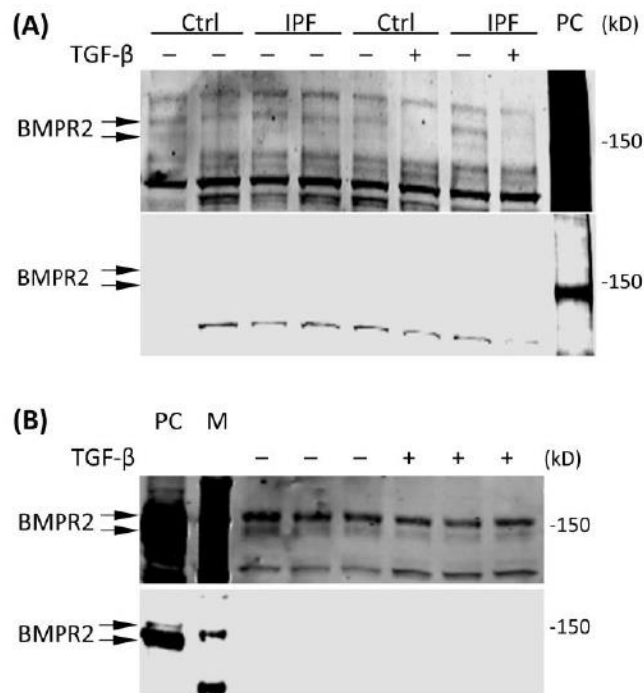
Declaration of interest

The authors report no conflicts of interest.

References

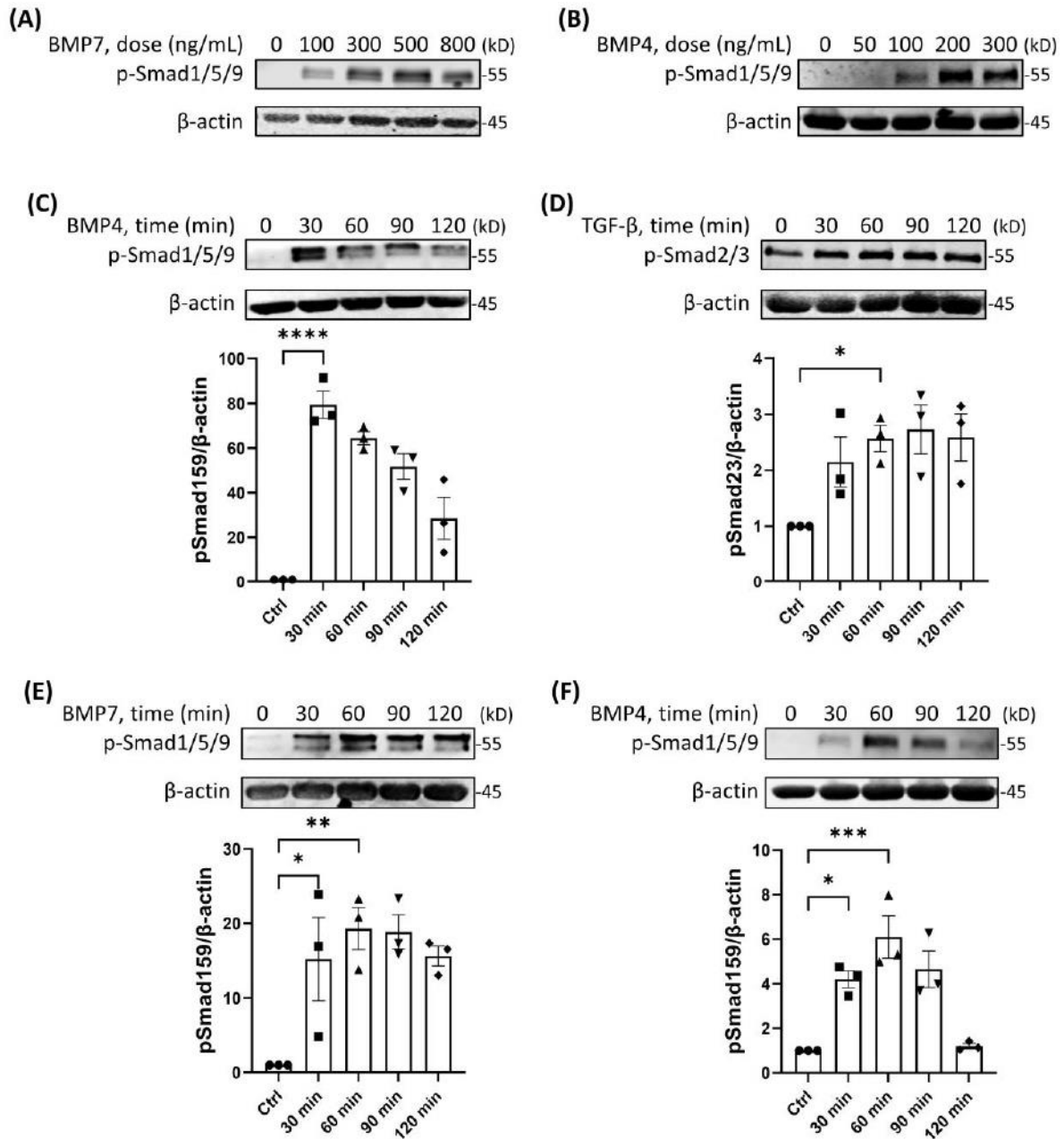
- Natsuzaka M, Chiba H, Kuronuma K, et al. Epidemiologic survey of Japanese patients with idiopathic pulmonary fibrosis and investigation of ethnic differences. *Am J Respir Crit Care Med*. 2014;190(7):773–779. doi:10.1164/rccm.201403-0566OC.
- King TE, Bradford WZ, Castro-Bernardini S, et al. A phase 3 trial of pirfenidone in patients with idiopathic pulmonary fibrosis. *N Engl J Med*. 2014;370(22):2083–2092. doi:10.1056/NEJMoa1402582.
- Richeldi L, Du Bois RM, Raghu G, et al. Efficacy and safety of nintedanib in idiopathic pulmonary fibrosis. *N Engl J Med*. 2014;370(22):2071–2082. doi:10.1056/NEJMoa1402584.
- Raghu G, Rochwerg B, Zhang Y, et al. An official ATS/ERS/JRS/ALAT clinical practice guideline: treatment of idiopathic pulmonary fibrosis. An update of the 2011 clinical practice guideline. *Am J Respir Crit Care Med*. 2015;192(2):e3–19. doi:10.1164/rccm.201506-1063ST.
- Fernandez IE, Eickelberg O. The impact of TGF- β on lung fibrosis: from targeting to biomarkers. *Proc Am Thorac Soc*. 2012;9(3):111–116. doi:10.1513/pats.201203-023AW.
- Bagnato G, Harari S. Cellular interactions in the pathogenesis of interstitial lung diseases. *Eur Respir Rev*. 2015;24(135):102–114. doi:10.1183/09059180.00003214.
- Derynck R, Zhang YE. Smad-dependent and Smad-independent pathways in TGF- β family signalling. *Nature*. 2003;425(6958):577–584. doi:10.1038/nature02006.
- Engel ME, McDonnell MA, Law BK, Moses HL. Interdependent SMAD and JNK signaling in transforming growth factor- β -mediated transcription. *J Biol Chem*. 1999;274(52):37413–37420. doi:10.1074/jbc.274.52.37413.
- Funaba M, Zimmerman CM, Mathews LS. Modulation of Smad2-mediated signaling by extracellular signal-regulated kinase. *J Biol Chem*. 2002;277(44):41361–41368. doi:10.1074/jbc.M204597200.
- Hocevar BA, Brown TL, Howe PH. TGF- β induces fibronectin synthesis through a c-Jun N-terminal kinase-dependent, Smad4-independent pathway. *Embo J*. 1999;18(5):1345–1356. doi:10.1093/emboj/18.5.1345.
- See F, Thomas W, Way K, et al. p38 mitogen-activated protein kinase inhibition improves cardiac function and attenuates left ventricular remodeling following myocardial infarction in the rat. *J Am Coll Cardiol*. 2004;44(8):1679–1689. doi:10.1016/j.jacc.2004.07.038.
- Jeffery TK, Upton PD, Trembath RC, Morrell NW. BMP4 inhibits proliferation and promotes myocyte differentiation of lung fibroblasts via Smad1 and JNK pathways. *Am J Physiol Lung Cell Mol Physiol*. 2005;288(2):L370–378. doi:10.1152/ajplung.00242.2004.
- Zeisberg M, Hanai J, Sugimoto H, et al. BMP-7 counteracts TGF- β 1-induced epithelial-to-mesenchymal transition and reverses chronic renal injury. *Nat Med*. 2003;9(7):964–968. doi:10.1038/nm888.
- Morrissey J, Hruska K, Guo G, Wang S, Chen Q, Klahr S. Bone morphogenetic protein-7 improves renal fibrosis and accelerates the return of renal function. *JASN*. 2002;13(Suppl 1):S14–S21. doi:10.1681/ASN.V13suppl_1s14.
- Chen BL, Peng J, Li QF, Yang M, Wang Y, Chen W. Exogenous bone morphogenetic protein-7 reduces hepatic fibrosis in *Schistosoma japonicum*-infected mice via transforming growth factor- β /Smad signaling. *WJG*. 2013;19(9):1405–1415. doi:10.3748/wjg.v19.i9.1405.
- Zhong L, Wang X, Wang S, Yang L, Gao H, Yang C. The anti-fibrotic effect of bone morphogenetic protein-7(BMP-7) on liver fibrosis. *Int J Med Sci*. 2013;10(4):441–450. doi:10.7150/ijms.5765.
- Liang D, Wang Y, Zhu Z, et al. BMP-7 attenuated silica-induced pulmonary fibrosis through modulation of the balance between TGF- β /Smad and BMP-7/Smad signaling pathway. *Chem Biol Interact*. 2016;243:72–81. doi:10.1016/j.cbi.2015.11.012.
- Izumi N, Mizuguchi S, Inagaki Y, et al. BMP-7 opposes TGF- β 1-mediated collagen induction in mouse pulmonary myofibroblasts through Id2. *Am J Physiol Lung Cell Mol Physiol*. 2006;290(1):L120–126. doi:10.1152/ajplung.00171.2005.
- Murray LA, Hackett TL, Warner SM, et al. BMP-7 does not protect against bleomycin-induced lung or skin fibrosis. *PLoS One*. 2008;3(12):e4039. doi:10.1371/journal.pone.0004039.
- De Langhe E, Cailotto F, De Vooght V, et al. Enhanced endogenous bone morphogenetic protein signaling

- protects against bleomycin induced pulmonary fibrosis. *Respir Res.* 2015;16:38. doi:10.1186/s12931-015-0202-x.
21. Dong Y, Geng Y, Li L, et al. Blocking follistatin-like 1 attenuates bleomycin-induced pulmonary fibrosis in mice. *J Exp Med.* 2015;212(2):235–252. doi:10.1084/jem.20121878.
 22. Fang Y, Zhang S, Li X, Jiang F, Ye Q, Ning W. Follistatin like-1 aggravates silica-induced mouse lung injury. *Sci Rep.* 2017;7(1):399. doi:10.1038/s41598-017-00478-0.
 23. Myllärniemi M, Lindholm P, Rynnänen MJ, et al. Gremlin-mediated decrease in bone morphogenetic protein signaling promotes pulmonary fibrosis. *Am J Respir Crit Care Med.* 2008;177(3):321–329. doi:10.1164/rccm.200706-945OC.
 24. Chen NY, D Collum S, Luo F, et al. Macrophage bone morphogenetic protein receptor 2 depletion in idiopathic pulmonary fibrosis and Group III pulmonary hypertension. *Am J Physiol Lung Cell Mol Physiol.* 2016;311(2):L238–254. doi:10.1152/ajplung.00142.2016.
 25. Bryant AJ, Robinson LJ, Moore CS, et al. Expression of mutant bone morphogenetic protein receptor II worsens pulmonary hypertension secondary to pulmonary fibrosis. *Pulm Circ.* 2015;5(4):681–690. doi:10.1086/683811.
 26. Reynolds AM, Xia W, Holmes MD, et al. Bone morphogenetic protein type 2 receptor gene therapy attenuates hypoxic pulmonary hypertension. *Am J Physiol Lung Cell Mol Physiol.* 2007;292(5):L1182–1192. doi:10.1152/ajplung.00020.2006.
 27. Schneider CA, Rasband WS, Eliceiri KW. NIH Image to ImageJ: 25 years of image analysis. *Nat Methods.* 2012;9(7):671–675. doi:10.1038/nmeth.2089.
 28. Long L, Crosby A, Yang X, et al. Altered bone morphogenetic protein and transforming growth factor-beta signaling in rat models of pulmonary hypertension: potential for activin receptor-like kinase-5 inhibition in prevention and progression of disease. *Circulation.* 2009;119(4):566–576. doi:10.1161/CIRCULATIONAHA.108.821504.
 29. Mendoza-Milla C, Valero Jiménez A, Rangel C, et al. Dehydroepiandrosterone has strong antifibrotic effects and is decreased in idiopathic pulmonary fibrosis. *Eur Respir J.* 2013;42(5):1309–1321. doi:10.1183/09031936.00027412.
 30. Roach KM, Roach KM, Duffy SM, et al. The K⁺ channel KCa3.1 as a novel target for idiopathic pulmonary fibrosis. *PLoS One.* 2013;8(12):e85244. doi:10.1371/journal.pone.0085244.
 31. Krempaska K, Barnowski S, Gavini J, et al. Azithromycin has enhanced effects on lung fibroblasts from idiopathic pulmonary fibrosis (IPF) patients compared to controls [corrected]. *Respir Res.* 2020;21(1):25. doi:10.1186/s12931-020-1275-8.
 32. Pegorier S, Campbell GA, Kay AB, Lloyd CM. Bone morphogenetic protein (BMP)-4 and BMP-7 regulate differentially transforming growth factor (TGF)-beta1 in normal human lung fibroblasts (NHLF). *Respir Res.* 2010;11:85. doi:10.1186/1465-9921-11-85.
 33. Yang G, Zhu Z, Wang Y, Gao A, Niu P, Tian L. Bone morphogenetic protein-7 inhibits silica-induced pulmonary fibrosis in rats. *Toxicol Lett.* 2013;220(2):103–108. doi:10.1016/j.toxlet.2013.04.017.
 34. Li X, An G, Wang Y, et al. Anti-fibrotic effects of bone morphogenetic protein-7-modified bone marrow mesenchymal stem cells on silica-induced pulmonary fibrosis. *Exp Mol Pathol.* 2017;102(1):70–77. doi:10.1016/j.yexmp.2016.12.010.
 35. Kadoya K, Togo S, Tulafu M, et al. Specific features of fibrotic lung fibroblasts highly sensitive to fibrotic processes mediated via TGF-β-ERK5 interaction. *Cell Physiol Biochem.* 2019;52(4):822–837. doi:10.33594/000000057.
 36. Jiang Q, Liu C, Liu S, et al. Dysregulation of BMP9/BMPR2/SMAD signalling pathway contributes to pulmonary fibrosis and pulmonary hypertension induced by bleomycin in rats. *Br J Pharmacol.* 2021;178(1):203–216. doi:10.1111/bph.15285.
 37. Wang Y, Ho CC, Bang E, et al. Bone morphogenetic protein 2 stimulates noncanonical SMAD2/3 signaling via the BMP type 1A receptor in gonadotrope-like cells: implications for FSH synthesis. *Endocrinology.* 2014;155(5):1970–1981. doi:10.1210/en.2013-1741.
 38. Holtzhausen A, Golzio C, How T, et al. Novel bone morphogenetic protein signaling through Smad2 and Smad3 to regulate cancer progression and development. *Faseb J.* 2014;28(3):1248–1267. doi:10.1096/fj.13-239178.
 39. Zhang H, Tian S, Klausen C, Zhu H, Liu R, Leung PC. Differential activation of noncanonical SMAD2/SMAD3 signaling by bone morphogenetic proteins causes disproportionate induction of hyaluronan production in immortalized human granulosa cells. *Mol Cell Endocrinol.* 2016;428:17–27. doi:10.1016/j.mce.2016.03.016.
 40. Katagiri T, Watabe T. Bone morphogenetic proteins. *Cold Spring Harb Perspect Biol.* 2016;8(6):a021899. doi:10.1101/cshperspect.a021899.
 41. Yanagisawa M, Nakashima K, Takeda K, et al. Inhibition of BMP2-induced, TAK1 kinase-mediated neurite outgrowth by Smad6 and Smad7. *Genes Cells.* 2001;6(12):1091–1099. doi:10.1046/j.1365-2443.2001.00483.x.
 42. Qi X, Li TG, Hao J, et al. BMP4 supports self-renewal of embryonic stem cells by inhibiting mitogen-activated protein kinase pathways. *Proc Natl Acad Sci USA.* 2004;101(16):6027–6032. doi:10.1073/pnas.0401367101.
 43. Moustakas A, Heldin CH. Non-Smad TGF-beta signals. *J Cell Sci.* 2005;118(Pt 16):3573–3584. doi:10.1242/jcs.02554.
 44. Reynolds AM, Holmes MD, Danilov SM, Reynolds PN. Targeted gene delivery of BMPR2 attenuates pulmonary hypertension. *Eur Respir J.* 2012;39(2):329–343. doi:10.1183/09031936.00187310.
 45. Harper RL, Maiolo S, Ward RJ, et al. BMPR2-expressing bone marrow-derived endothelial-like progenitor cells alleviate pulmonary arterial hypertension in vivo. *Respirology.* 2019;24(11):1095–1103. doi:10.1111/resp.13552.



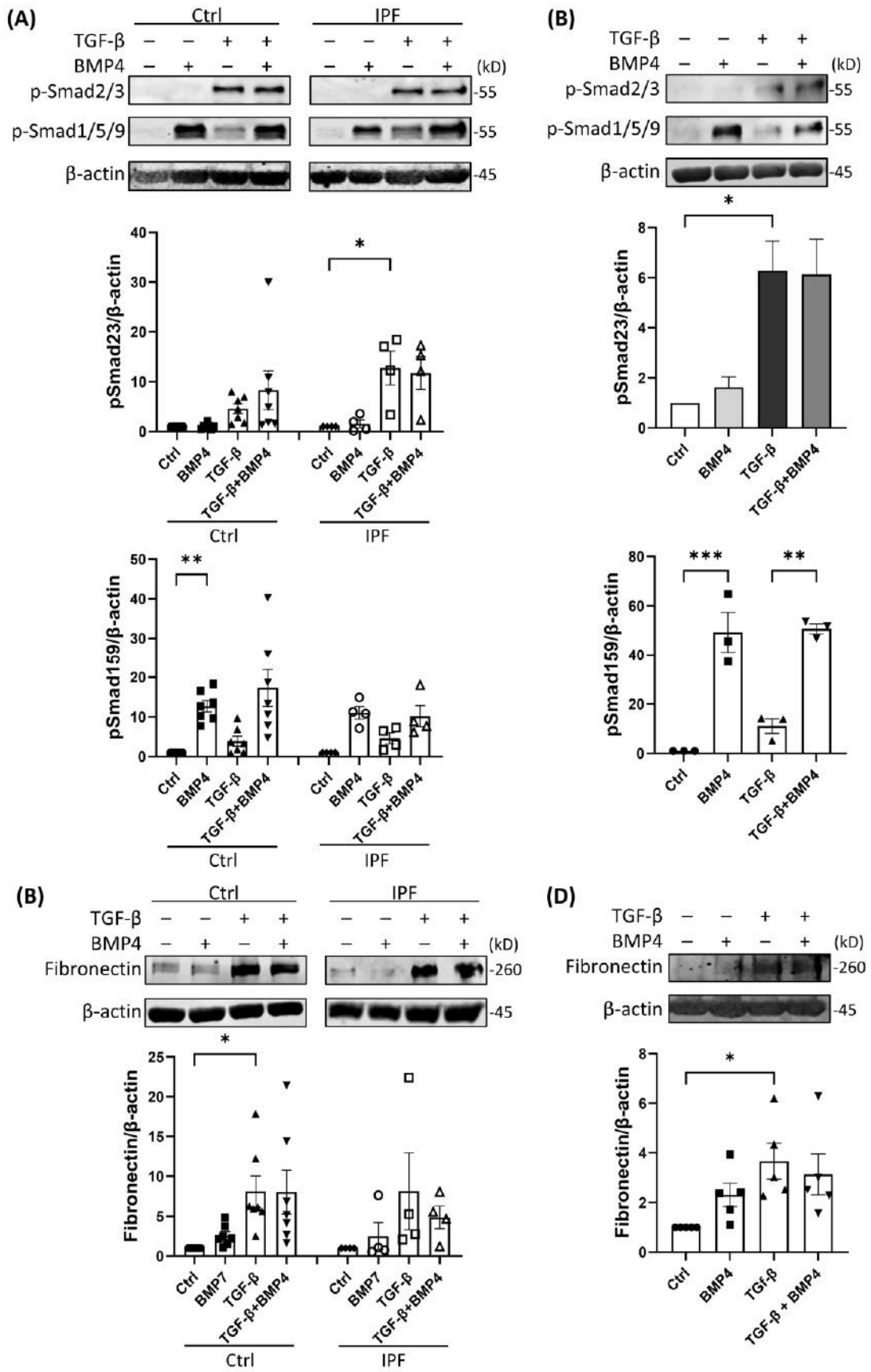
1
2
3
4
5
6
7
8
9
10
11
12

Fig. S1. BMPR2 bands in Fig. 2 together with positive controls. The BMPR2 Western blot image for (A) HLFs used for Fig. 2A and C and (B) RLFs used for Fig. 2E, together with positive controls. The contrast is adjusted for non-transduced (top) or transduced (bottom) BMPR2 bands. HLFs infected with AdBMPR2 were used as positive controls for BMPR2 bands. BMPR2 is usually detected as double bands, which present slightly above and below the marker of 150 kD. Strong nonspecific bands are observed at the 100 kD level. As the intensity of the transduced BMPR2 bands is considerably stronger than that of non-transduced BMPR2, it is impossible to show both the transduced and non-transduced BMPR2 bands on the same image. The strength of the two bands differed and was inconsistent in each experiment. PC; positive control, M; protein marker.



1
 2 **Fig. S2. Dose setting of BMPs and time course of Smad phosphorylation after**
 3 **stimulation with TGF-β or BMPs.** Dose-dependent study of Smad1/5/9 phosphorylation
 4 induced by (A) BMP7 was increased from 0-300 ng/mL, and (B) BMP4 was increased
 5 from 0-200 ng/mL, where doses of 300 ng/mL of BMP7 and 200 ng/mL of BMP4 were
 6 chosen for future studies. (C) Smad1/5/9 phosphorylation was induced by BMP4
 7 stimulation of more than 30 min in HLFs, determined by Western blot (n=3). (D) Smad2/3
 8 phosphorylation was induced by TGF-β stimulation of more than 60 min in RLFs,
 9 determined by Western blot (n = 3). (E, F) Smad1/5/9 phosphorylation was similarly
 10 induced by BMP7 or 4 in RLFs after 60 mins, determined by Western blot (n=3). Values
 11 are presented as mean ± SE and analysed by one-way ANOVA followed by Sidak's
 12 multiple comparison test. Based on these time-course studies, 60 mins of incubation time
 13 was used for all future studies of p-Smads. Values indicate the ratios to the values of the

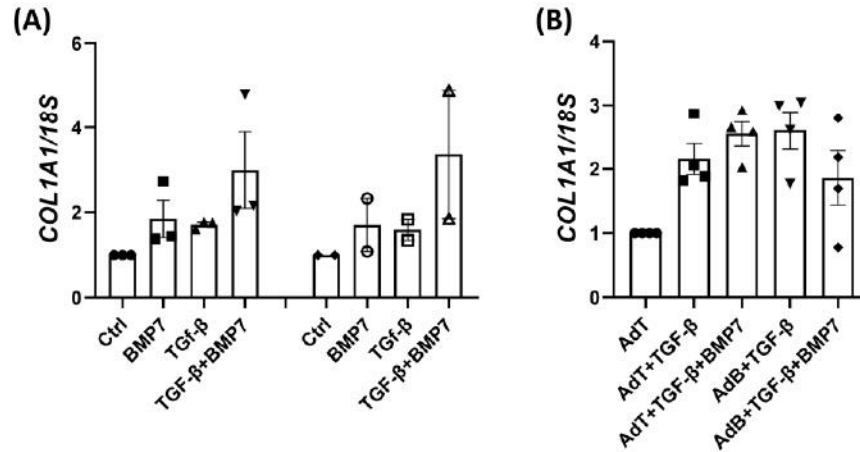
1 cells not treated with TGF- β or BMPs. * $P < 0.05$; ** $P < 0.01$; *** $P < 0.005$; **** $P <$
2 0.0001.
3



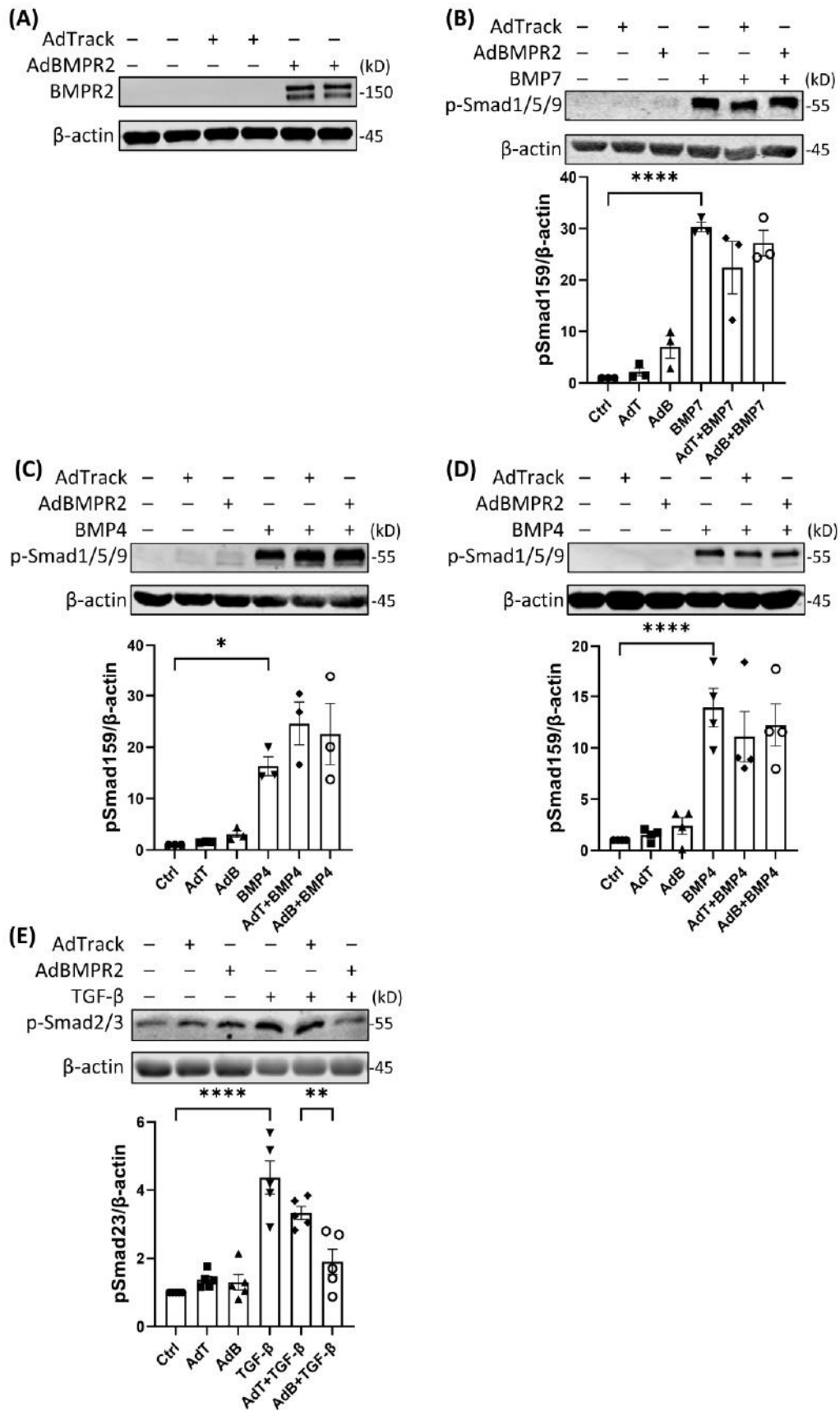
1

2 **Fig. S3. BMP4 did not suppress the TGF- β -induced changes in HLFs.** (A, C) TGF- β -
 3 induced Smad2/3 phosphorylation and fibronectin production were not suppressed by

1 BMP4 in HLFs from both healthy controls (n=7) and IPF patients (n=4), determined by
2 Western blot with representative immunoblots from a healthy control and an IPF patient.
3 (B, D) TGF- β -induced Smad2/3 phosphorylation and fibronectin production were not
4 suppressed by BMP4 in RLFs (n=3). Values are presented as mean \pm SE and analysed by
5 one-way ANOVA followed by Sidak's multiple comparison test. Values indicate the ratios
6 to the values of the cells not treated with TGF- β and/or BMPs. * $P < 0.05$; ** $P < 0.01$;
7 *** $P < 0.005$.
8
9
10
11



1
2 **Fig. S4. mRNA of collagen 1 was not suppressed by BMP7 alone but was suppressed**
3 **in BMPR2-transduced HLFs.** (A) TGF-β-induced fibronectin production was not
4 suppressed by BMP7 in HLFs from both healthy controls (n=3) and IPF patients (n=2),
5 determined by qRT-PCR. (B) BMPR2 transduction did not significantly suppress, but
6 showed a trend of suppressing, TGF-β-induced fibronectin production in HLFs from a
7 healthy control (n=4). Values are presented as mean ± SE and analysed by one-way
8 ANOVA. Values indicate the ratios to the values of the cells infected with AdTrack and not
9 treated with TGF-β and/or BMPs.
10



1

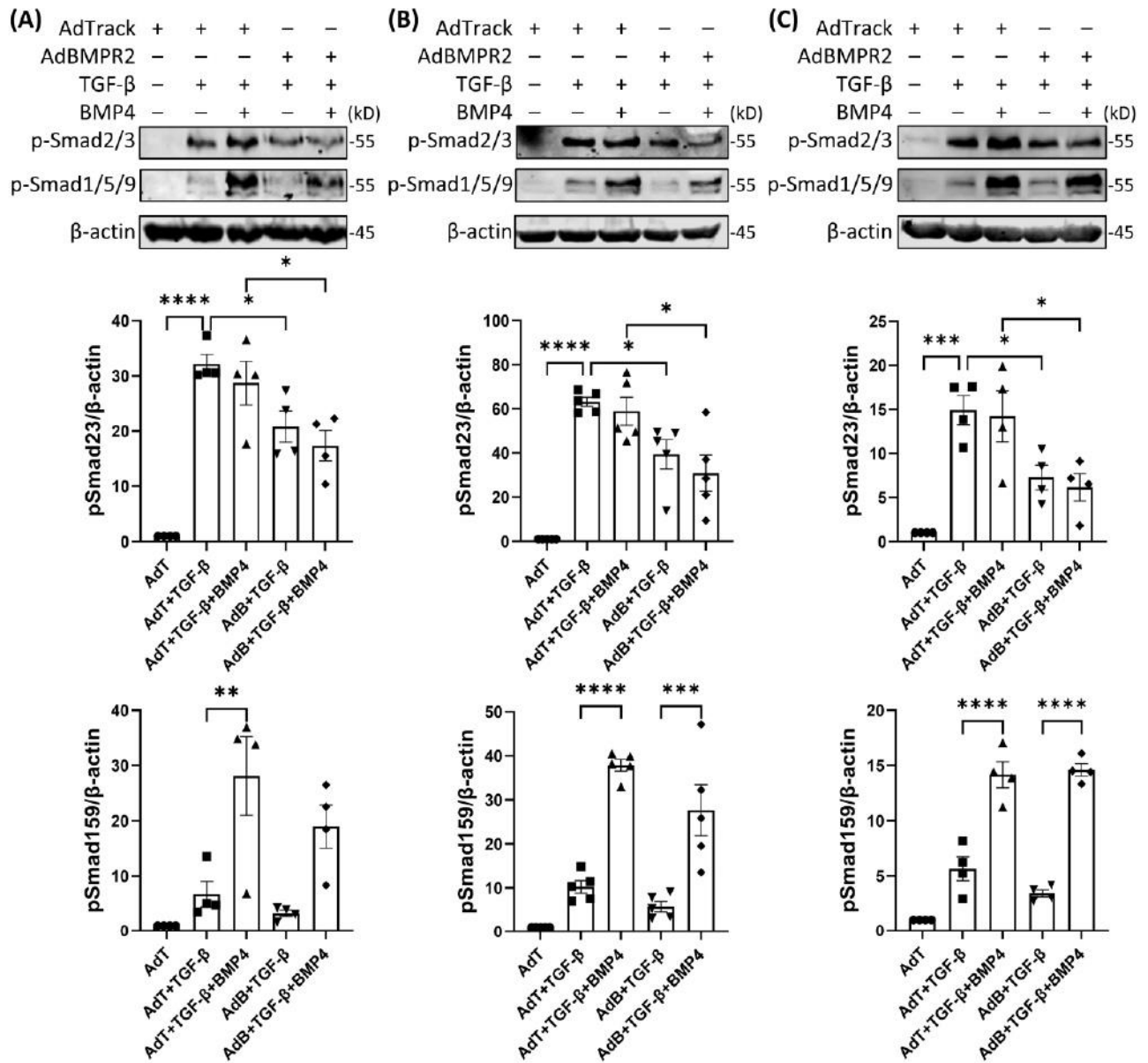
2

Fig. S5. BMPR2 transduction using adenovirus did not promote BMP-induced

3

Smad1/5/9 phosphorylation in lung fibroblasts. (A) BMPR2 was strongly expressed in

1 RLFs infected with AdBMP2, determined by Western blot. (B) BMP2 transduction did
2 not promote BMP7-induced Smad1/5/9 phosphorylation in RLFs (n=3). (C, D) BMP2
3 transduction did not promote BMP4-induced Smad1/5/9 phosphorylation in HLFs from a
4 healthy control (n=3) (C) and in RLFs (n=4) (D). (E) BMP2 transduction suppressed
5 TGF- β -induced Smad2/3 phosphorylation even without BMP stimulation in RLFs (n=5).
6 Values are presented as mean \pm SE and analysed by one-way ANOVA followed by Sidak's
7 multiple comparison test. Values indicate the ratios to the values of the cells infected with
8 AdTrack and not treated with TGF- β or BMPs. * $P < 0.05$; ** $P < 0.01$; **** $P < 0.001$.
9



1
 2 **Fig. S6. BMPR2 transduction using adenovirus suppressed TGF-β-induced Smad2/3**
 3 **phosphorylation in lung fibroblasts.** (A-C) BMPR2 transduction suppressed TGF-β-
 4 induced Smad2/3 phosphorylation regardless of the levels of p-Smad1/5/9 in HLFs from a
 5 healthy control (n=4) (A) and an IPF patient (n=5) (B), and in RLFs (n=4) (C). Values are
 6 presented as mean ± SE and analysed by one-way ANOVA followed by Sidak's multiple
 7 comparison test. Values indicate the ratios to the values of the cells infected with AdTrack
 8 and not treated with TGF-β and/or BMPs. * $P < 0.05$; ** $P < 0.01$; *** $P < 0.005$; **** P
 9 < 0.001 .

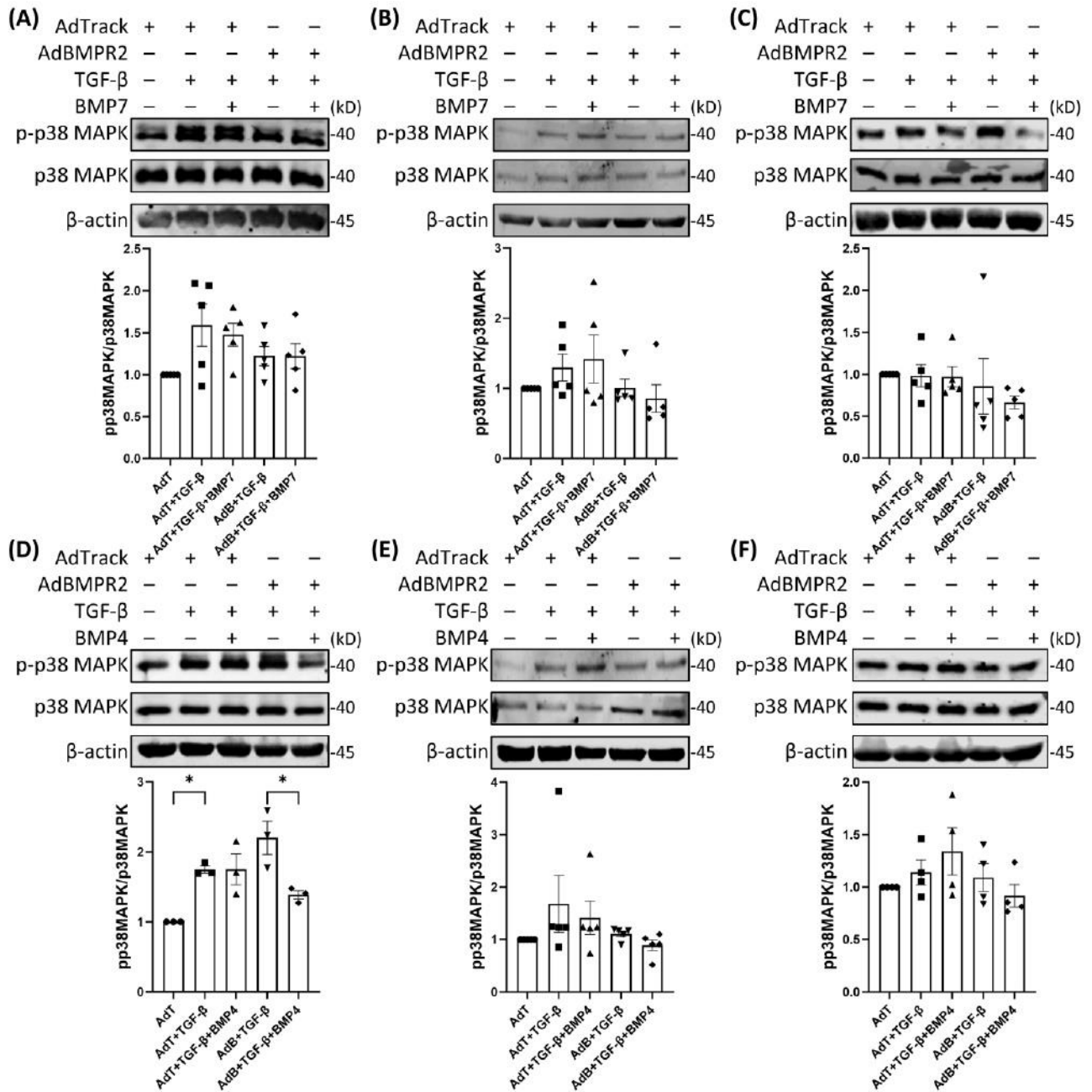


Fig. S7. BMPR2 transduction may suppress TGF- β -induced p38 MAPK

phosphorylation in lung fibroblasts. (A-F) Though statistically insignificant, BMPR2 transduction using adenovirus showed trends of suppressing TGF- β -induced p38 MAPK phosphorylation in lung fibroblasts from (A, D) healthy controls (n=4), (B, E) IPF patients (n=5) and (C, F) RLFs (n=4). Values are presented as mean \pm SE and analysed by one-way ANOVA followed by Sidak's multiple comparison test. Values indicate the ratios to the values of the cells infected with AdTrack and not treated with TGF- β or BMPs. * $P < 0.05$; ** $P < 0.01$.

1
2
3
4
5
6
7
8
9
10

Part III

Transduction of BMPR2 to human and rat lung fibroblasts using exosomes secreted by BMPR2-transduced ECFCs

1. Overview

EVs including exosomes are produced by various cell types, including stem cells, progenitor cells and inflammatory cells. Intracellular materials, such as micro RNAs, proteins and DNAs, as well as membrane-bound proteins are enveloped in or presented on the surface of exosomes and released from the cell. These exosomes are then absorbed by other cells. Therefore, it is considered that exosomes have role of mediating cell-to-cell communication through this transmission process (Figure 3-1). EPCs are known to be one of the major sources of EVs in various contexts (152, 153, 160-163).

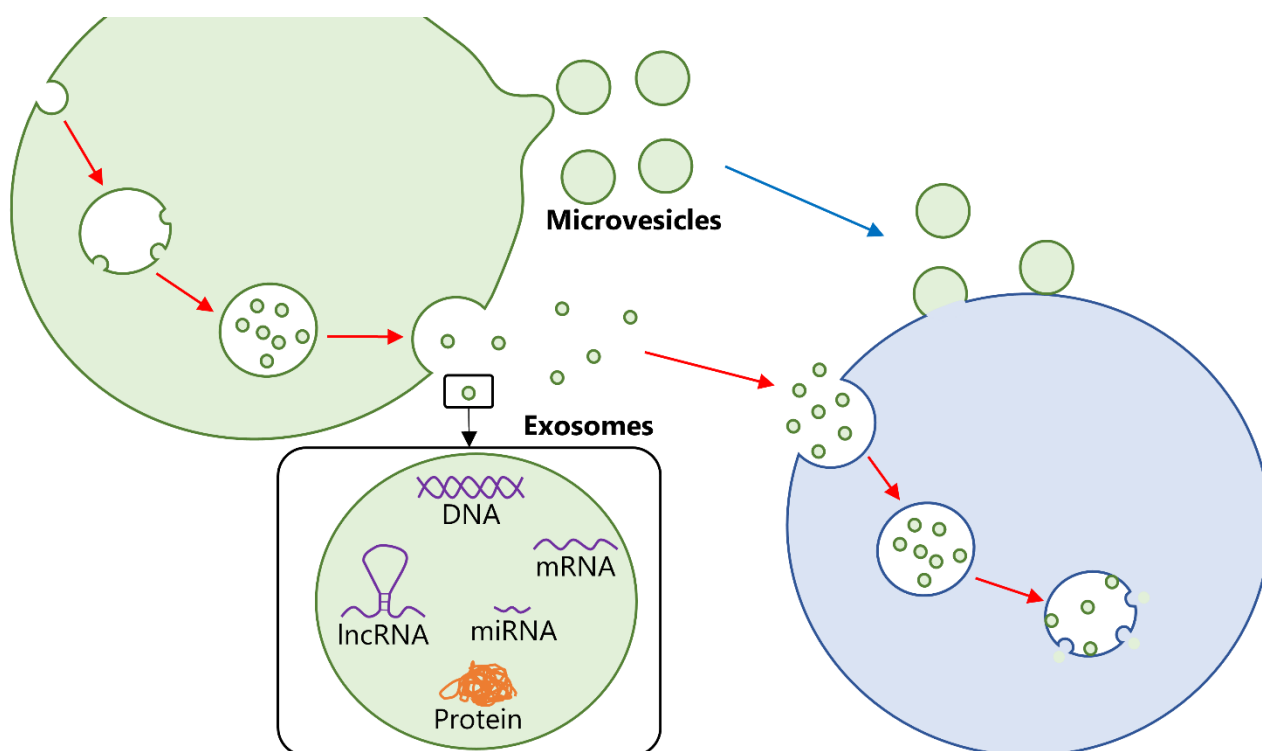


Figure 3-1. Cell-to-cell communication via EVs. EV, extracellular vesicle; mRNA, messenger RNA; lncRNA, long non-coding RNA; miRNA, micro-RNA.

According to a decade of research, EVs have shown to have potential as a biomarker and therapeutic agent of various diseases. In the field of pulmonary fibrosis, EVs isolated from serum, sputum, or primary lung fibroblasts of IPF patients contain profibrotic micro-RNAs, and these EVs were reported to be correlated with mortality and disease severity (232-234). Although EV-based therapy has never been applied for treating human IPF, in some studies using

pulmonary fibrosis experimental models, EVs derived from MSCs have shown an effect of ameliorating pulmonary fibrosis via miRNAs and/or MMPs and TIMPs contained in the EVs (235-239). However, despite EVs having a potential to be manipulated artificially, such artificially modified EVs have not been used for treating pulmonary fibrosis even in experimental settings yet.

As described in Part I (Introduction section, 5.3), our group has previously reported that intravenous injection of AdBMPR2 targeting pulmonary endothelium could attenuate PAH in rat and mouse models (178-183). Most recently, our group has demonstrated that intravenous injection of rat bone marrow-derived EPCs transduced with AdBMPR2 can increase the expression of BMPR2 in the lungs and attenuate monocrotaline-induced rat PAH both hemodynamically and histologically (184). The biodistribution study evaluated using EPCs transduced with luciferase reporter adenovirus revealed that though more than 99% of EPCs accumulated in the lungs 1-6 hours after injection, vast majority were lost by 24 hours. In view of this short retention time, the mechanism for the effects of this cell therapy may be due to paracrine effect via EVs.

For applying this cell-based therapy to the field of pulmonary fibrosis, I have firstly clarified that the exosomes from BMPR2-transduced human ECFCs/rat EPCs are transmitted and transduce BMPR2 to lung fibroblasts. Moreover, I have tried to evaluate the effect of BMPR2 transduction using exosomes on TGF- β -induced fibronectin production.

2. Methods

2.1 Human and rat samples

Blood samples were collected from healthy people for isolating ECFCs, which was approved by Central Adelaide Local Health Network Human Research Ethics Committee with informed written consent obtained in accordance with the “Declaration of Helsinki”. Blood samples were obtained at Royal Adelaide Hospital, Adelaide, SA, Australia.

Lungs and femurs were collected from male F344 rats for isolating rat lung fibroblasts (RLFs) and EPCs, which was approved by the University of South Australia Animal Ethics Committee (U18-19) and undertaken as per the guidelines established by the “Australian Code of Practice for the Care and Use of Animals for Scientific Purposes”.

2.2 Cell lines and provided primary cells

HEK-293 cells were used for adenovirus amplification and grown in Dulbecco's Modified Eagle's Medium (DMEM) with HEPES buffer with Ham's F12 Nutrient Mixture (50:50) (Gibco, Grand Island, NY, USA), 10% foetal calf serum (FCS) (Lonza, Basel, Switzerland), L-glutamine (2 mM) (Cosmo Bio, Tokyo, Japan), sodium pyruvate (1 mM) (Gibco), penicillin (62.5 µg/ml) and streptomycin (100 µg/mL) (Gibco, Grand Island, NY, USA). Human lung fibroblasts (HLFs) isolated from healthy people and IPF patients were provided by Dr. D. Knight (University of Newcastle, Callaghan, NSW, Australia) and Dr. M. Rojas (University of Pittsburgh, Pittsburgh, PA, USA). HLFs were grown in DMEM with 10% FCS. All cells were grown in a 5% CO₂-atmosphere at 37°C.

2.3 RLF isolation from lung

RLFs were isolated from Fischer 344 rats that were humanely killed using CO₂ asphyxiation. Animals were housed in the University of South Australia Core Animal Facility (Adelaide, SA, Australia). Their lungs were collected into DMEM and immediately stored on ice. They were then minced into small pieces and incubated at 37°C with collagenase type III (30 mg) and DNase type I (750 µg) (Worthington Biochemical, Lakewood, NJ, USA) in a volume of 30 mL media for 60-80 min with gentle shaking. Then the cell suspension was filtered through a 70-µm cell strainer. The cell pellet from this filtered media was resuspended in DMEM with 15% FCS and seeded after incubation with red cell lysis solution. After 4 days, the media was

changed to DMEM with 10% FCS. After 2 weeks, cells were passaged and used for further experiments at passage 1-4.

2.4 Isolation of ECFCs from human peripheral blood

Human peripheral blood samples were taken in Lithium Heparin blood collection tubes from healthy volunteers for isolating human ECFCs. The blood was processed with Lymphoprep™ (Stemcell Technologies, VIC, Australia) to isolate the mononuclear cells. These were cultured on 48-well plates prepared with Collagen (Sigma-Aldrich, St. Louis, MO, USA) coating in endothelial selective media; EGM-2 (Lonza) with 20% FCS (Hyclone, Noble Park North, VIC, Australia). After 2-4 weeks, colonies of hECFCs appear and these were picked and expanded over 2 weeks to give sufficient numbers of ECFCs. The cells were used for subsequent experiments between passage 4-7.

2.5 Isolation of EPCs from rat bone marrow

Isolation of rat EPCs was performed using Fischer 344 rats that were humanely killed using CO₂ asphyxiation. Femurs were removed and bone marrow was flushed with EGM-2MV. Then the cell suspension was spun, the cell pellet was resuspended in EGM-2MV with 20% FCS (Hyclone) and seeded. Following 6-9 days of culture, cells were observed under a microscope for the typical endothelial-like cell 'cobblestone' appearance. Characterisation of EPCs isolated through this procedure was previously carried out by positive von Willebrand factor staining, increased acetylated low density lipoprotein uptake, tube formation in Matrigel, and expression of cell surface markers as CD309^{dim}, CD45^{dim}, CD146^{dim} and CD34⁺ determined by flow cytometry (184).

2.6 Viral construction

AdCMVBMPR2myc (AdBMPR2 henceforth), a replication-incompetent serotype 5 adenoviral vector, and control adenovirus (AdTrack) containing the cytomegalovirus promoter driving expression of reporter genes luciferase and green fluorescent protein were prepared as previously described (180). Viral titre was determined by 50% tissue culture infectious dose assay using HEK-293 cells and particle titre by optical density at 260 nm.

2.7 Adenoviral transduction of BMPR2 to human ECFCs/rat EPCs and purification of exosomes in their conditioned media

Human ECFCs or rat EPCs were either untransduced or transduced with AdTrack (containing green fluorescent protein (GFP) and luciferase reporter genes) or AdBMPR2 when they were grown up to 80% confluency. The cells were incubated with virus at 150 pfu/ml for 3 days. The transduction media was then removed, and cells were washed with PBS. The exosome collection media (EGM-2 for human ECFCs or EGM-2MV for rat EPCs) (Lonza) was applied with 1% exosome-free FCS (Hyclone). This media was collected at 24 h and 48 h and spun at 300 g for 10 min to remove cell debris. The supernatant was spun at 100,000 g for 2 h to pellet the EVs. The supernatant was removed, and the EVs were re-suspended in PBS for treatment of cells or in protein lysis buffer directly for Western blot. Protein assay was performed to quantify the exosomes contained in the solution.

2.8 BMPR2 transduction to HLFs/RLFs and treatment with TGF- β /BMPs

The next day after seeding the HLFs/RLFs, the culture media was replaced with transduction media containing exosomes derived from either human ECFCs or rat EPCs for treating HLFs or RLFs, respectively, at a concentration of 20 μ g/mL (this means suspending exosomes (20 μ g protein in 1 mL culture media). After incubation for 4 days, the transduction media was removed, and cells were washed with phosphate-buffered saline (PBS). Then the cells were incubated with the media containing recombinant human TGF- β 1 (Pepro Tech, Rocky Hill, NJ, USA) of 2 ng/mL and/or recombinant human BMP7 (Pepro Tech) of 300 ng/mL or recombinant human BMP4 (Pepro Tech) of 200 ng/mL. For evaluating production of ECM proteins, after 3 days of incubation, cells were harvested and processed for Western blot. To evaluate phosphorylation of the Smad signalling proteins, serum starvation for 24 h was performed prior to the incubation with TGF- β and/or BMP7 or 4 at the same concentration as above for 1 h. After the treatment, cells were harvested for Western blot.

2.9 Western Blot

Samples were lysed with ice cold PierceTM RIPA buffer (Thermo ScientificTM, Waltham, MA, USA) containing proteinase inhibitor (cOmpleteTM Mini, Sigma-Aldrich, St. Louis, MO, USA) and phosphatase inhibitor cocktail (HaltTM, Thermo ScientificTM). Protein quantification was performed using DC protein assay kit (Bio-Rad Laboratories, Hercules, CA, USA). Protein samples (15-30 μ g) were loaded on 10% polyacrylamide/SDS gels, electrophoresed and electroblotted to a 0.2 μ m Nitrocellulose membrane (Bio-Rad Laboratories). Membranes were blocked with

Odyssey Blocking Buffer (LI-COR Biosciences, Lincoln, NE, USA) for 1 h at room temperature. The membranes were then incubated overnight at 4°C with primary antibodies in Odyssey Blocking Buffer; rabbit anti-phosphorylated (p-)Smad1/5/9 and p-Smad2/3 (1:1000) and rabbit anti- β -actin (1:2000) (Cell Signalling Technology, Danvers, MA, USA), rabbit anti-fibronectin (1:250) (Proteintech, Rosemont, IL, USA) and mouse anti-BMP2 (1:250) (BD Biosciences). The secondary antibodies used were goat anti-rabbit 800, donkey anti-rabbit 680 and goat anti-mouse 680 (1:20000) (LI-COR Biosciences) and incubated for 1 h at room temperature. Membrane scanning was performed on the Odyssey Imaging System (LI-COR Biosciences) and data analysis was carried out using Image Studio Lite version 5.2 (LI-COR Biosciences). Values of each sample were calculated as the integrated intensity counts using the intensity of β -actin as a reference, which reflect the relative fluorescence of each band.

2.10 Statistical analysis

Data are expressed as mean \pm standard error (SE). Results are expressed as the relative values using the value of control sample in each experiment as a reference (i.e., there are no error bars for control data). One-way ANOVA was used for intergroup analysis. When the *F* value indicated significance, the Sidak's test was carried out using GraphPad Prism version 9 (GraphPad Software, San Diego, CA, USA) for multiple comparisons. A value of $p < 0.05$ was considered to be statistically significant.

3. Results

3.1 Lung fibroblasts treated with exosomes from BMPR2-transduced human ECFCs/rat EPCs showed elevation of BMPR2

In the exosomes purified from culture media of ECFCs/rat EPCs pre-treated with AdBMPR2, significantly elevated BMPR2 expression was observed compared to the exosomes from the cells not transduced with BMPR2 (Figure 3-2A, B). When HLFs/RLFs were treated with those BMPR2-harboring exosomes, BMPR2 levels in the cell lysates were significantly elevated (Figure 3-2C, D). At this point, whether the elevation of BMPR2 in lung fibroblasts was due to the transmission of BMPR2 from exosomes to the cells or just due to the sedimentation of BMPR2-harboring exosomes on the surface of the cells was unclear.

3.2 BMPR2 transduced by exosomes reduced fibronectin production in lung fibroblasts

I have tried to evaluate the effect of BMPR2 overexpression for suppressing TGF- β -induced profibrotic responses in lung fibroblasts using above-mentioned exosome-mediated transduction of BMPR2. In HLFs, TGF- β -induced fibronectin production was suppressed by treatment with BMPR2-exosomes, regardless of supplementary BMP ligands (Figure 3-3A, B).

However, the HLFs treated with BMPR2-exosomes were obviously few and damaged, or almost dead at the time of collection. When it comes to RLFs, the cells treated with exosomes (both AdTrack-exosomes and BMPR2-exosomes) were also almost dead and the protein concentration of those samples were not enough for running following experiments. Therefore, treatment with BMPR2-exosomes was revealed to be very toxic for lung fibroblasts in this experimental condition. This might partly be due to the antifibrotic treatment effect of overexpressed BMPR2. However, given the fact that BMPR2 transduced by adenovirus showed much milder antifibrotic effect on lung fibroblasts and could not show any effect in the absence of BMP7 in Section II, the severe toxicity of exosome therapy here may not be only by the antifibrotic effect of BMPR2. As it is impossible to avoid contamination by adenovirus when purifying exosomes by ultracentrifugation, toxicity by adenovirus can be one of the explanations, which can explain the toxic effect of AdTrack-exosomes on RLFs. Although the viral load in the exosome solution should be much lower than that in viral solution used for direct adenoviral transduction, as the exosomes were added to the media on day 2 and incubated until day 6 after seeding the cells, even such a small viral load might have a

significant impact on the viability of very small number of cells on culture wells (in adenoviral transduction studies, the transduction media was applied when the cells reached to 80% confluency and removed 2 days later). Another explanation is the effect of ECFCs/rat EPCs-derived exosomes themselves against lung fibroblasts, but if the findings from AdTrack-exosomes in Figure 3-3A and B are true, this possibility is low in HLFs.

Lower dose of exosomes and shorter treatment term were also tried, but exosomes less than 10 µg/mL or treatment less than 3 days were not sufficient for detecting increase of BMPR2 in lung fibroblasts (data not shown).

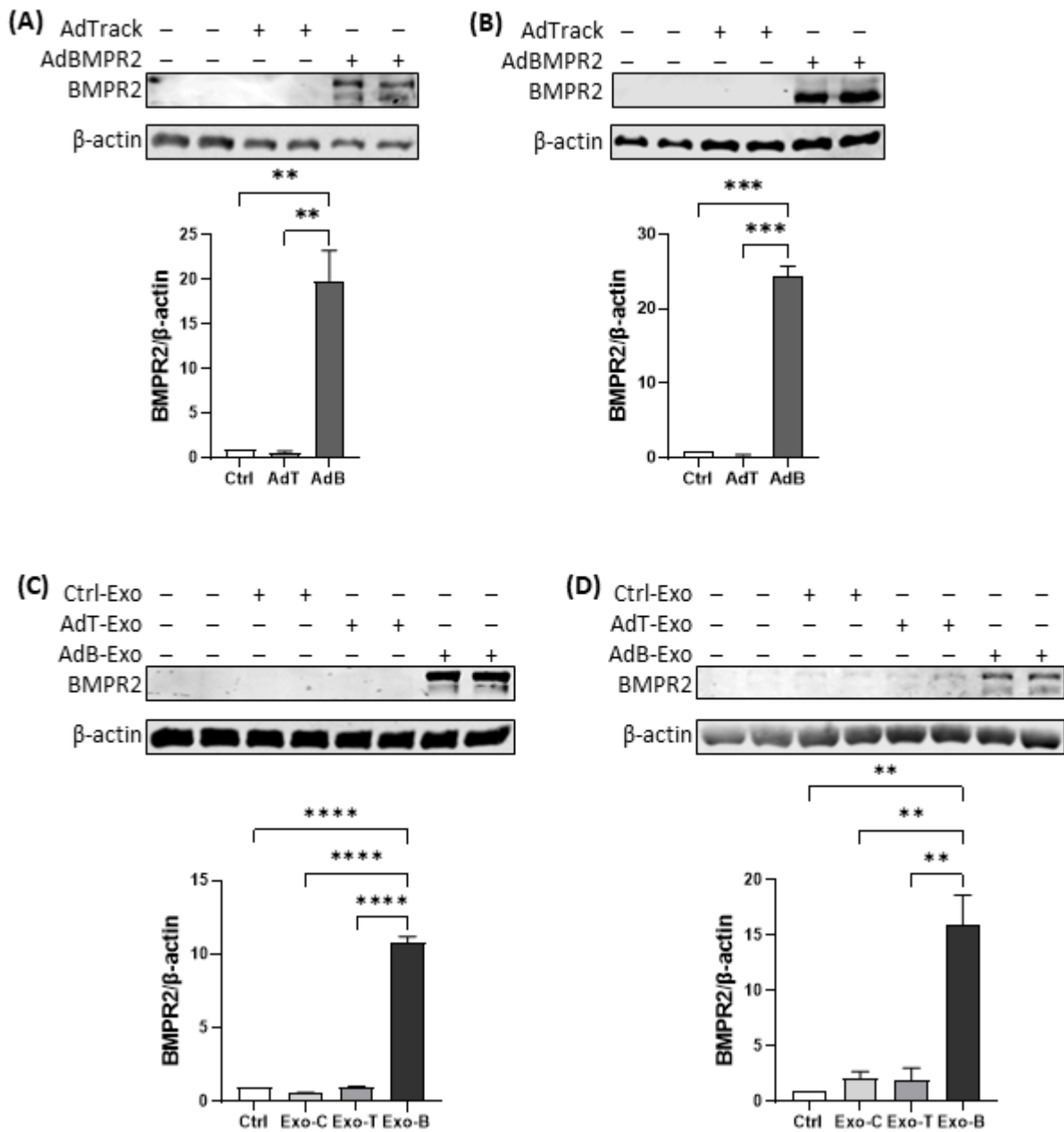


Figure 3-2. Lung fibroblasts treated with exosomes from BMPR2-transduced ECFCs/rat EPCs showed elevation of BMPR2. (A-B) BMPR2 was strongly expressed in exosomes from (A) BMPR2-transduced ECFCs and (B) rat EPCs, determined by Western blot (n=2). (C-D) BMPR2 was significantly increased in cell lysates of (C) HLFs and (D) RLFs treated with exosomes from human ECFCs or rat EPCs, respectively, determined by Western blot (n=2). Ctrl, control; AdT, AdTrack; AdB, AdBMPR2; Exo-C, exosomes derived from cells not infected with

adenovirus; Exo-T: exosomes derived from AdTrack-infected cells; Exo-B, exosomes derived from AdBMPR2-infected cells. ** $P < 0.01$; *** $P < 0.005$; **** $P < 0.001$.

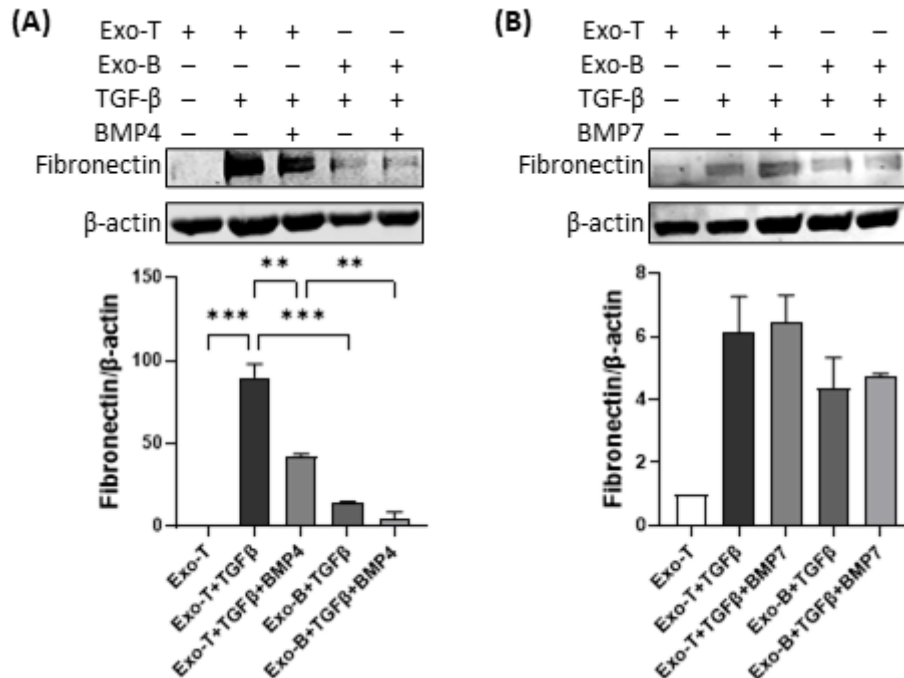


Figure 3-3. Fibronectin production was decreased in HLFs treated with exosomes from BMPR2-transduced ECFCs. (A-B) Fibronectin production was decreased in HLFs treated with exosomes from BMPR2-transduced ECFCs, regardless of administration of (A) BMP4, or (B) BMP7, determined by Western blot (n=2). Exo-T: exosomes derived from AdTrack-infected cells; Exo-B, exosomes derived from AdBMPR2-infected cells. ** $P < 0.01$; *** $P < 0.005$.

*Though the results could become different by modifying the experimental protocol to maintain lung fibroblasts survival, since this study attempted to reveal background mechanism of the treatment effect in vivo (elaborated in Part IV) but the in vivo study had failed, further optimisation study was not carried out.

Part IV

**Treatment of rats with bleomycin-induced
pulmonary fibrosis using BMPR2-transduced rat
EPCs**

1. Overview

I have tried to elucidate the efficacy of tail vein injection of BMPR2-transduced rat EPCs on pulmonary fibrosis in rat model. The concept of this treatment strategy is as follows.

- 1) EPCs (ECFCs) have potential to home to the sites of vascular damage to promote vasculogenesis (150, 151), and microvascular injury is one of the typical findings in the lungs from pulmonary fibrosis.
- 2) Since EPCs have potential of secreting EVs (152, 153), EPCs carrying BMPR2 may secrete BMPR2-carrying EVs at the site where they accumulate.
- 3) BMPR2-transduced rat EPCs injected from tail veins accumulate in lungs of rats with monocrotaline-induced PAH and stayed for less than 24 hours, according to our previous study (184). Despite such a short-term accumulation, BMPR2 was transduced to the lungs and the expression was sustained for at least 14 days, that suggests that BMPR2 was transmitted from EPCs to the lungs which may be via EVs while the EPCs were in the lungs. Importantly, this approach reduced the monocrotaline-induced pulmonary vascular remodelling and reduced pulmonary hypertension.
- 4) According to the results in Part III, exosomes secreted from BMPR2-transduced EPCs can be transmitted to lung fibroblasts.
- 5) According to the results in Part II, TGF- β -induced fibronectin production was suppressed in BMPR2-transduced lung fibroblasts.

Combining all these points, I have expected that tail vein injection of BMPR2-transduced EPCs is effective for pulmonary fibrosis. I attempted to evaluate the efficacy of this cell-based treatment on rat bleomycin-induced pulmonary fibrosis model.

2. Methods

The experimental methods not mentioned in Part III are elaborated here.

2.1 Preparation of BMPR2-transduced rat EPCs for intravenous injection

Femurs were collected from EPC donor rats 11 days before intravenous injection and processed for isolating EPCs as described in Part III. The culture media was replaced on day 7 with normal media or transduction media containing AdTrack or AdBMPR2 of 150 pfu/ml, and cells were incubated for 3 days (this protocol was originally 100 pfu/ml and for only 1 day but was modified afterward). The transduction media was then removed on day 10, and cells were washed with PBS and incubated with EGM-2MV (Lonza) applied with 1% FCS (Hyclone) for further 24 h. On day 11, EPCs were released from the culture plate, counted, and resuspended in sterile PBS at a concentration of 1×10^6 cells/mL.

2.2 Creation of rat bleomycin-induced pulmonary fibrosis model and treatment with BMPR2-transduced rat EPCs

For dose-optimisation of bleomycin, Fischer 344 rats at 8-10 weeks were treated with intratracheally administered bleomycin sulphate (Cayman Chemical, Ann Arbor, MI, USA) (1, 1.5, 2, 4, 6, 8 or 10 mg/kg in a total volume of 2 mL/kg saline) or the same volume of saline on day 0 and were held under normal animal housing conditions. Lungs were collected on day 14 or earlier if the rats reached humane killing endpoints and processed for haematoxylin/eosin (HE) staining and protein/mRNA assays. Eventually, the dose of bleomycin was set at 1.5 mg/kg. For evaluating if the injected EPCs accumulate in lungs, rats were treated with bleomycin on day 0 and taken tail vein injection of EPCs (1×10^6 cells/rat) infected with or without AdBMPR2 on day 7. Lungs were collected 1 and 6 hours after injection and processed for HE stains and protein assay.

For EPC-treatment studies, rats were assigned to 5 groups ($n = 8$ /group) as follows: saline, bleomycin, bleomycin + control (non-infected) EPCs, bleomycin + AdTrack-infected EPCs and bleomycin + AdBMPR2-infected EPCs. Bleomycin sulphate or the same volume of saline were administered intratracheally on day 0. For the experiments evaluating the effect of BMPR2-transduced EPCs for preventing development of pulmonary fibrosis, rats in the bleomycin + EPCs groups were given tail vein injection of relevant EPCs (1×10^6 cells/rat) on day 1 and their lungs were collected on day 14 (14-day prevention study). To evaluate the effect for treating already established pulmonary fibrosis, tail vein injection

was performed on day 7-10 and lungs were collected on day 21 (21-day treatment study). The collected lungs were separated in right and left lobes, and the right lung lobes were snap frozen and homogenised for protein/mRNA assays, while the left lobes were fixed with 10% formalin for histopathological evaluation.

2.3 Hematoxylin-Eosin staining

The left lung lobes were fixed with 10% formalin for 24 h and submitted to the Adelaide Medical School Histology Services (Adelaide, SA, Australia) for routine histological examination. Sections of 5 μm were heat mounted (58°C for 1 h) on coated glass slides (InstrumeC, Sandringham, VIC, Australia), deparaffinised with xylene and stained with Hematoxylin and Eosin.

2.4 Modified Ashcroft's score

To assess the degree of pulmonary fibrosis, the modified Ashcroft's score proposed by Hübner et al (240) was evaluated. In each slide, whole sections were assessed at high-power ($\times 200$) for severity of interstitial fibrosis and allotted a score between 0 and 8 using a predetermined scale of severity for each field. The mean score of all the fields was taken as the fibrosis score for the section.

2.5 Collagen assay

To quantify collagen content in rat lung tissues, lung homogenate was at first digested with 6 M hydrochloric acid at 120°C for 3 h. The supernatant was used for following assay using Hydroxyproline assay kit (Sigma-Aldrich) per manufacturer's protocol. The absorbance of the reaction solutions at 560 nm were measured and hydroxyproline content was calculated and expressed as $\mu\text{g}/\text{mg}$ lung.

2.6 Western Blot

For rat lung protein extraction, lung homogenates were lysed with the Long's lysis buffer (177) containing proteinase inhibitor (cOmplete™ Mini, Sigma-Aldrich) and phosphatase inhibitor cocktail (Halt™, Thermo Scientific™). Protein quantification was performed using DC protein assay kit (Bio-Rad Laboratories, Hercules, CA, USA). Following procedures from protein quantification to taking images are elaborated in Part III (2.9). Values of each sample were calculated as the integrated intensity counts using the intensity of β -actin as a reference, which reflect the relative fluorescence of each band.

2.7 Quantitative real time polymerase chain reaction (qRT-PCR)

RNA was isolated from lung homogenates using mirVana™ miRNA Isolation Kit (Invitrogen™) according to the manufacturer's instructions. The purity and quantity of RNA were assessed using the NanoDrop™ One/One^c UV-VS Spectrophotometer (Thermo Scientific™, Waltham, MA, USA). The GoTaq™ 1-Step RT-qPCR System (Promega, Madison, WI, USA) was used for preparation of cDNA and qRT-PCR reaction. Each reaction contained 50 ng of total RNA in a volume of 14 µL. Reactions were performed on CFX Connect Real-Time PCR Detection System (Bio-Rad Laboratories) with the following conditions: reverse transcription at 45°C for 15 min, reverse transcript inactivation and hot-start activation at 95°C for 10 min, followed by quantitative PCR of 40 cycles of 95 °C for 10 s and 60°C for 30 s. All assays were run in duplicate. The Cq is defined as the PCR cycle at which the fluorescent signal of the reporter dye crosses an arbitrarily placed threshold in the exponential phase. The sample with a Cq value over 40 or with a melt curve with a different peak from that of other samples treated with the same primer was considered as invalid and was not useful for further analysis. The sequences of the primer pairs were summarized in Table 4-1. Values of each sample were expressed as $2^{-\Delta\Delta Cq}$ using *18s* as a housekeeping gene and the ΔCq value of one of the control samples as a reference.

Table 4-1. Quantitative real-time polymerase chain reaction primer sequences

Species	Gene	Primer sequence (5'-3')	Length (bp)
Rat	bmpr2	F AGTTTGGGGAACCGAGGCAC	238
		R AAGCAGGAGGGCAAAGAAAAGA	
	col1a1	F ACGAGTCACACCGGAACTTG	97
		R CAATGTCCAAGGGAGCCACA	
	fn1	F GTTACCCTTCCACACCCCAA	186
		R CCCCAGAGGACGTTGTTAG	
	18s	F GCAATTATTCCCCATGAACG	123
		R GGCCTCACTAAACCATCCAA	

F: forward; R: reverse.

2.8 Statistical analysis

Data are expressed as mean \pm standard error (SE). Results are expressed as the relative values using the average value of control samples as a reference. One-way ANOVA or student's *t*-test was used for intergroup analysis. When the *F* value

indicated significance, the Sidak's test was carried out using GraphPad Prism version 9 (GraphPad Software, San Diego, CA, USA) for multiple comparisons. A value of $p < 0.05$ was considered to be statistically significant.

3. Results

3.1 Optimisation of bleomycin dosage and the protocols for intratracheal administration and monitoring

According to a preliminary study I have performed in Japan prior to coming to Australia, the optimal dosage of bleomycin was estimated to be 10 mg/kg, because the sufficient pulmonary fibrosis was induced (Figure 4-1A) and all animals had survived with expected range of body weight loss (Figure 4-1B). Additionally, bleomycin of this dose reduced *bmpr2* mRNA in fibrotic lungs (Figure 4-1C) like the findings demonstrated in Part II. In this study, the extent of fibrosis induced by doses of 4 and 6 mg/kg were not sufficient and body weight of the rats treated with those doses were recovered completely 14 days after administration of bleomycin.

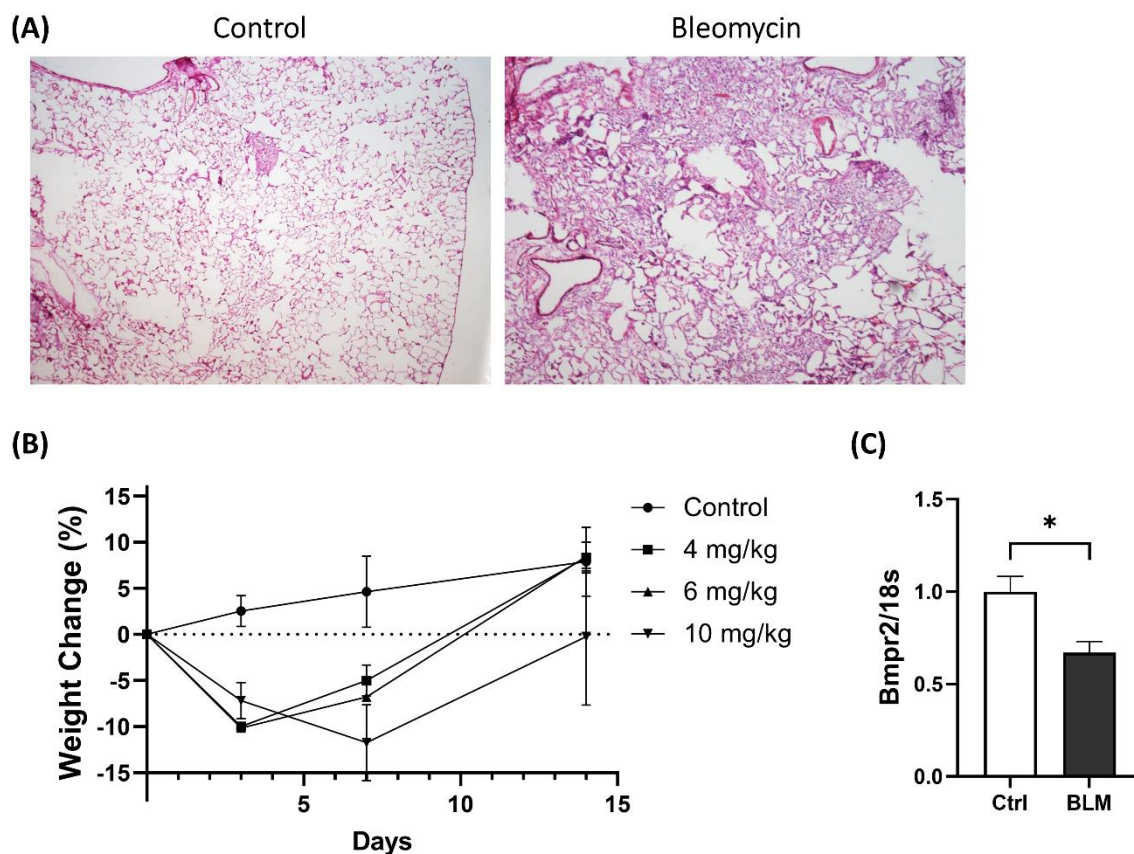


Figure 4-1. The optimal bleomycin dosage was estimated at 10 mg/kg (preliminary optimisation study in Nagoya University). (A) HE stains of lung sections. The sections from the lungs of rats treated with bleomycin showed formation of fibrosis and infiltration of inflammatory cells mainly in the alveolar wall of the surrounding areas of bronchi/bronchiole. (B) Body weight of rats was reduced by bleomycin administration, while it was recovered up to

the similar levels of saline control group on day 14 in the 4 and 6 mg/kg groups (saline control group: n=4; 4 and 6 mg/kg groups: n=2/each group; 10 mg/kg group: n=5). (C) *bmpr2* mRNA was reduced by administration of bleomycin, determined by qRT-PCR. * $P < 0.05$.

Based on these findings, I firstly tried to evaluate the efficacy and toxicity of bleomycin of 4, 6, 8 and 10 mg/kg (n=5/dose) for replicating the results I had obtained in Japan and confirming the best dose. Most of the rats showed weight loss of 5-10% with significant body condition deterioration after 2 days from bleomycin administration. Two of them were found dead on day 4 and 9 of them (2 of them were from the lowest dose group) were killed humanely by day 5 according to the prespecified humane endpoints. Bilateral patchy lung damage (with similar extent in right and left lobes from a same rat) was observed in lung sections from the rats treated with bleomycin, while there was no specific abnormality in the lung sections from control group animals (Figure 4-2A). Lung lesions (mononuclear inflammatory cell infiltration) presented mainly in the alveolar wall of the surrounding areas of bronchi/bronchiole, which was consistent with the damage due to aspiration of bleomycin. There was no finding suggestive of infection, such as intra-alveolar fibrin deposition or granulomatous lesions. Gram and Grocott stains were negative (Figure 4-2B, C).

Given the unexpectedly high mortality rate, the first study was terminated, and a new optimisation study was planned using bleomycin of lower doses (1, 1.5 and 2 mg/kg). In this dose range, all rats treated with 1-1.5 mg/kg bleomycin had survived for 14 days with mild-moderate body condition worsening. All rats in 2 mg/kg group were humanely killed on day 7 due to the unexpected signs of moderate-high toxicity. Body weight loss was the most severe in 2 mg/kg group (Figure 4-2D), though 2 of 5 rats in 1.5 mg/kg group showed similar extent of weight loss. The lung sections showed patchy fibrosis distributed similarly to the lesions observed in the first optimisation study. Modified Ashcroft's score on day 14 after bleomycin administration was calculated and significant increase of the score was observed in 1.5 mg/kg group, while fibrosis was very mild in 1 mg/kg group and the score was not significantly different compared with control group. Although the rats in 2 mg/kg group had been killed on day 7, their fibrosis was more severe than that in 1.5 mg/kg group (Figure 4-2E).

Based on the two optimisation studies, the dose of bleomycin used in the following studies had set at 1.5 mg/kg for achieving sufficient pulmonary fibrosis with minimum toxicity.

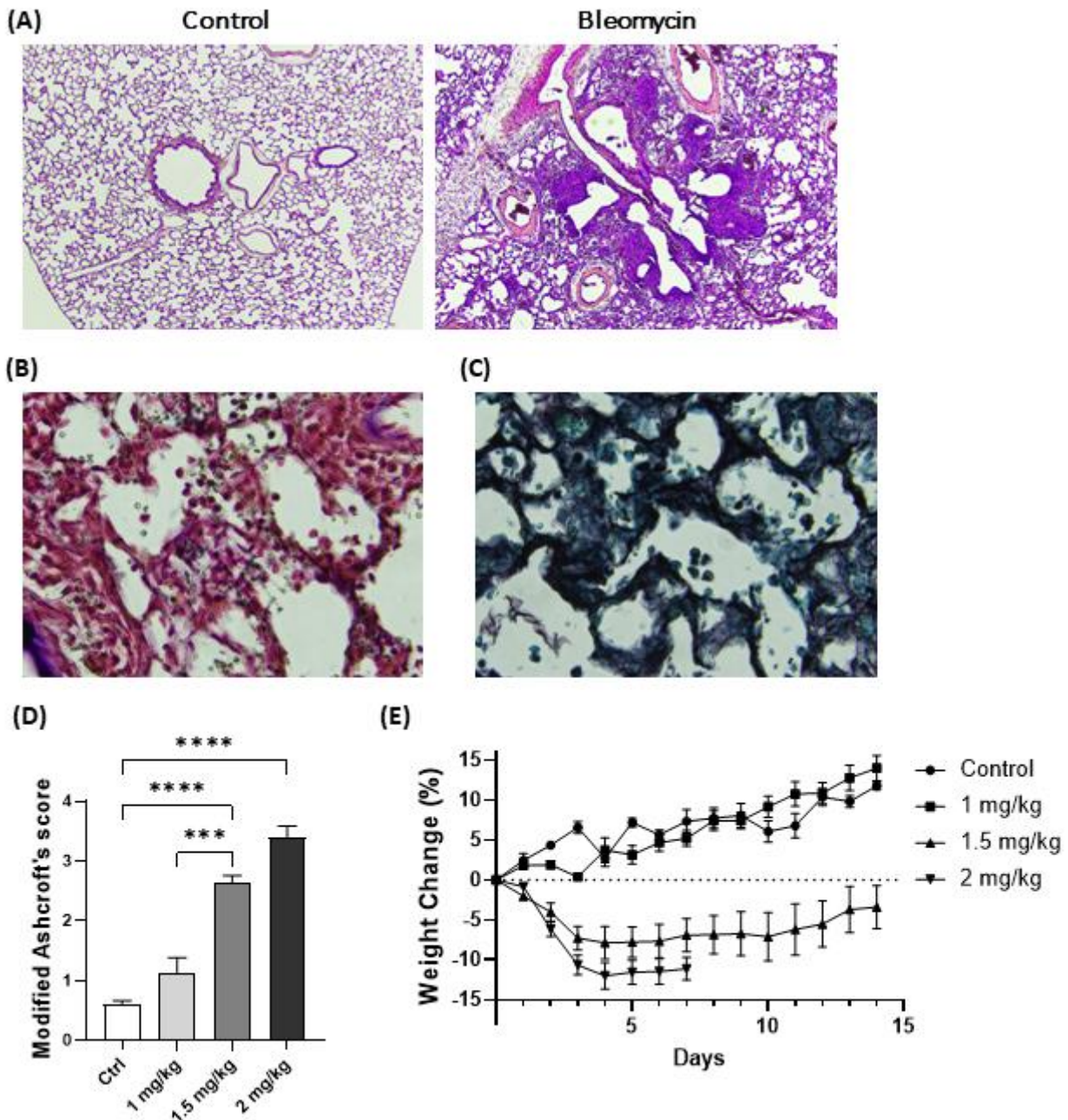


Figure 4-2. The optimal bleomycin dosage was set at 1.5 mg/kg. (A) HE stains of lung sections in the first optimisation study. The sections from the lungs of rats treated with bleomycin showed infiltration of inflammatory cells mainly in the alveolar wall of the surrounding areas of bronchi/bronchiole. (B) Gram stains of damaged lung sections were negative. (C) Grocott stains of damaged lung sections showed no evidence of pneumocystis infection in the lungs. (D) Modified Ashcroft's score was significantly increased in 1.5 mg/kg group (on day 14) and 2 mg/kg group (on day 7) compared with control group, while fibrosis was very mild in 1 mg/kg group (on day 14) (n=5/group). (E) Body weight of rats was reduced

in 1.5 and 2 mg/kg groups, while control and 1 mg/kg groups showed similar extent of gradual weight gain after intratracheal administration of saline or bleomycin. *** $P < 0.005$; **** $P < 0.001$.

3.2 Intravenously injected EPCs accumulated in the lungs of rats with bleomycin-induced pulmonary fibrosis shortly after injections

After the above-mentioned dose-setting studies, a batch of rats were assigned to a group of BMPR2-transduced EPC treatment in the 14-day prevention study and treated with both bleomycin and BMPR2-transduced EPCs. BMPR2 showed a trend of increase in the lungs from those rats when the lungs were harvested 14 days after injection (Figure 4-3A), but the difference between bleomycin only group and BMPR2-transduced EPC group was not statistically significant as the inter-sample variance was quite big (Figure 4-4). Additionally, the expected antifibrotic effects of increased BMPR2 were not detected.

Suspecting that EPCs could not be delivered to the lungs sufficiently and/or the load of transduced BMPR2 was too low to show consistent biological effects, I have increased the dose of virus for treating EPCs (100 to 150 pfu/mL) and extended the term for incubation with virus (1 to 3 days). If the lungs of bleomycin-induced pulmonary fibrosis rats were harvested at 1 or 6 hours after tail vein injection of BMPR2-transduced rat EPCs, BMPR2 was significantly increased in the lungs compared with the lungs from the rats not treated with rat EPCs (Figure 4-3B). However, even using EPCs treated with the modified protocol, BMPR2 was not significantly increased in the lungs 14 days after EPC injection (Figure 4-3C, data from the 21-day treatment study).

Therefore, BMPR2-transduced rat EPCs could accumulate in the rat lungs shortly (1-6 hours) after intravenous injections but mostly washed out after then and inconsistently preserved 14 days later. Despite the difficulty to detect a long-term consistent increase in expression of BMPR2, it was uncertain if the duration of expression would still be sufficient to influence the bleomycin-induced fibrotic process, so it was decided to proceed to a therapy study. This approach was in part justified by our prior experience with the monocrotaline PAH model, where transient upregulation of BMPR2 was shown to be sufficient to modify the physiological outcomes in that setting.

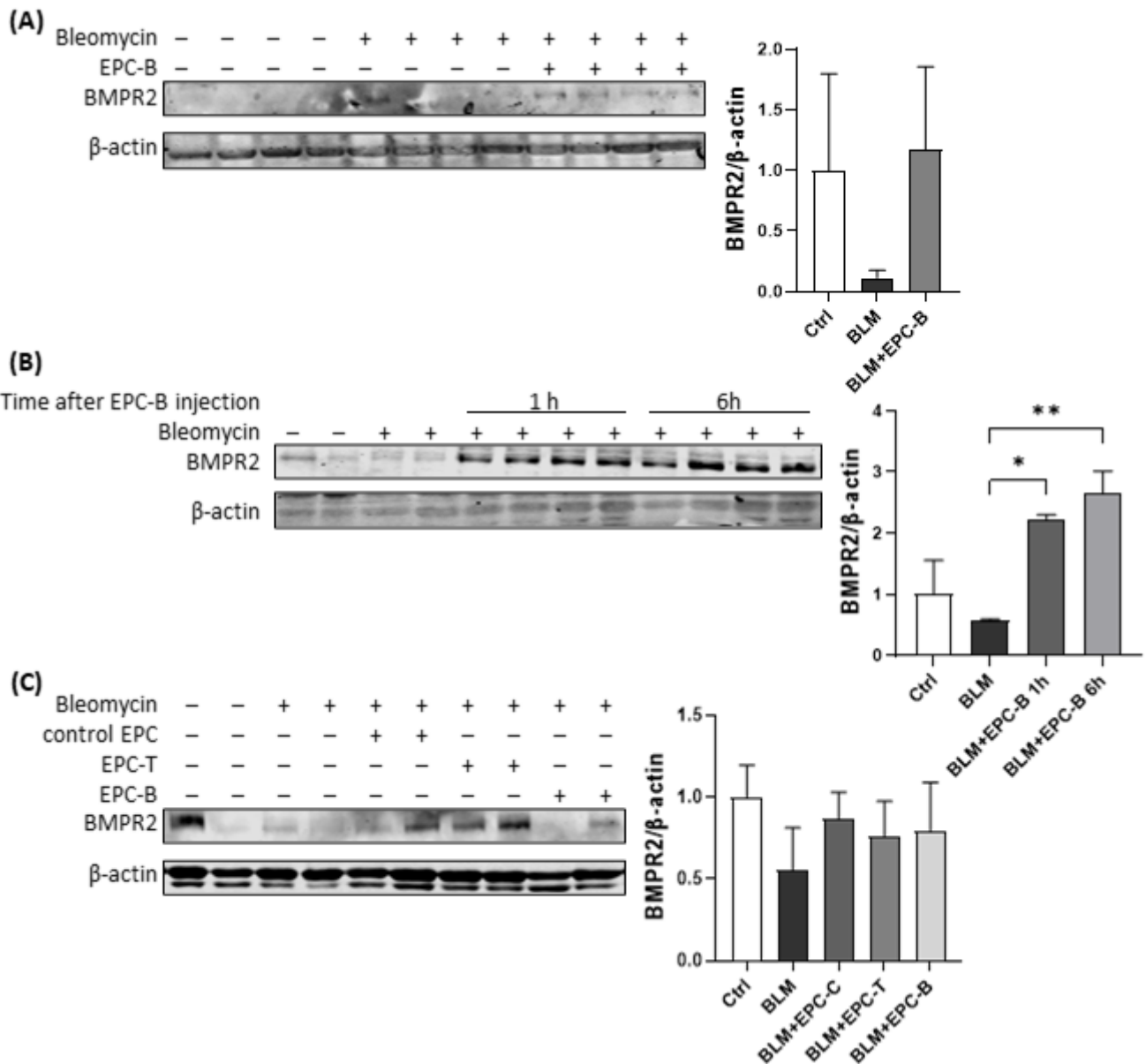


Figure 4-3. Rat EPCs injected from tail veins of rats with bleomycin-induced pulmonary fibrosis accumulated in the lungs shortly after injections. (A) BMPR2 tended to be increased in the lungs of rats with bleomycin-induced pulmonary fibrosis treated with BMPR2-transduced rat EPCs when evaluated 14 days after injections, though statistically insignificant because of large inter-sample variabilities, determined by Western blot (n=8/group, data were from the 14-day prevention study). (B) Significant increase of BMPR2 was observed in the lungs of rats with bleomycin-induced pulmonary fibrosis treated with BMPR2-transduced rat EPCs when evaluated 1 and 6 hours after injections, determined by Western blot (n=4/group). (C) BMPR2 was not increased in the lungs of rats with bleomycin-induced pulmonary fibrosis treated with BMPR2-transduced rat EPCs when evaluated 14 days after injections, determined

by Western blot (n=8/group, data were from the 21-day treatment study). EPC-B, rat EPCs infected by AdBMPR2; Ctrl, control; BLM, bleomycin; EPC-C, control rat EPCs not infected by adenovirus; EPC-T, rat EPCs infected by AdTrack. * $P < 0.05$; ** $P < 0.01$.

3.3 BMPR2-transduced EPC treatment might reduce collagen production in pulmonary fibrosis, though further validation is warranted

After the above-mentioned optimisation studies, I tried to evaluate the effect of tail vein injection of BMPR2-transduced rat EPCs on bleomycin-induced pulmonary fibrosis. However, in this main study, bleomycin administration based on the optimised protocol had not induced pulmonary fibrosis in rat lungs consistently as observed in the optimisation studies. As only 11 out of 35 rats showed sufficient fibrosis in their lungs after bleomycin administration, the freshness of bleomycin solution was considered to be a cause of this problem. So, then I tried to avoid storing bleomycin solution for more than 2 weeks after reconstitution, but the rats having showed sufficient fibrosis in the following studies were still only 24 out of 48 rats. Therefore, because of such inconsistent induction of pulmonary fibrosis, I could not evaluate the genuine effect of BMPR2-transduced EPCs in the 21-day treatment study where all of bleomycin treatment other than control EPC group has failed. On the other hand, all rats assigned to saline control, bleomycin only, and BMPR2-transduced EPC groups in the 14-day prevention study have shown sufficiently severe pulmonary fibrosis. Therefore, I could run some preliminary experiments to evaluate the effect of BMPR2-transduced EPCs for preventing pulmonary fibrosis by directly comparing the results between bleomycin only group and BMPR2-transduced EPC group, though it was impossible to assess the impact of EPCs or adenovirus themselves.

According to the preliminary results from the 14-day prevention study, body weight loss in bleomycin-treated rats was significantly more than that in control rats (Figure 4-4A), while that was not different between bleomycin only group and BMPR2-transduced EPC group. BMPR2 showed a trend of increase in the lungs from BMPR2-transduced EPC group rats (Figure 4-3A), though the trend of mRNA expression was inconsistent with this result (Figure 4-4B). Though modified Ashcroft's score was significantly increased by bleomycin administration, histopathological improvement was not observed in lungs treated with BMPR2-transduced EPCs (Figure 4-4C). Hydroxyproline assay was performed for quantifying collagen content in the lungs. Hydroxyproline was slightly, but significantly reduced in BMPR2-transduced EPC group compared with bleomycin

only group (Figure 4-4D). However, given that the value was the same between control and bleomycin only groups, the reliability of the assay was doubtful. Similarly, fibronectin production was not altered by both bleomycin administration and EPC treatment (Figure 4-4E, F). On the other hand, *col1A1* mRNA was increased by bleomycin administration and reduced by BMPR2-transduced EPC injection, though statistically insignificant (Figure 4-4G). Again, I cannot conclude that BMPR2-transduced EPC therapy is effective for suppressing collagen production, because the results from control EPC group and AdTrack-infected EPC group are unusable as the induction of pulmonary fibrosis by bleomycin failed.

*Due to time restriction, I was unable to pursue re-optimising the bleomycin treatment protocol and restudying some parts of the studies where the induction of pulmonary fibrosis had failed.

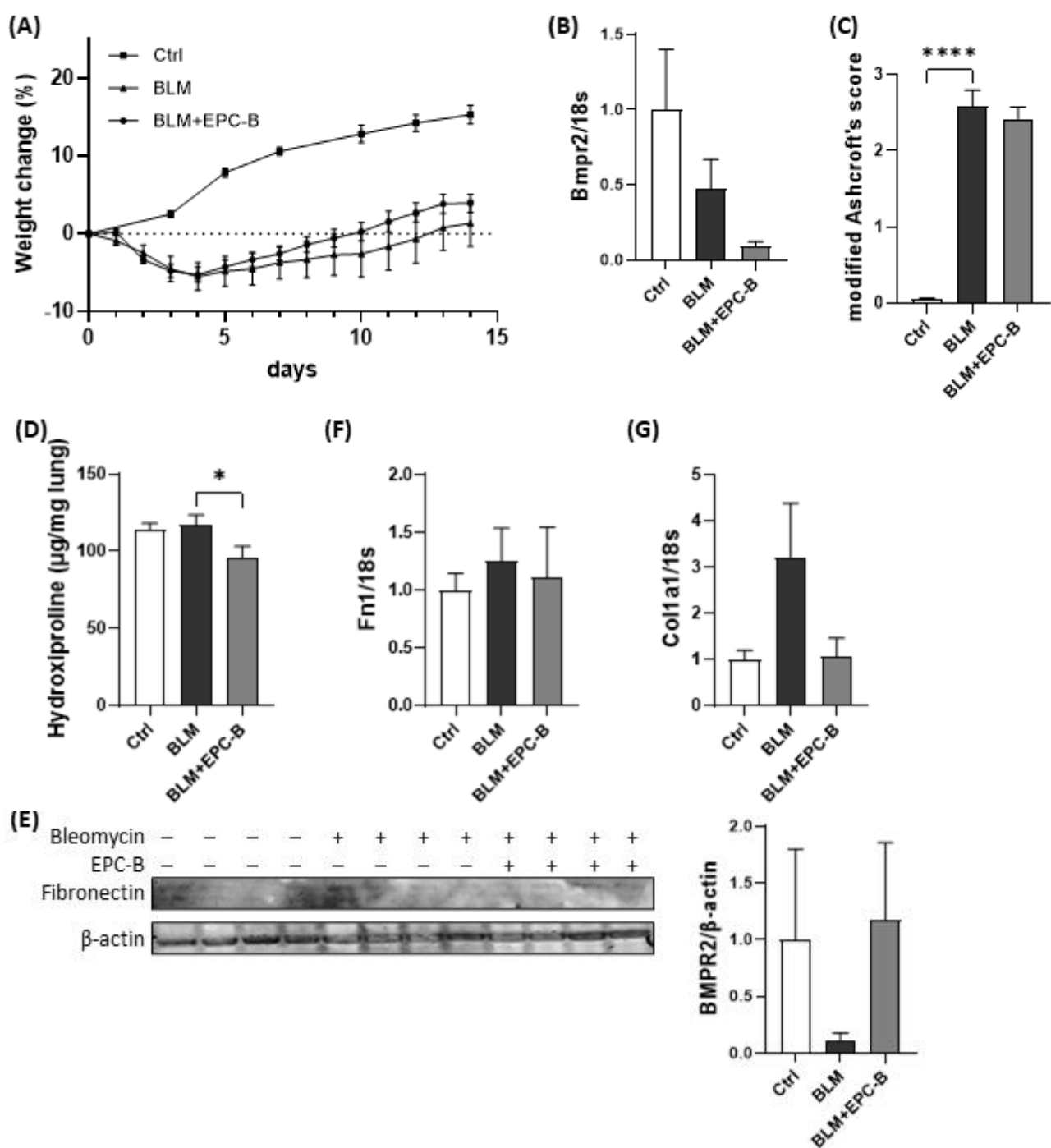


Figure 4-4. Rat EPCs injected from tail veins of rats with bleomycin-induced pulmonary fibrosis accumulated in the lungs shortly after injections. (A) Body weight of rats was reduced by bleomycin administration, but BMPR2-transduced EPC treatment did not have an impact on weight change. (B) *bmpr2* mRNA levels were not increased by BMPR2-transduced EPC treatment, determined by qRT-PCR. (C) Modified Ashcroft's score was significantly increased by bleomycin administration, but BMPR2-transduced EPC treatment did not show an effect on improving histopathological finding in fibrotic lungs. (D) Hydroxyproline was reduced

by BMPR2-transduced EPC treatment, however, was not increased by bleomycin administration, determined by hydroxyproline assay. (E-F) Fibronectin production was not increased by bleomycin administration and not altered by BMPR2-transduced EPC treatment, determined by Western blot (E) and qRT-PCR (F). (G) *col1a1* mRNA levels tended to be increased by bleomycin administration and decreased by BMPR2-transduced EPC treatment, determined by qRT-PCR. N=8/group in all experiments. Ctrl, control; BLM, bleomycin; EPC-B, rat EPCs infected by AdBMPR2; EPC-C, control rat EPCs not infected by adenovirus; EPC-T, rat EPCs infected by AdTrack. * $P < 0.05$; ** $P < 0.01$. * $P < 0.05$; **** $P < 0.0001$.

Part V

**Probable UIP pattern on chest CT is insufficient for
making a definitive diagnosis of IPF**

Statement of Authorship

Title of Paper	Probable usual interstitial pneumonia pattern on chest CT: Is it sufficient for a diagnosis of idiopathic pulmonary fibrosis?
Publication Status	<input checked="" type="checkbox"/> Published <input type="checkbox"/> Accepted for Publication <input type="checkbox"/> Unpublished and Unsubmitted work written in draft style
Publication Details	<u>Fukihara J</u> , Kondoh Y, Brown KK, Kimura T, Kataoka K, Matsuda T, Yamano Y, Suzuki A, Furukawa T, Sumikawa H, Takahashi O, Johkoh T, Tanaka T, Fukuoka J, Hashimoto N, Hasegawa Y. Probable usual interstitial pneumonia pattern on chest CT: Is it sufficient for a diagnosis of idiopathic pulmonary fibrosis? <i>Eur Respir J</i> 2020;55(4):1802465. PMID: 32029448. DOI: 10.1183/13993003.02465-2018.

Principal Author

Name of Principal Author (Candidate)	Jun Fukihara		
Contribution to the Paper	Designed the study, collected the data, performed statistical analysis, interpreted the results, drafted and revised the manuscript.		
Overall percentage (%)	80%		
Certification:	This paper reports on original research I conducted during the period of my Higher Degree by Research candidature and is not subject to any obligations or contractual agreements with a third party. I am the primary author of this paper.		
Signature	<table border="1"><tr><td>Date</td><td>16/Jun/2021</td></tr></table>	Date	16/Jun/2021
Date	16/Jun/2021		

Co-Author Contributions

By signing the Statement of Authorship, each author certifies that:

- the candidate's stated contribution to the publication is accurate (as detailed above);
- permission is granted for the candidate to include the publication in the thesis; and
- the sum of all co-author contributions is equal to 100% less the candidate's stated contribution.

Name of Co-Author	Yasuhiro Kondoh		
Contribution to the Paper	Supported the design of the study, data collection and interpretation of the results, made a final diagnosis for each patient, performed CT classification as one of the radiological interpreters, and edited the manuscript.		
Signature	<table border="1"><tr><td>Date</td><td>16/Jun/2021</td></tr></table>	Date	16/Jun/2021
Date	16/Jun/2021		

Name of Co-Author	Kevin K Brown		
Contribution to the Paper	Supported the interpretation of the results and edited the manuscript.		
Signature	<table border="1"><tr><td>Date</td><td>16/Jun/2021</td></tr></table>	Date	16/Jun/2021
Date	16/Jun/2021		

Please cut and paste additional co-author panels here as required.

Name of Co-Author	Tomoki Kimura		
Contribution to the Paper	Supported data collection and edited the manuscript.		
Signature		Date	16/Jun/2021

Name of Co-Author	Kensuke Kataoka		
Contribution to the Paper	Supported data collection and edited the manuscript.		
Signature		Date	16/Jun/2021

Name of Co-Author	Toshiaki Matsuda		
Contribution to the Paper	Supported data collection and edited the manuscript.		
Signature		Date	16/Jun/2021

Name of Co-Author	Yasuhiko Yamano		
Contribution to the Paper	Supported data collection and edited the manuscript.		
Signature		Date	16/Jun/2021

Name of Co-Author	Atsushi Suzuki		
Contribution to the Paper	Supported the design of the study and data collection.		
Signature		Date	16/Jun/2021

Name of Co-Author	Taiki Furukawa		
Contribution to the Paper	Supported the design of the study, data collection and statistical analysis.		
Signature		Date	16/Jun/2021

Name of Co-Author	Hiromitsu Sumikawa		
Contribution to the Paper	Made a radiological diagnosis for each patient and performed CT classification as one of the radiologists.		
Signature		Date	16/Jun/2021

Name of Co-Author	Osamu Takahashi		
Contribution to the Paper	Supported statistical analysis and the interpretation of the results and edited the manuscript.		
Signature		Date	16/Jun/2021

Name of Co-Author	Takeshi Johkoh		
Contribution to the Paper	Made a radiological diagnosis for each patient and performed CT classification as one of the radiologists and edited the manuscript.		
Signature		Date	16/Jun/2021

Name of Co-Author	Tomonori Tanaka		
Contribution to the Paper	Made a histopathological diagnosis for each patient and performed histopathological classification as one of the pathologists.		
Signature		Date	16/Jun/2021

Name of Co-Author	Junya Fukuoka		
Contribution to the Paper	Made a histopathological diagnosis for each patient and performed histopathological classification as one of the pathologists.		
Signature		Date	16/Jun/2021

Name of Co-Author	Naozumi Hashimoto		
Contribution to the Paper	Supported the design of the study and interpretation of the results.		
Signature		Date	16/Jun/2021

Name of Co-Author	Yoshinori Hasegawa		
Contribution to the Paper	Supported the design of the study and interpretation of the results.		
Signature		Date	16/Jun/2021

Name of Co-Author			
Contribution to the Paper			
Signature		Date	

Name of Co-Author			
Contribution to the Paper			
Signature		Date	

Name of Co-Author			
Contribution to the Paper			
Signature		Date	

Name of Co-Author			
Contribution to the Paper			
Signature		Date	

Name of Co-Author			
Contribution to the Paper			
Signature		Date	



Probable usual interstitial pneumonia pattern on chest CT: is it sufficient for a diagnosis of idiopathic pulmonary fibrosis?

Jun Fukihara^{1,2}, Yasuhiro Kondoh², Kevin K. Brown³, Tomoki Kimura², Kensuke Kataoka², Toshiaki Matsuda², Yasuhiko Yamano², Atsushi Suzuki^{1,2}, Taiki Furukawa⁴, Hiromitsu Sumikawa⁵, Osamu Takahashi⁶, Takeshi Johkoh⁷, Tomonori Tanaka⁸, Junya Fukuoka⁹, Naozumi Hashimoto¹ and Yoshinori Hasegawa¹

Affiliations: ¹Dept of Respiratory Medicine, Nagoya University Graduate School of Medicine, Nagoya, Japan. ²Dept of Respiratory Medicine and Allergy, Tosei General Hospital, Seto, Japan. ³Dept of Medicine, National Jewish Health, Denver, CO, USA. ⁴Dept of Medical IT Center, Nagoya University Hospital, Nagoya, Japan. ⁵Dept of Radiology, Osaka International Cancer Institute, Osaka, Japan. ⁶Support Unit for Conducting Clinically Essential Study, St Luke's International University Graduate School of Public Health, Tokyo, Japan. ⁷Dept of Radiology, Kinki Central Hospital of Mutual Aid Association of Public School Teachers, Itami, Japan. ⁸Dept of Pathology, Kinki University Faculty of Medicine, Osakasayama, Japan. ⁹Dept of Pathology, Nagasaki University Graduate School of Biomedical Sciences, Nagasaki, Japan.

Correspondence: Yasuhiro Kondoh, Dept of Respiratory Medicine and Allergy, Tosei General Hospital, 160 Nishioiwake-cho, Seto, Aichi, Japan, 489-8642. E-mail: lung@tosei.or.jp

 @ERSpublications

Except when the final diagnosis is IPF, idiopathic interstitial pneumonia (IIP) patients with a probable usual interstitial pneumonia (UIP) pattern on chest CT have a longer survival time and time to first acute exacerbation than those with a UIP pattern <http://bit.ly/2FOJa2F>

Cite this article as: Fukihara J, Kondoh Y, Brown KK, *et al.* Probable usual interstitial pneumonia pattern on chest CT: is it sufficient for a diagnosis of idiopathic pulmonary fibrosis? *Eur Respir J* 2020; 55: 1802465 [<https://doi.org/10.1183/13993003.02465-2018>].

ABSTRACT Recent studies have suggested that in patients with an idiopathic interstitial pneumonia (IIP), a probable usual interstitial pneumonia (UIP) pattern on chest computed tomography (CT) is sufficient to diagnose idiopathic pulmonary fibrosis (IPF) without histopathology.

We retrospectively compared the prognosis and time to first acute exacerbation (AE) in IIP patients with a UIP and a probable UIP pattern on initial chest CT.

One hundred and sixty IIP patients with a UIP pattern and 242 with a probable UIP pattern were identified. Probable UIP pattern was independently associated with longer survival time (adjusted hazard ratio 0.713, 95% CI 0.536–0.950; $p=0.021$) and time to first AE (adjusted hazard ratio 0.580, 95% CI 0.389–0.866; $p=0.008$). In subjects with a probable UIP pattern who underwent surgical lung biopsy, the probability of a histopathological UIP pattern was 83%. After multidisciplinary discussion and the inclusion of longitudinal behaviour, a diagnosis of IPF was made in 66% of cases. In IPF patients, survival time and time to first AE were not associated with CT pattern. Among subjects with a probable UIP pattern, compared to non-IPF patients, survival time and time to first AE were shorter in IPF patients.

In conclusion, IIP patients with a probable UIP pattern on initial chest CT had a better prognosis and longer time to first AE than those with a UIP pattern. However, when baseline data and longitudinal behaviour provided a final diagnosis of IPF, CT pattern was not associated with these outcomes. This suggests diagnostic heterogeneity among patients with a probable UIP pattern.

This article has an editorial commentary: <https://doi.org/13993003.00590-2020>

This article has supplementary material available from erj.ersjournals.com

Received: 29 Dec 2018 | Accepted after revision: 31 Dec 2019

Copyright ©ERS 2020

Introduction

Idiopathic pulmonary fibrosis (IPF) is a chronic, progressive idiopathic interstitial pneumonia (IIP) with poor prognosis that is characterised histopathologically by a usual interstitial pneumonia (UIP) pattern [1]. Due to its poor prognosis, an accurate diagnosis is important. According to the recently published Fleischner Society white paper [1] and the 2018 IPF guidelines [2], in the appropriate clinical setting a “UIP pattern” on computed tomography (CT) (subpleural basal predominance, reticular abnormality and honeycombing) is sufficient to establish a diagnosis of IPF without the need for a surgical lung biopsy (SLB). On the other hand, patients with a “probable UIP pattern” (the same criteria as for a UIP pattern but without honeycombing and with traction bronchiectasis), an “indeterminate for UIP pattern” (subpleural basal predominance, evidence of fibrosis not suggestive of a specific aetiology) or an “alternative diagnosis” on CT require SLB for a definitive diagnosis. However, a substantial number of patients will not undergo surgery for a variety of reasons, including refusal or excessive perioperative risk (e.g. severe physiologic impairment or comorbidities), and remain without a definitive diagnosis.

In the previous IPF guidelines, published in 2011 [3], the current probable UIP and indeterminate for UIP patterns were collectively classified as “possible UIP pattern”. In the two INPULSIS trials [4], which evaluated the efficacy and safety of nintedanib in the treatment of IPF, IIP subjects who showed a fibrosing interstitial pneumonia with a combination of traction bronchiectasis and a possible UIP pattern on CT were considered to have a diagnosis of IPF, without the need for SLB. In a *post hoc* analysis, the IPF subjects enrolled with a possible UIP pattern and traction bronchiectasis showed similar disease progression and treatment responsiveness to subjects enrolled with IPF as diagnosed based strictly on the 2011 guidelines [5]. Additionally, BROWNELL *et al.* [6] have revealed that an increasing extent of traction bronchiectasis increases the positive predictive value (PPV) of a possible UIP pattern for an underlying histopathological UIP pattern. Others have reported that traction bronchiectasis on CT is correlated with a poor prognosis in patients with fibrotic IIP [7, 8]. These results are considered to be supportive evidence for the diagnostic value of possible UIP pattern with traction bronchiectasis (*i.e.* the current probable UIP pattern) on CT for histopathological UIP pattern.

However, the INPULSIS trials [4] recruited patients who were clinically suspected to have IPF by physicians with expertise in the diagnosis of interstitial lung disease (ILD). Therefore, it is possible that the PPV of a possible UIP pattern with traction bronchiectasis for histopathological UIP pattern and a diagnosis of IPF was higher in the INPULSIS trials than would be seen in a real-world setting (*i.e.* populations seen in routine clinical practice). Additionally, the validity of the inclusion criteria of the INPULSIS trials has never been evaluated from the perspective of survival time, a fundamental concern of both clinicians and patients.

To estimate the validity of this approach, we compared survival time in IIP patients having a UIP pattern with that in patients having a probable UIP pattern, in a real-world setting. We also compared time to first acute exacerbation (AE) between the two CT patterns.

Patients and methods

Study design and population

This study was approved by the institutional review board of Tosei General Hospital (Seto, Aichi, Japan). Informed consent was not required as the data were collected retrospectively and anonymously analysed.

A retrospective review of consecutive patients with ILD evaluated at Tosei General Hospital from January 2008 to March 2013 was performed. Patients included were those who underwent an initial workup for a suspected diagnosis of IIP and whose CT scans at initial workup were available. Patients excluded were those with an indeterminate for UIP or an alternative diagnosis pattern on CT [2], a diagnosis of connective tissue disease (CTD), chronic hypersensitivity pneumonitis (CHP) or other identifiable causes of ILD, those with concurrently associated malignant diseases, those lost to follow up within 1 year of the initial workup for reasons other than death and those who did not undergo a pulmonary function test (PFT) at the initial workup. All patients with clinically suspected IIP prior to SLB were included in the analysis, regardless of final diagnosis.

All patients with a UIP pattern or a probable UIP pattern on CT were included in the statistical analyses and we compared survival time and time to first AE between the two CT patterns. The same analyses were also performed in patients with a diagnosis of IPF and between IPF and non-IPF diagnoses in patients with a probable UIP pattern.

Data collection

Patient characteristics and test results were collected retrospectively from clinical charts. Initial workup data including PFTs, arterial blood gas analyses and CT scans conducted within 1 month were collected. Forced vital capacity (FVC) and diffusing capacity of the lung for carbon monoxide (D_{LCO}) were expressed as

percentages of the predicted values [9, 10]. The final follow-up date was December 31, 2016. The date of initial evaluation, date of last follow-up with survival status and date of diagnosis of the first AE were also recorded.

Definition of an AE

An AE was defined as a clinical event meeting all the following criteria [11]: 1) an acute respiratory deterioration characterised by evidence of new widespread alveolar abnormality; 2) acute worsening or development of dyspnoea within 1 month; 3) CT scan of the chest with new bilateral ground-glass opacity superimposed on a background pattern consistent with UIP; and 4) deterioration not fully explained by cardiac failure, fluid overload or infection.

Radiological and histopathological evaluation

All CT scans were independently reviewed by two experienced thoracic radiologists (TJ and HS) and an experienced thoracic physician (YK). To evaluate inter-observer variability, scans from 100 patients chosen at random from the study population were reviewed by each reviewer and Fleiss' κ -value was calculated. Published criteria were used to categorise CT scans as definite, probable or indeterminate for UIP pattern, or as findings of an alternative diagnosis [2]. Furthermore, each reviewer was blinded to the clinical and histopathological information. Given the κ -value (0.66, 95% CI 0.52–0.79), radiological interpretation of eligible cases was performed by one of the three reviewers.

A subset of patients had undergone SLB and all lung biopsy specimens were anonymised for histopathological analysis, and reviewed by two experienced pulmonary pathologists (JF and TT) who were blinded to clinical and radiological information and consulted each other about histopathological decisions. Published criteria were used to categorise histopathological findings [2].

Final diagnoses of ILDs

As the institute where the study was conducted was a local public hospital as well as a tertiary referral hospital, almost all patients were seen at least once every 3 months in the first year after initial workup, and every 3–6 months in the following years. All information regarding emergency department visits and/or hospitalisation was also captured. Under these circumstances, all available follow-up information was reviewed when making the final clinical diagnoses.

When histopathological information was available, the final diagnoses were established through multidisciplinary discussion (MDD) by clinicians, radiologists and pathologists with reference to the published criteria for IPF [2] and the classification for IIPs [12]. During the MDD, the clinical context and course, chest imaging and histopathology (if available) were reviewed in order to provide a final diagnosis. A diagnosis of “unclassifiable ILD” was made for patients with a non-IPF final diagnosis and histopathological features suggesting an alternative diagnosis (cellular inflammatory infiltration apart from areas of honeycombing, prominent lymphoid hyperplasia including secondary germinal centres, or a distinctly bronchiolocentric distribution including extensive peribronchiolar metaplasia). A diagnosis of CHP was made when histopathological features and clinical course were compatible, even if a history of exposure to specific antigens was lacking.

If histopathology was not available, the diagnosis of IPF was made when the clinical context was that of an IIP and the CT showed a UIP pattern. The patients with a probable UIP pattern on CT but no histopathology were provisionally classified as IPF when the likelihood of the diagnosis was believed to be >70% [12], while being classified as unclassifiable ILD when the clinical context was that of an IIP and clinical course did not suggest a specific diagnosis [12–14]. Findings suggestive of CTD, CHP and other identifiable causes or associations were actively sought out at the time of initial workup and during follow-up. We validated the clinical unclassifiable ILD diagnoses using a second approach (supplementary material).

Statistical analysis

Continuous variables were presented as medians with interquartile range (IQR) as they showed a non-normal distribution. Categorical variables were summarised by number of patients and percentage. To assess the differences in variables between subgroups, the Mann–Whitney U-test was used for continuous variables and the Pearson Chi-squared test was used for categorical variables. Survival time and time to first AE were measured from the date of initial workup until the date of death or the first diagnosis of AE, respectively. The Kaplan–Meier method was applied to show unadjusted survival curves, and mortality rate and AE rate were shown per 100 person-years.

Cox proportional hazards models were used to evaluate the associations between CT pattern or IPF diagnosis and survival time. The prognostic impacts were adjusted by demographic information generally associated with survival time: age, gender, baseline FVC [15], baseline D_{LCO} [16–18] and use of anti-fibrotics [4, 19]. Competing risk analyses were used to evaluate the associations between CT pattern or IPF diagnosis and time to first AE, in order to account for competing risks such as death from disease

progression without AE. The predictive values for time to first AE were adjusted by variables that have been reported to be associated with AE: baseline FVC [20–23], baseline D_{LCO} [21, 24] and use of anti-fibrotics. Multiple imputation analyses were performed to estimate survival time and time to first AE under the assumption of missing data. We carried out some imputations using all potential predictor variables in each imputation model. The overall proportion of patients with missing data was 2%, in all of whom D_{LCO} could not be assessed at baseline due to excessively low pulmonary function.

The adjusted annual rate of change in FVC was analysed with the use of a random coefficient regression model (with random slopes and intercepts) that included sex, age and height as covariates. The impact of CT pattern and IPF diagnosis were determined using estimated slopes for each study group on the basis of the time-by-treatment interaction term from the mixed model. Missing data were assumed to be missing at random and were not imputed.

All statistical tests were two sided and p-values of less than 0.05 were considered statistically significant. Statistical analyses were carried out using SPSS version 25.0 (SPSS Inc., Chicago, IL, USA) and Stata version 13.1 (StataCorp, College Station, TX, USA).

Results

Patient characteristics

A total of 682 patients underwent an initial workup for suspected IIP that included a CT scan of the chest. After excluding 280 patients, 160 patients with a UIP pattern and 242 with a probable UIP pattern were identified (figure 1). The validity of this sample size for the analyses performed was confirmed (supplementary material). Median follow-up time was 42.9 months (range 0.8–104.4 months).

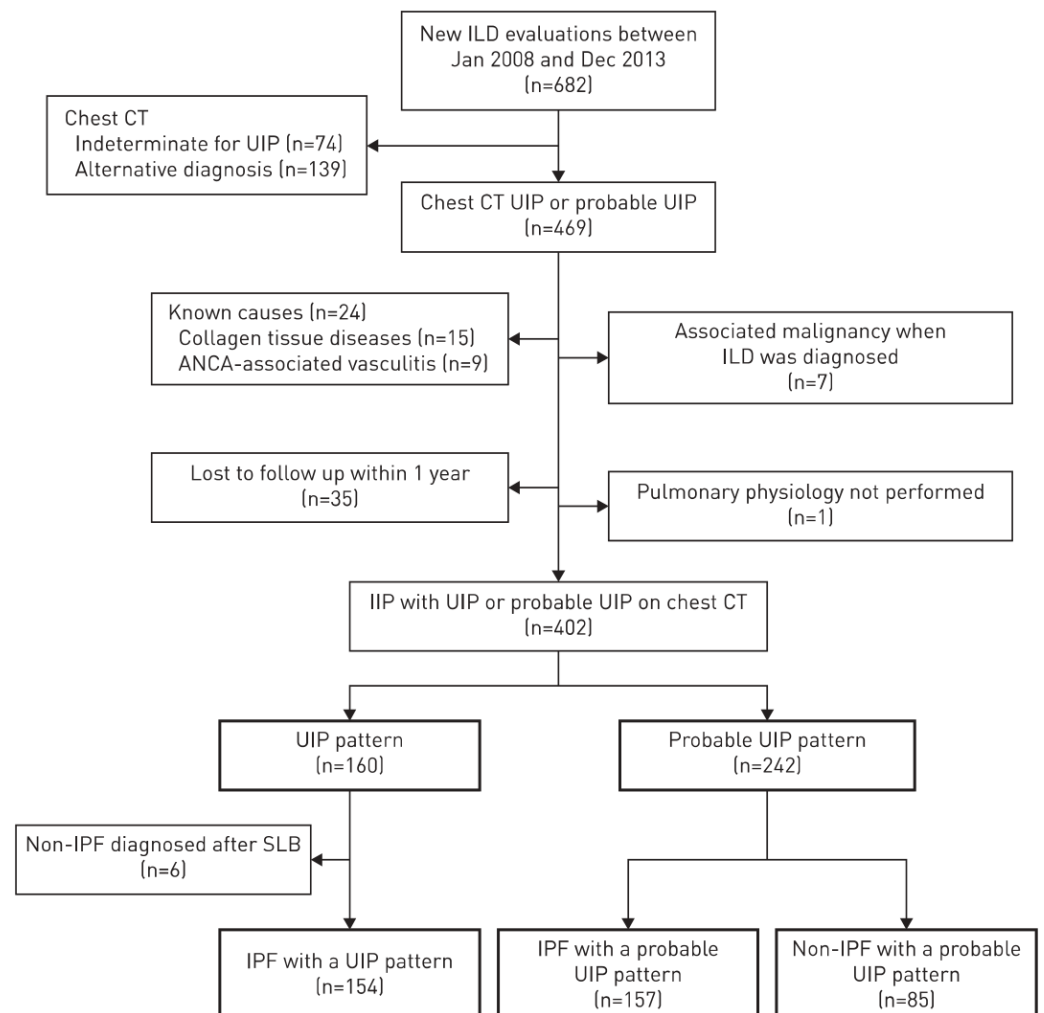


FIGURE 1 Screening and inclusion scheme for patients in the study. ILD: interstitial lung disease; CT: computed tomography; UIP: usual interstitial pneumonia; ANCA: anti-neutrophil cytoplasmic antibody; IIP: idiopathic interstitial pneumonia; IPF: idiopathic pulmonary fibrosis; SLB: surgical lung biopsy.

The clinical characteristics (table 1) showed significantly fewer males and smokers among patients with a probable UIP pattern and those with a non-IPF diagnosis when compared with other groups. Those with IPF and a UIP pattern showed a significantly lower FVC. The prevalence of a histopathological UIP pattern was 82% (27 out of 32) for a UIP pattern and 83% (90 out of 109) for a probable UIP pattern on chest CT, while the probability of an MDD diagnosis of IPF declined to 66% (72 out of 109) with a probable UIP pattern.

Prognosis: UIP pattern versus probable UIP pattern

The median survival time was 43.5 months for UIP pattern and 72.1 months for probable UIP pattern (figure 2a). Median time to first AE was 86.0 months for UIP pattern and 93.1 months for probable UIP pattern (figure 2b). In the imputed dataset, probable UIP pattern was independently associated with longer survival time (adjusted hazard ratio 0.722, 95% CI 0.540–0.965; $p=0.028$) (table 2) and longer time to first AE (adjusted hazard ratio 0.586, 95% CI 0.387–0.888; $p=0.012$) (table 3).

Prognosis of IPF: UIP pattern versus probable UIP pattern

Among subjects with a final diagnosis of IPF, survival time, time to first AE and their predictors were compared between those with a UIP pattern and those with a probable UIP pattern. Although survival time was longer in those with a probable UIP pattern, time to first AE was similar in the two groups (42.6 months *versus* 67.4 months and 86.0 months *versus* 90.9 months, respectively). CT pattern was not significantly associated with survival time (adjusted hazard ratio 0.883, 95% CI 0.640–1.218; $p=0.447$) (table 2) or time to first AE (adjusted hazard ratio 0.803, 95% CI 0.517–1.248; $p=0.329$) (table 3) in the imputed dataset.

TABLE 1 Characteristics of patients in the study

Characteristic	UIP pattern on CT (n=160)	Probable UIP pattern on CT		
		Total (n=242)	IPF (n=157)	non-IPF (n=85)
Age years	69 [65–72]	67 [61–71] [#]	66 [61–71] [#]	68 [62–71]
Male gender	131 (82)	185 (76)	126 (80)	59 (69) [#]
Smokers	129 (81) (n=159)	171 (71) [#]	116 (74)	55 (65) [#]
Smoking pack-years	39.0 [15.0–55.0] (n=159)	30.0 [0.0–50.0] [#]	30.0 [0.0–51.0]	30.0 [0.0–46.5] [#]
FVC L	2.40 [1.85–2.93]	2.73 [2.01–3.27] [#]	2.78 [2.07–3.28] [#]	2.60 [2.04–3.29]
FVC % predicted	74.0 [63.8–89.4]	88.3 [72.8–100.4] [#]	87.4 [72.8–99.9] [#]	89.2 [72.7–102.2] [#]
D_{LCO} % predicted	52.8 [41.0–66.6] (n=155)	65.6 [52.4–82.9] [#] (n=238)	63.1 [51.7–79.3] [#] (n=155)	69.6 [55.9–87.3] [#] (n=83)
P_{aO_2} mmHg	78.0 [70.8–87.7] (n=155)	82.3 [74.7–90.7] [#] (n=230)	82.0 [76.0–91.4] [#] (n=154)	82.4 [73.4–89.2] (n=76)
Treatment				
Anti-fibrotics	87 [54]	115 [48]	92 [59]	23 [27] ^{#,‡}
Corticosteroids	18 [11]	41 [17]	24 [15] [#]	17 [20] [#]
Histopathological pattern	n=32	n=109	n=72	n=37
Definite/probable UIP	27 [84]	90 [83]	71 [99]	19 [51] ⁺
Indeterminate for UIP	2 [6]	5 [5]	1 [1]	4 [11]
Alternative diagnosis	3 [9]	14 [13]	0 [0]	14 [38]
Final diagnosis (with SLB)				
IPF	26 [81]	72 [66]	72 [100]	0 [0]
NSIP	1 [3]	8 [7]	0 [0]	8 [22]
Unclassifiable ILD	4 [13]	22 [20]	0 [0]	22 [59]
Other	1 [3]	7 [19]	0 [0]	7 [19]
Final diagnosis (with clinical diagnosis)				
IPF	154 [96]	157 [65]	157 [100]	0 [0]
NSIP	1 [1]	8 [3]	0 [0]	8 [9]
Unclassifiable ILD	4 [3]	70 [29]	0 [0]	70 [82]
Other	1 [1]	7 [3]	0 [0]	7 [8]

Data are presented as median (IQR) or n (%) unless otherwise stated. UIP: usual interstitial pneumonia; CT: computed tomography; IPF: idiopathic pulmonary fibrosis; FVC: forced vital capacity; D_{LCO} : diffusing capacity of the lung for carbon monoxide; P_{aO_2} : arterial oxygen tension; SLB: surgical lung biopsy; NSIP: nonspecific interstitial pneumonia; ILD: interstitial lung disease; IQR: interquartile range. [#]: significantly different compared with a UIP pattern on CT; [‡]: significantly different compared with a probable UIP pattern and IPF diagnosis; ⁺: has features that raise concerns about the likelihood of an alternative diagnosis, such as a cellular inflammatory infiltration apart from areas of honeycombing, prominent lymphoid hyperplasia including secondary germinal centres and a distinctly bronchiolocentric distribution that could include extensive peribronchiolar metaplasia.

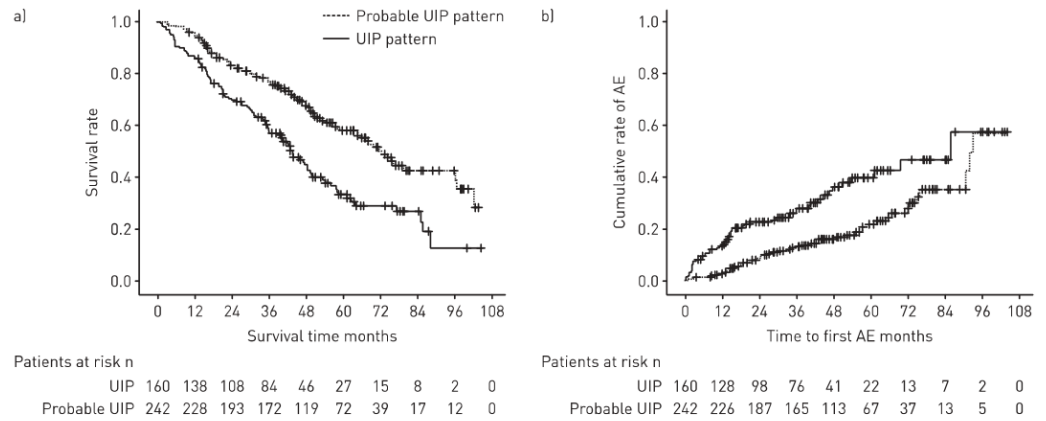


FIGURE 2 Kaplan–Meier curves of subjects with a usual interstitial pneumonia (UIP) pattern and those with a probable UIP pattern. a) Overall survival: the adjusted hazard ratio [0.722, 95% CI 0.540–0.965; p=0.028] for a probable UIP pattern (versus a UIP pattern) was evaluated by Cox proportional hazard analysis. b) Time to first acute exacerbation (AE): adjusted hazard ratio [0.586, 95% CI 0.387–0.888; p=0.012] for a probable UIP pattern (versus a UIP pattern) was evaluated by competing risk analysis.

Prognosis of probable UIP pattern: final diagnosis of IPF versus non-IPF

Survival time, time to first AE and factors associated with them were evaluated in IPF and non-IPF subjects with a probable UIP pattern. Both survival time (67.4 months versus median not reached) and time to first AE (90.9 months versus median not reached) were numerically shorter in IPF. In the imputed dataset, a final diagnosis of IPF was independently associated with survival time (adjusted hazard ratio 1.879, 95% CI 1.138–3.103; p=0.014) (table 2) and time to AE (adjusted hazard ratio 2.935, 95% CI 1.206–7.145; p=0.018) (table 3).

The adjusted annual rate of change in FVC did not significantly differ between UIP pattern and probable UIP pattern, nor did it differ between the two CT patterns in subjects with IPF. In subjects with a probable UIP pattern, the annual decline was significantly larger in those with a diagnosis of IPF than of non-IPF (supplementary material).

In the analyses carried out with the non-imputed dataset, survival time and time to first AE did not differ significantly between UIP pattern and probable UIP pattern, nor did they differ between the two CT patterns in subjects with IPF. In subjects with a probable UIP pattern, survival time was significantly shorter in those with a diagnosis of IPF than of non-IPF, but the difference in time to first AE was not significant.

Detail data for the adjusted annual rate of change in FVC and results from the non-imputed dataset are shown in the supplementary material.

TABLE 2 Mortality rate and Cox proportional hazard analysis for survival time

Parameters	Patients n	Deaths n	Mortality rate [#] (95% CI)	Adjusted hazard ratio (95% CI)	p-value [¶]
All patients					
UIP pattern on CT	160	99	19.8 [16.2–24.1]	Reference	0.028
Probable UIP pattern on CT	242	103	10.6 [8.8–12.9]	0.722 [0.540–0.965]	
IPF only					
UIP pattern on CT	154	96	20.5 [16.8–25.0]	Reference	0.447
Probable UIP pattern on CT	157	77	12.1 [9.7–15.2]	0.883 [0.640–1.218]	
Probable UIP pattern only					
Final diagnosis of non-IPF	85	26	7.8 [5.3–11.4]	Reference	0.014
Final diagnosis of IPF	157	77	12.1 [9.7–15.2]	1.879 [1.138–3.103]	

Hazard ratios were based on data modified by the multiple imputation method and adjusted by age, sex, baseline (% predicted) forced vital capacity (FVC), baseline (% predicted) diffusing capacity of the lung for carbon monoxide (D_{LCO}) and use of anti-fibrotics. UIP: usual interstitial pneumonia; CT: computed tomography; IPF: idiopathic pulmonary fibrosis. [#]: mortality rate per 100 person-years; [¶]: p-value for the hazard ratio.

TABLE 3 Acute exacerbation (AE) rate and competing risk analysis for time to first AE

Parameters	Patients n	AEs n	AE rate [#] (95% CI)	Adjusted hazard ratio (95% CI)	p-value [¶]
All patients					
UIP pattern on CT	160	51	11.1 [8.5–14.7]	Reference	0.012
Probable UIP pattern on CT	242	49	5.3 [4.0–7.0]	0.586 [0.387–0.888]	
IPF only					
UIP pattern on CT	154	49	11.5 [8.7–15.2]	Reference	0.329
Probable UIP pattern on CT	157	40	6.7 [4.9–9.1]	0.803 [0.517–1.248]	
Probable UIP pattern only					
Final diagnosis of non-IPF	85	9	2.7 [1.4–5.2]	Reference	0.018
Final diagnosis of IPF	157	40	6.7 [4.9–9.1]	2.935 [1.205–7.145]	

Hazard ratios were based on data modified by the multiple imputation method and adjusted by baseline (% predicted) forced vital capacity (FVC), baseline (% predicted) diffusing capacity of the lung for carbon monoxide (D_{LCO}) and use of anti-fibrotics. UIP: usual interstitial pneumonia; CT: computed tomography; IPF: idiopathic pulmonary fibrosis. [#]: AE rate per 100 person-years; [¶]: p-value for the hazard ratio.

Discussion

The INPULSIS [4] trials regarded the presence of an IIP and a probable UIP pattern as sufficient for diagnosing IPF without SLB, and showed that these subjects had a similar rate of disease progression compared to those with guideline-diagnosed IPF [5]. Based on that result and in the appropriate clinical context, patients with a probable UIP pattern can be expected to have comparable longitudinal disease behaviour to those who meet the guideline definition of IPF. However, the validity of this finding in the real-world or from the perspective of survival time has never been tested.

Our study provides new information about probable UIP pattern in a real-world setting. Among patients initially evaluated for an IIP, a probable UIP pattern is 50% more common than a UIP pattern. Prognostically, we demonstrate that patients with a probable UIP pattern on CT generally have a longer survival time and longer time to first AE than those with a UIP pattern, even after adjustment for other known prognostic factors. However, our data support the specific INPULSIS trial data (*i.e.* when patients with a final MDD diagnosis of IPF were analysed, the diagnosis predicted a poor prognosis and CT pattern was not a significant predictor of outcome), while recognising that, in our study, the diagnosis of IPF was made with the combination of baseline and longitudinal follow-up data, making it not applicable for predicting prognosis at initial presentation. Although there are some inconsistencies between the results from the imputed and non-imputed datasets, it is likely because those patients in whom D_{LCO} could not be measured due to extremely poor pulmonary function were excluded from the multivariate analyses in the non-imputed dataset. Exclusion of these subjects with the most severely impaired lung function possibly resulted in the reduction of the intergroup prognostic differences.

The probability of a histopathological UIP pattern in patients with a probable UIP pattern on CT remains controversial. Although some studies have reported PPVs of possible UIP pattern, according to the 2011 guidelines (*i.e.* ignoring the existence of traction bronchiectasis), for histopathological UIP pattern of more than 90% [25, 26], these studies have dealt with patients from randomised controlled trials for IPF (*i.e.* patients already diagnosed with IPF by expert ILD physicians). Consequently, there is unavoidable selection bias that may lead to an elevated PPV and, in real-world cohorts, the PPVs have been lower (approximately 60–70%) [6, 27, 28]. BROWNELL *et al.* [6] reported that the extent of traction bronchiectasis can increase the PPV of possible UIP pattern for histopathological UIP pattern and CHUNG *et al.* [29] found a prevalence of histopathological UIP pattern in patients with a probable UIP pattern that was similar to ours (82.4%). Thus, the inclusion of traction bronchiectasis in the definition of possible UIP pattern likely increases the PPV of histopathological UIP pattern. On the other hand, our cohort showed a final diagnosis of IPF of only 62% after MDD, suggesting that MDD is still important in making a definitive diagnosis of IPF in patients with a probable UIP pattern.

The extent of fibrosis on CT scan has been reported as a prognostic factor in both IPF [7, 17, 30] and fibrotic IIP [8, 18, 31]. However, quantification of the extent of fibrosis is difficult and alternative approaches to radiological evaluation have also been adopted to evaluate prognosis. SUMIKAWA *et al.* [7] showed the existence of traction bronchiectasis to be a prognostic factor, while JEONG *et al.* [32] reported that IPF with honeycombing had poorer prognosis than that without honeycombing. Although some studies demonstrated no statistical difference in survival between a UIP pattern and a possible UIP pattern in patients with fibrotic IIP based on log rank tests, the Kaplan–Meier curves shown in those articles suggest that, with greater numbers or longer follow-up, subjects with a possible UIP pattern might have

better outcomes [15, 33]. Our real-world data shows longer survival in patients with a probable UIP pattern compared with a UIP pattern, even though the definition includes the presence of traction bronchiectasis. However, in cohorts limited to subjects with a final diagnosis of IPF, we found no survival difference between UIP pattern and probable UIP pattern after adjustment for other relevant variables, as compatible with past reports [7, 34, 35].

Regarding non-radiological baseline prognostic factors, although the number of studies evaluating the prognostic impact of CT findings in multivariate analysis together with non-radiological variables is limited, the extent of fibrosis on CT and D_{LCO} or FVC have been reported as independent prognostic factors in patients with IPF [16, 17] and fibrotic IIP [15, 18]. In our study, probable UIP pattern (compared to UIP pattern) was independently associated with prognosis even when age, gender and usage of anti-fibrotics were included together with those physiological parameters.

AE has a significant impact on mortality [11], and a low FVC [20–23], low D_{LCO} [21, 24] and recent decline in FVC [20, 36, 37] are all reported to be risk factors for AE in IPF. Although AE is also reported in patients with non-IPF ILDs [38–40], it is more frequent in IPF than in IIP with a pattern other than UIP on CT scan [23]. Our results are consistent with these findings; however, as IPF patients with a probable UIP pattern showed a risk for AE similar to those with a UIP pattern in our cohort, it should be noted that an IPF diagnosis is more important than the CT pattern in predicting time to AE.

There are a number of limitations to this study. First, this was a retrospective study from a large clinical practice and the baseline disease severity varied among the groups. Patients with a UIP pattern generally had more severe disease than those in other groups. Although adjusted for well-recognised prognostic factors, caution is still necessary when interpreting our results. Moreover, treatment was not standardised and all decisions regarding starting and ending treatment rested with the individual physician, making it difficult to evaluate the effect of treatment on outcomes. As such, prospective validation will be needed to clarify these points. Secondly, the study was conducted at a single institute and all patients were Japanese, making it difficult to generalise to other cohorts.

In conclusion, in our real-world IIP cohort, patients with a probable UIP pattern had a generally better prognosis and lower risk of AE at any time point than those with a UIP pattern. Moreover, probable UIP pattern was an independent prognostic factor and associated with time to first AE. As probable UIP pattern did not predict survival in patients with a final diagnosis of IPF, diagnostic heterogeneity associated with a probable UIP pattern likely explains the difference between the two groups. As such, care is needed when extrapolating diagnostic evidence from clinical trials for IPF.

Conflict of interest: None declared.

Support statement: This work was supported in part by a grant-in-aid for the interstitial lung disease research group from the Japanese Ministry of Health, Labour and Welfare (H29-023). Funding information for this article has been deposited with the Crossref Funder Registry.

References

- 1 Lynch DA, Sverzellati N, Travis WD, *et al.* Diagnostic criteria for idiopathic pulmonary fibrosis: a Fleischner Society white paper. *Lancet Respir Med* 2018; 6: 138–153.
- 2 Raghu G, Remy-Jardin M, Myers JL, *et al.* Diagnosis of idiopathic pulmonary fibrosis. An official ATS/ERS/JRS/ALAT clinical practice guideline. *Am J Respir Crit Care Med* 2018; 198: e44–e68.
- 3 Raghu G, Collard HR, Egan JJ, *et al.* An official ATS/ERS/JRS/ALAT statement: idiopathic pulmonary fibrosis: evidence-based guidelines for diagnosis and management. *Am J Respir Crit Care Med* 2011; 183: 788–824.
- 4 Richeldi L, du Bois RM, Raghu G, *et al.* Efficacy and safety of nintedanib in idiopathic pulmonary fibrosis. *N Engl J Med* 2014; 370: 2071–2082.
- 5 Raghu G, Wells AU, Nicholson AG, *et al.* Effect of nintedanib in subgroups of idiopathic pulmonary fibrosis by diagnostic criteria. *Am J Respir Crit Care Med* 2017; 195: 78–85.
- 6 Brownell R, Moua T, Henry TS, *et al.* The use of pretest probability increases the value of high-resolution CT in diagnosing usual interstitial pneumonia. *Thorax* 2017; 72: 424–429.
- 7 Sumikawa H, Johkoh T, Colby TV, *et al.* Computed tomography findings in pathological usual interstitial pneumonia: relationship to survival. *Am J Respir Crit Care Med* 2008; 177: 433–439.
- 8 Edey AJ, Devaraj AA, Barker RP, *et al.* Fibrotic idiopathic interstitial pneumonias: HRCT findings that predict mortality. *Eur Radiol* 2011; 21: 1586–1593.
- 9 Sasaki H, Nakamura M, Kida K, *et al.* [Reference value for spirogram and partial pressure of arterial blood gas in Japanese adults]. *Nihon Kokyūki Gakkai Zasshi* 2001; 39: S1–S17.
- 10 Knudson RJ, Kaltenbom WT, Knudson DE, *et al.* The single-breath carbon monoxide diffusing capacity: reference equations derived from a healthy nonsmoking population and effects of hematocrit. *Am Rev Respir Dis* 1987; 135: 805–811.
- 11 Collard HR, Ryerson CJ, Corte TJ, *et al.* Acute exacerbation of idiopathic pulmonary fibrosis: an International Working Group report. *Am J Respir Crit Care Med* 2016; 194: 265–275.
- 12 Ryerson CJ, Corte TJ, Lee JS, *et al.* A standardized diagnostic ontology for fibrotic interstitial lung disease: an international working group perspective. *Am J Respir Crit Care Med* 2017; 196: 1249–1254.

- 13 Travis WD, Costabel U, Hansell DM, *et al.* An official American Thoracic Society/European Respiratory Society statement: update of the international multidisciplinary classification of the idiopathic interstitial pneumonias. *Am J Respir Crit Care Med* 2013; 188: 733–748.
- 14 Ryerson CJ, Urbanir TH, Richeldi L, *et al.* Prevalence and prognosis of unclassifiable interstitial lung disease. *Eur Respir J* 2013; 42: 750–757.
- 15 Novelli F, Tavanti L, Cini S, *et al.* Determinants of the prognosis of idiopathic pulmonary fibrosis. *Eur Rev Med Pharmacol Sci* 2014; 18: 880–886.
- 16 Mogulkoc N, Brutsche MH, Bishop PW, *et al.* Pulmonary function in idiopathic pulmonary fibrosis and referral for lung transplantation. *Am J Respir Crit Care Med* 2001; 164: 103–108.
- 17 Lynch DA, Godwin JD, Safrin S, *et al.* High-resolution computed tomography in idiopathic pulmonary fibrosis. Diagnosis and prognosis. *Am J Respir Crit Care Med* 2005; 172: 488–493.
- 18 Shin KM, Lee KS, Chung MP, *et al.* Prognostic determinants among clinical, thin-section CT, and histopathologic findings for fibrotic idiopathic interstitial pneumonias: tertiary hospital study. *Radiology* 2008; 249: 328–337.
- 19 King TE Jr., Bradford WZ, Castro-Bernardini S, *et al.* A phase 3 trial of pirfenidone in patients with idiopathic pulmonary fibrosis. *N Engl J Med* 2014; 370: 2083–2092.
- 20 Kondoh Y, Taniguchi H, Katsuta T, *et al.* Risk factors of acute exacerbation of idiopathic pulmonary fibrosis. *Sarcoidosis Vasc Diffuse Lung Dis* 2010; 27: 103–110.
- 21 Song JW, Hong SB, Lim CM, *et al.* Acute exacerbation of idiopathic pulmonary fibrosis: incidence, risk factors and outcome. *Eur Respir J* 2011; 37: 356–363.
- 22 Ohshimo S, Ishikawa N, Horimasu Y, *et al.* Baseline KL-6 predicts increased risk for acute exacerbation of idiopathic pulmonary fibrosis. *Respir Med* 2014; 108: 1031–1039.
- 23 Arai T, Kagawa T, Sasaki Y, *et al.* Heterogeneity of incidence and outcome of acute exacerbation in idiopathic interstitial pneumonia. *Respirology* 2016; 21: 1431–1437.
- 24 Mura M, Porretta MA, Bargagli E, *et al.* Predicting survival in newly diagnosed idiopathic pulmonary fibrosis: a 3-year prospective study. *Eur Respir J* 2012; 40: 101–109.
- 25 Raghu G, Lynch D, Godwin JD, *et al.* Diagnosis of idiopathic pulmonary fibrosis with high-resolution CT in patients with little or no radiological evidence of honeycombing: secondary analysis of a randomised, controlled trial. *Lancet Respir Med* 2014; 2: 277–284.
- 26 Yagihashi K, Huckleberry J, Colby TV, *et al.* Radiologic-pathologic discordance in biopsy-proven usual interstitial pneumonia. *Eur Respir J* 2016; 47: 1057–1059.
- 27 Salisbury ML, Xia M, Murray S, *et al.* Predictors of idiopathic pulmonary fibrosis in absence of radiologic honeycombing: a cross sectional analysis in ILD patients undergoing lung tissue sampling. *Respir Med* 2016; 118: 88–95.
- 28 Kondoh Y, Taniguchi H, Kataoka K, *et al.* Clinical spectrum and prognostic factors of possible UIP pattern on high-resolution CT in patients who underwent surgical lung biopsy. *PLoS One* 2018; 13: e0193608.
- 29 Chung JH, Chawla A, Peljto AL, *et al.* CT scan findings of probable usual interstitial pneumonitis have a high predictive value for histologic usual interstitial pneumonitis. *Chest* 2015; 147: 450–459.
- 30 Nagao T, Nagai S, Hiramoto Y, *et al.* Serial evaluation of high-resolution computed tomography findings in patients with idiopathic pulmonary fibrosis in usual interstitial pneumonia. *Respiration* 2002; 69: 413–419.
- 31 Lee HY, Lee KS, Jeong YJ, *et al.* High-resolution CT findings in fibrotic idiopathic interstitial pneumonias with little honeycombing: serial changes and prognostic implications. *Am J Roentgenol* 2012; 199: 982–989.
- 32 Jeong YJ, Lee KS, Müller NL, *et al.* Usual interstitial pneumonia and non-specific interstitial pneumonia: serial thin-section CT findings correlated with pulmonary function. *Korean J Radiol* 2005; 6: 143–152.
- 33 Lee JW, Shehu E, Gjonbrataj J, *et al.* Clinical findings and outcomes in patients with possible usual interstitial pneumonia. *Respir Med* 2015; 109: 510–516.
- 34 Gruden JF, Panse PM, Leslie KO, *et al.* UIP diagnosed at surgical lung biopsy, 2000–2009: HRCT patterns and proposed classification system. *Am J Roentgenol* 2013; 200: W458–W467.
- 35 Qadrelli S, Molinari L, Ciallella L, *et al.* Radiological versus histopathological diagnosis of usual interstitial pneumonia in the clinical practice: does it have any survival difference? *Respiration* 2010; 79: 32–37.
- 36 Kondoh Y, Taniguchi H, Ebina M, *et al.* Risk factors for acute exacerbation of idiopathic pulmonary fibrosis: extended analysis of pirfenidone trial in Japan. *Respir Investig* 2015; 53: 271–278.
- 37 Reichmann WM, Yu YF, Macaulay D, *et al.* Change in forced vital capacity and associated subsequent outcomes in patients with newly diagnosed idiopathic pulmonary fibrosis. *BMC Pulm Med* 2015; 15: 167.
- 38 Park IN, Kim DS, Shim TS, *et al.* Acute exacerbation of interstitial pneumonia other than idiopathic pulmonary fibrosis. *Chest* 2007; 132: 214–220.
- 39 Suda T, Kaida Y, Nakamura Y, *et al.* Acute exacerbation of interstitial pneumonia associated with collagen vascular diseases. *Respir Med* 2009; 103: 846–853.
- 40 Tachikawa R, Tomii K, Udea H, *et al.* Clinical features and outcome of acute exacerbation of interstitial pneumonia: collagen vascular diseases-related versus idiopathic. *Respiration* 2012; 83: 20–27.

1 **Results**

2 *Validation of sample size*

3 The sample size was calculated to provide 80% power to detect a between-group
4 difference of survival time. Based on a past study comparing survival time of patients with
5 a UIP pattern and those with a probable UIP pattern [1], median 3-year survival time was
6 assumed to be 40% in UIP pattern group and 55% in possible UIP pattern (not probable
7 UIP pattern) group. Based on these assumptions, when the ratio of sample number of UIP
8 pattern and probable UIP pattern was estimated to be 1:2, the sample size was calculated as
9 155 patients in UIP pattern group and 233 patients in probable UIP pattern group for a
10 Kaplan-Meier analysis at a significance level of $< 5\%$. The actual sample size of this study
11 was 160 patients in UIP pattern group and 242 patients in probable UIP pattern group.

12

13 *Validation of the diagnostic approach*

14 To confirm the validity of the diagnoses we made for our cohort, we made a specific
15 provisional diagnosis when the likelihood of the disease was $> 70\%$, the same as a high
16 confidence provisional diagnosis proposed by Ryerson et al [2]. In terms of those who we
17 originally made a diagnosis of unclassifiable interstitial lung disease (ILD) with a probable
18 usual interstitial pneumonia (UIP) pattern on chest computed tomography (CT) and
19 without histopathology, only 3 out of 48 patients were recognized as having a high
20 likelihood of a specific disease: 1 idiopathic pulmonary fibrosis (IPF), 1
21 pleuroparenchymal fibroelastosis and 1 smoking-related ILD. All IPF diagnoses did not
22 change, as in our clinical practice, we usually make a diagnosis of IPF when the likelihood
23 is suggested to be $>70\%$. These changes did not affect the results of our analyses.

24

25 *Annual rate of change in forced vital capacity*

1 The adjusted annual rate of change in forced vital capacity (FVC) was not significantly
2 different between UIP pattern and probable UIP pattern. The rate was -150 ml/year in UIP
3 pattern as compared with -120 ml/year in probable UIP pattern (difference, -30 ml/year
4 [95% confidence interval (95%CI), -10-40]; $p = 0.414$). Similarly, it was not significantly
5 different between the two CT patterns in subjects with a diagnosis of IPF (-160 ml/year in
6 UIP pattern vs. -190 ml/year in probable UIP pattern; difference, 30 ml/year [95%CI, -50-
7 10]; $p = 0.515$). In subjects with a probable UIP pattern, it was significantly larger in those
8 with a diagnosis of IPF (-200 ml/year) than of non-IPF (10 ml/year) (difference, -200
9 ml/year [95%CI, -290--110]; $p < 0.001$).

10

11 **References**

- 12 1. Lee JW, Shehu E, Gjonbrataj J, Bahn YE, Rho BH, Lee MY, Choi WI. Clinical
13 findings and outcomes in patients with possible usual interstitial pneumonia. *Respir*
14 *Med* 2015; 109: 510-516.
- 15 2. Ryerson CJ, Corte TJ, Lee JS, Richeldi L, Walsh SLF, Myers JL, Behr J, Cottin V,
16 Danoff SK, Flaherty KR, Lederer DJ, Lynch DA, Martinez FJ, Raghu G, Travis WD,
17 Udwadia Z, Wells AU, Collard HR. A standardized diagnostic ontology for fibrotic
18 interstitial lung disease: An international working group perspective. *Am J Respir Crit*
19 *Care Med* 2017; 196: 1249-1254.

20

21

TABLE S1 Cox proportional hazard analysis for survival time		
Parameters	Adjusted HR [95%CI]	P-value for HR
All patients		
UIP pattern on CT	Ref.	
Probable UIP pattern on CT	0.749 [0.557-1.008]	0.056
IPF only		
UIP pattern on CT	Ref.	
Probable UIP pattern on CT	0.885 [0.638-1.227]	0.464
Probable UIP pattern only		
Final diagnosis of non-IPF	Ref.	
Final diagnosis of IPF	1.791 [1.079-2.974]	0.024
Based on the non-imputed data. Hazard ratios were adjusted by age, sex, baseline forced vital capacity (% predicted), baseline diffusing capacity for the lung of carbon monoxide (% predicted) and use of antifibrotics. HR: hazard ratio; 95% CI: 95% confidence interval; UIP: usual interstitial pneumonia; CT: computed tomography; IPF: idiopathic pulmonary fibrosis.		

1
2

TABLE S2 Competing risk analysis for time to first acute exacerbation		
Parameters	Adjusted HR [95%CI]	P-value for HR
All patients		
UIP pattern on CT	Ref.	
Probable UIP pattern on CT	0.704 [0.462-1.074]	0.103
IPF only		
UIP pattern on CT	Ref.	
Probable UIP pattern on CT	0.881 [0.563-1.377]	0.577
Probable UIP pattern only		
Final diagnosis of non-IPF	Ref.	
Final diagnosis of IPF	2.212 [0.960-5.097]	0.062
Based on the non-imputed data. Hazard ratios were adjusted by baseline forced vital capacity (% predicted), baseline diffusing capacity for the lung of carbon monoxide (% predicted) and use of antifibrotics. AE: acute exacerbation; HR: hazard ratio; 95% CI: 95% confidence interval; UIP: usual interstitial pneumonia; CT: computed tomography; IPF: idiopathic pulmonary fibrosis.		

1
2

Part VI

Discussion

1. Summary of the studies and achievements

Throughout this PhD period, I could find some new things in the field of pulmonary fibrosis from both molecular cell biological and clinical aspects.

Firstly, I have attempted to evaluate the efficacy of BMPR2 transduction as a therapy for pulmonary fibrosis. I could reveal that BMPR2 is downregulated in the lungs from rats with bleomycin-induced pulmonary fibrosis, which may be due to the proliferation of lung fibroblasts where BMPR2 is not highly expressed. Although the treatment with BMP7 or 4 did not modulate TGF- β -induced profibrotic phenotypes in lung fibroblasts, adenovirus-mediated BMPR2 transduction into those cells reduced phosphorylation of Smad2/3 and production of fibronectin solely or in cooperation with BMP7.

Thereafter, I have tried to evaluate the efficacy of cell therapy using BMPR2-transduced rat EPCs on pulmonary fibrosis. Since this therapy was suspected to work via the transmission of BMPR2 to the damaged lung areas mediated by exosomes released from the gene-modified EPCs (184), I at first confirmed that exosomes derived from BMPR2-transduced human ECFCs/rat EPCs can deliver BMPR2 to lung fibroblasts. However, the exosome-treatment protocol I had used was so toxic for lung fibroblasts that further validation for antifibrotic effect of the transduced BMPR2 was not successful *ex vivo*. I have also attempted to assess the effect of the BMPR2-transduced rat EPCs on rats with bleomycin-induced pulmonary fibrosis, and the cell-therapy showed a trend of suppressing collagen production in lungs. However, the study could not be completed during my PhD period, as the creation of the disease model with a consistent level of fibrosis could not be achieved.

In another study, I have evaluated the validity of the current diagnostic criteria for IPF, which has significant impact on the interpretation of the aetiology of IPF and on eligibility of clinical trials. Although IIP patients with a probable UIP pattern on chest CT could be included in some recent clinical trials for IPF, I had elucidated that a significant number of patients with a non-IPF final diagnosis could be present in the CT-probable UIP pattern group unless IPF was strongly suspected by ILD experts. Such diagnostic heterogeneity was significantly related with longer survival time and time to the first acute exacerbation of probable UIP pattern group in comparison with UIP pattern group. These results suggested the importance of accurate clinical assessment of possibility of IPF, and the risk of overdiagnosis of IPF among non-IPF patients with a better prognosis when

applying the approach of exempting lung biopsy in patients with a probable UIP pattern on chest CT.

2. Impact of BMPR2 overexpression on the TGF- β -induced profibrotic responses in lung fibroblasts

One of the important findings I have established through the experiments in Part II is the confirmation of relatively low BMPR2 expression in lung fibroblasts compared with epithelial or endothelial cells, and the excessive proliferation of fibroblasts may be a cause of reduction of total BMPR2 in fibrotic lungs. Additionally, I could also demonstrate that TGF- β stimulation reduces BMPR2 in both human and rat lung fibroblasts. There are just a few reports describing the BMPR2 expression in fibrotic lungs (123, 124), and none of them have focused on lung fibroblasts.

In my study, BMPs were not effective for attenuating TGF- β -induced profibrotic phenotypes in lung fibroblasts when administered solely. Although BMPs are generally regarded as having antifibrotic properties, the effects of them are not consistent among different reports (104-110, 112). Considering that some studies reported BMP-induced activation of Smad2/3 in a variety of cells including lung fibroblasts (241, 242), the role of BMPs may vary depending on the cell types and context.

On the other hand, TGF- β -induced profibrotic phenotypes was suppressed in lung fibroblasts overexpressing BMPR2. If those profibrotic phenotypes are regulated by the Smad signalling, there are some discrepancies among the findings that 1) BMPs did not reduce p-Smad2/3 or fibronectin when administered solely, 2) overexpression of BMPR2 reduced p-Smad2/3 even in the absence of supplemental BMPs, and 3) fibronectin was reduced only when BMPR2-transduced fibroblasts were treated with BMP7. Therefore, some of the non-Smad signalling pathways should be involved in those phenomena. Though the phosphorylation of p38 MAPK was evaluated in my study as one of the major non-Smad pathways activated by TGF- β , a robust trend of its alteration was not confirmed. Further studies are warranted regarding downstream signalling cascades explaining the findings I have seen through this study. As there are no reports describing the effect of BMPR2 overexpression in lung fibroblasts, my report is the first one evaluating it.

More detailed discussions are in the paper attached in Part II. Based on the results mentioned above, I am motivated to pursue future studies to apply our

laboratory's new technique of delivering a specific gene to lungs using gene-modified EPCs and to evaluate the antifibrotic properties of BMPR2 in a pulmonary fibrosis animal model.

3. Exosome-mediated BMPR2 transmission and its effect on the TGF- β -induced profibrotic responses in lung fibroblasts

The laboratory where I have studied has previously reported that BMPR2-transduced rat EPCs showed a treatment effect on PH in a rat model (184). As human ECFCs have a property of homing to the sites of vascular injury or hypoxia (132-134), it seems a reasonable idea to use rat EPCs as a vector of a specific gene to damaged vascular endothelium in PH. Based on the result from a biodistribution study, EPCs injected from tail vein accumulate in the lungs shortly after injection but are washed out within 24 h (184). Nevertheless, BMPR2 increase had persisted in the lungs from PH rats for a few weeks more. Therefore, the treatment effect of this BMPR2-transduced EPC therapy was suspected to be mediated by cell-to-cell communication between the EPCs and lung cells via exosomes delivering BMPR2 released from the EPCs.

In my study, I have attempted to apply this BMPR2-transduced EPC therapy to a rat pulmonary fibrosis model. Prior to the *in vivo* study, I have at first evaluated if the exosomes released from BMPR2-transduced human ECFCs/rat EPCs can be absorbed by lung fibroblasts and if the BMPR2 transduced via the exosomes have antifibrotic properties against TGF- β -induced phenotypes as shown in adenoviral transduction study in Part II.

Through the optimisation experiments, I have confirmed that the exosomes from BMPR2-transduced human ECFCs/rat EPCs contain BMPR2 of significantly higher levels than the exosomes from control (non-transduced) cells. Additionally, lung fibroblasts treated with those BMPR2-containing exosomes expressed significantly high BMPR2. At this stage, it could not be denied that the BMPR2 detected by Western blot of lung fibroblasts harvested directly from culture plates did not represent truly transduced BMPR2, but just detected the exosomes themselves which precipitated on the surface of the fibroblasts. Therefore, it is necessary to evaluate the function, i.e., antifibrotic effect against the TGF- β stimuli, of the increased BMPR2 in lung fibroblasts.

However, in the main part of this study, I could not keep lung fibroblasts sufficiently alive for 3 days after transduction which are necessary to stimulate the cells with TGF- β /BMPs. A significant number of fibroblasts had died or been

damaged during this term, which is suspected to be due to the toxicity of adenovirus slightly contained in the exosomes or the in the media of exosome solution. The data presented in this thesis are only from the experiments in which at least the cells treated with AdTrack-exosomes have mostly survived, but there were indeed a significant number of experiments that failed to collect cell samples due to cell death before the endpoint dates both in the groups of AdTrack- and AdBMPR2-exosomes. Although it was true that the survival rate of the cells looked slightly higher in the cells treated with AdBMPR2-exosomes, we cannot conclude that the difference of fibronectin levels between the cells treated with AdTrack- and AdBMPR2-exosomes were merely due to the effect of transduced BMPR2. Compared with adenoviral transduction performed in the studies of Part II, the term for incubation with transduction media was twice longer in this exosome study, which might have a significant impact on cell survival even if the total contaminated viral load is much smaller than adenoviral transduction study. Furthermore, given that the BMPR2 expression levels in lung fibroblasts were gradually increased time-dependently over 4-day incubation period for exosome treatment, it might be possible that the BMPR2 was transduced not only via the exosomes but also via the contaminated adenovirus.

Use of shorter duration of incubation with transduction media or of lower dose of exosomes were also attempted. However, those “milder” treatment strategies could not achieve sufficient BMPR2 increase which was detectable by Western blot (data not shown). Additionally, as the transduction efficiency of exosomes was much lower than that of adenovirus, it was necessary to culture human ECFCs/rat EPCs of no less than 8-12 x 175 cm² culture flasks even for running a small, triplicated experiment with just 5 different conditions using exosomes at a concentration of 20 µg/mL. Because of such excessively large size and high workload of the study, and unexpectedly high toxicity of exosome therapy, I had to give up finding a better experimental condition for this study during my PhD period.

Further optimisation of this study is warranted in order to establish a less toxic treatment protocol. For this purpose, use of immunoaffinity capture method in a well-established MACS[®] procedure may be one of the options for increasing the purity of exosomes, though the adenovirus contained inside exosomes cannot be removed and the total amount of exosomes obtained through this method will become less than the ultracentrifuge protocol. Creation of BMPR2-carrying, much

less toxic lentiviral vector instead of adenoviral vector may be another solution worth trying.

4. Creation of bleomycin-induced pulmonary fibrosis model and accumulation of intravenous BMPR2-transduced rat EPCs in rat lungs

Although the study above was not successful in clearly showing an effect of transferring BMPR2 by exosomes, I have simultaneously tried to evaluate the effect of intravenous injection of BMPR2-transduced EPCs in rats with bleomycin-induced pulmonary fibrosis. However, I could not successfully establish the disease model and had to give up completing this study in my PhD.

The bleomycin-induced pulmonary fibrosis rodent model is one of the most well-established and broadly used animal models for studying pulmonary fibrosis (243). At first, I have used bleomycin hydrochloride (Nippon Kayaku, Tokyo, Japan) for optimisation studies performed in Japan, but as the same bleomycin was not traded in Australia, I had to change the brand of bleomycin after coming to Australia. Though a dose of 10 mg/kg was well tolerated in my Japanese model, the similar dose was revealed to be too toxic when the brand of bleomycin was changed. The suspected reasons of such a different response to bleomycin between two countries other than the brand include the source of rats and colonisation of *Pneumocystis*. Although we have used the same strain of rats (Fischer 344) as that used in Japan, the source of the rats was different, which might also cause differed sensitivity to bleomycin. It was also wondered that the Australian rats may have been colonised with *Pneumocystis*, though we could not confirm this.

As a result, the extent of body condition deterioration observed in my Japanese model was at an unacceptable level in Australian ethical criteria (15-20% body weight loss from baseline was frequently observed, and 5-10% of animals could be found dead before the endpoint in my Japanese model). Therefore, I had to reoptimize the dosage of bleomycin and create a rat model with much milder pulmonary fibrosis, and eventually set a dose of 1.5 mg/kg for the following studies.

In spite of the above-mentioned prudent dose setting, the model could not still be well-established in the following studies: about a half of rats administered with intratracheal bleomycin did not show sufficiently severe pulmonary fibrosis. Although the reconstituted bleomycin can generally be stored at -80°C for up to 3 months, as there was a trend of developing milder fibrosis in the first 35 rats

treated with bleomycin solution reconstituted more than 1 month prior to administration, I have used fresher bleomycin reconstituted within 1 month for the following 48 rats.

However, the rate of the rats showing insufficient fibrosis was not reduced. Given that the extent of fibrosis was almost the same level within each batch of rats, I cannot deny that the age or weight of rats might have some impacts on the extent of fibrosis. However, the failures of induction of fibrosis were observed in rats with various age (8-12 weeks) and weight (180-230 g) within the range defined in the prespecified protocol, and there were no obvious correlations between those parameters and extent of fibrosis. Another possible explanation for the fibrosis induction failures is that the dose of 1.5 mg/kg is just on the “borderline” level, which can cause both success and failure of induction of fibrosis equally and had just accidentally induced fibrosis successfully in the optimisation studies. This hypothesis has to be verified through a repeat optimisation study for doses of 1.5-2.0 mg/kg, but it may be difficult to carry out studies using this model under the current ethical criteria as the toxicity of bleomycin observed in a batch of rats treated with a dose of 2.0 mg/kg was unacceptable based on the ethical criteria.

In terms of the intravenous injection of gene-modified EPCs, it was expected that BMPR2 expression is increased shortly (1-6 hours) after injection of BMPR2-transduced EPCs as shown in our previous article regarding treatment of rat PH model using this cell-based therapy (184). Given the long-lasting effect of BMPR2-transduced EPCs (at least for 8-10 days after injection) observed despite the very short-term stay of EPCs in the lungs in this study (184), it was speculated that the transmission of BMPR2 from EPCs to lung cells via exosomes had the transduced BMPR2 work longer at the lungs. It is however plausible that even a brief upregulation of BMPR2 was sufficient to interrupt the inflammatory cascade that had been set in motion by monocrotaline. Given that, it was at least plausible that brief upregulation of BMPR2 might interrupt the inflammatory cascade induced by a single administration of bleomycin. In my pulmonary fibrosis rat model, BMPR2 expression was also increased 1 and 6 hours after intravenous injection of BMPR2-transduced EPCs as expected, while the increase was not persistent for 14 days after injection. Nevertheless, in the 14-day prevention study, I could reveal that collagen production was significantly suppressed by BMPR2-transduced EPC injection, though I have to mention that there are some limitations in this study, e.g. there are not control EPC or AdTrack-infected EPC groups which are necessary for interpreting if the positive treatment effects are due to the BMPR2 transduced into

injected EPCs, histopathological improvement was not brought about by BMPR2-transduced EPCs, and three groups (control, bleomycin only and BMPR2-transduced EPC groups) had been treated at different timing and with different bleomycin batches, that can cause batch effects. In terms of the 21-day treatment study, I have challenged after a small optimisation study for maximising the dosage of AdBMPR2 used for BMPR2 transduction into EPCs prior to intravenous injection, but the rat model creation failed as stated.

As discussed in Part II, adenoviral transduction of BMPR2 into lung fibroblasts has shown a positive effect on suppression of profibrotic responses induced by TGF- β . Furthermore, based on the treatment effect of BMPR2-transduced EPCs observed (though just partly) in the above-mentioned 14-day prevention study, I think overexpression of BMPR2 is still worthy to try in vivo after reoptimizing the study protocol including the dosage of bleomycin. It may also be possible to consider an alternate fibrosis model, although bleomycin is by far the most common model used.

5. Importance of radiological pattern for diagnosing homogeneous IPF

In another study, I have tackled another important issue of pulmonary fibrosis from a clinical aspect. Considering the application of new treatments to IPF patients in the future, I have evaluated the validity of the current diagnostic criteria for IPF, which has significant impact on the interpretation of the aetiology of IPF and on eligibility of clinical trials targeting IPF.

IIP patients with a probable UIP pattern on chest CT, who need to undergo surgical lung biopsy to get a definitive diagnosis according to the current guideline (3), could be included in some recent clinical trials for IPF (17, 231). This approach was supported by a result from the post-hoc analysis of the INPULSIS trials (11) showing that the annual decline in FVC from baseline in those patients was similar to that in patients with IPF diagnosed strictly based on the guideline (202), and officially described in the diagnostic criteria proposed by Fleischner Society (244), in which probable UIP pattern on chest CT is insisted to be a sufficient finding for making a diagnosis of IPF without confirming histopathological findings.

However, I had elucidated that a significant number of patients with a non-IPF final diagnosis could exist in the CT-probable UIP pattern group unless IPF was strongly suspected by ILD experts. Such diagnostic heterogeneity was significantly related with longer survival time and time to the first acute exacerbation of

probable UIP pattern group in comparison with UIP pattern group. These results suggested the importance of accurate clinical assessment regarding the possibility of IPF, and the risk of overdiagnosis of IPF among non-IPF patients with a better prognosis when applying the approach of exempting lung biopsy in patients with a probable UIP pattern on chest CT.

Based on those discussions, Raghu et al. recently described that the necessity of SLB should be considered in patients with a probable UIP pattern on chest CT if IPF is not highly suspected clinically (245). Although significant benefits of antifibrotics in progressive fibrosing ILDs other than IPF have recently been found (212), it has also been shown that the effectiveness of the treatment was significantly different between different detailed diagnoses (246). Further studies regarding “what are the clinical findings suggestive of IPF” and the importance of making a “precise” definitive diagnosis of ILD are warranted to generalise clinical interpretations by experts. More detailed discussions are described in the article attached in Part V.

6. Conclusions

BMPR2 was reduced in fibrotic lesions of lungs with pulmonary fibrosis and in lung fibroblasts treated with TGF- β . In addition, adenovirus-mediated BMPR2 transduction could suppress Smad2/3 phosphorylation solely and fibronectin production in cooperation with BMP7. BMPR2 was increased in lung fibroblasts when treated with exosomes derived from BMPR2-transduced human ECFCs/rat EPCs, but further study is necessary to clarify if this increase is due to the transduction of BMPR2 into fibroblasts or just due to the sedimentation of exosomes on the surface of fibroblasts. BMPR2-transduced EPCs could be accumulated in the lungs of rats with bleomycin-induced pulmonary fibrosis shortly after injection from their tail vein. The effect of this cell-based therapy needs to be evaluated using well-optimised animal model showing pulmonary fibrosis consistently.

Patients with a probable UIP pattern had a better prognosis and lower risk of acute exacerbation than those with a UIP pattern. As probable UIP pattern did not predict survival in patients with a final diagnosis of IPF, diagnostic heterogeneity associated with a probable UIP pattern likely explains the difference between the two groups. As such, prudent clinical evaluation is important for making a diagnosis of IPF and care is needed when interpreting evidence from clinical trials for IPF.

Bibliography

1. Travis WD, Costabel U, Hansell DM, King TE, Lynch DA, Nicholson AG, et al. An official American Thoracic Society/European Respiratory Society statement: Update of the international multidisciplinary classification of the idiopathic interstitial pneumonias. *Am J Respir Crit Care Med.* 2013;188(6):733-48.
2. Natsuzaka M, Chiba H, Kuronuma K, Otsuka M, Kudo K, Mori M, et al. Epidemiologic survey of Japanese patients with idiopathic pulmonary fibrosis and investigation of ethnic differences. *Am J Respir Crit Care Med.* 2014;190(7):773-9.
3. Raghu G, Remy-Jardin M, Myers JL, Richeldi L, Ryerson CJ, Lederer DJ, et al. Diagnosis of Idiopathic Pulmonary Fibrosis. An Official ATS/ERS/JRS/ALAT Clinical Practice Guideline. *Am J Respir Crit Care Med.* 2018;198(5):e44-e68.
4. Raghu G, Collard HR, Egan JJ, Martinez FJ, Behr J, Brown KK, et al. An official ATS/ERS/JRS/ALAT statement: idiopathic pulmonary fibrosis: evidence-based guidelines for diagnosis and management. *Am J Respir Crit Care Med.* 2011;183(6):788-824.
5. Collard HR, Ryerson CJ, Corte TJ, Jenkins G, Kondoh Y, Lederer DJ, et al. Acute Exacerbation of Idiopathic Pulmonary Fibrosis. An International Working Group Report. *Am J Respir Crit Care Med.* 2016;194(3):265-75.
6. Raghu G, Mageto YN, Lockhart D, Schmidt RA, Wood DE, Godwin JD. The accuracy of the clinical diagnosis of new-onset idiopathic pulmonary fibrosis and other interstitial lung disease: A prospective study. *Chest.* 1999;116(5):1168-74.
7. Hunninghake GW, Zimmerman MB, Schwartz DA, King TE, Lynch J, Hegele R, et al. Utility of a lung biopsy for the diagnosis of idiopathic pulmonary fibrosis. *Am J Respir Crit Care Med.* 2001;164(2):193-6.
8. Hunninghake GW, Lynch DA, Galvin JR, Gross BH, Müller N, Schwartz DA, et al. Radiologic findings are strongly associated with a pathologic diagnosis of usual interstitial pneumonia. *Chest.* 2003;124(4):1215-23.
9. Chung JH, Chawla A, Peljto AL, Cool CD, Groshong SD, Talbert JL, et al. CT scan findings of probable usual interstitial pneumonitis have a high predictive value for histologic usual interstitial pneumonitis. *Chest.* 2015;147(2):450-9.
10. Brownell R, Moua T, Henry TS, Elicker BM, White D, Vittinghoff E, et al. The use of pretest probability increases the value of high-resolution CT in diagnosing usual interstitial pneumonia. *Thorax.* 2017;72(5):424-9.

11. Raghu G, Wells AU, Nicholson AG, Richeldi L, Flaherty KR, Le Maulf F, et al. Effect of Nintedanib in Subgroups of Idiopathic Pulmonary Fibrosis by Diagnostic Criteria. *Am J Respir Crit Care Med.* 2017;195(1):78-85.
12. Troy LK, Grainge C, Corte TJ, Williamson JP, Vallely MP, Cooper WA, et al. Diagnostic accuracy of transbronchial lung cryobiopsy for interstitial lung disease diagnosis (COLDICE): a prospective, comparative study. *Lancet Respir Med.* 2020;8(2):171-81.
13. Noth I, Anstrom KJ, Calvert SB, de Andrade J, Flaherty KR, Glazer C, et al. A placebo-controlled randomized trial of warfarin in idiopathic pulmonary fibrosis. *Am J Respir Crit Care Med.* 2012;186(1):88-95.
14. Raghu G, Anstrom KJ, King TE, Lasky JA, Martinez FJ, Network IPFCR. Prednisone, azathioprine, and N-acetylcysteine for pulmonary fibrosis. *N Engl J Med.* 2012;366(21):1968-77.
15. Raghu G, Behr J, Brown KK, Egan JJ, Kawut SM, Flaherty KR, et al. Treatment of idiopathic pulmonary fibrosis with ambrisentan: a parallel, randomized trial. *Ann Intern Med.* 2013;158(9):641-9.
16. King TE, Bradford WZ, Castro-Bernardini S, Fagan EA, Glaspole I, Glassberg MK, et al. A phase 3 trial of pirfenidone in patients with idiopathic pulmonary fibrosis. *N Engl J Med.* 2014;370(22):2083-92.
17. Richeldi L, du Bois RM, Raghu G, Azuma A, Brown KK, Costabel U, et al. Efficacy and safety of nintedanib in idiopathic pulmonary fibrosis. *N Engl J Med.* 2014;370(22):2071-82.
18. Sumikawa H, Johkoh T, Colby TV, Ichikado K, Suga M, Taniguchi H, et al. Computed tomography findings in pathological usual interstitial pneumonia: relationship to survival. *Am J Respir Crit Care Med.* 2008;177(4):433-9.
19. Edey AJ, Devaraj AA, Barker RP, Nicholson AG, Wells AU, Hansell DM. Fibrotic idiopathic interstitial pneumonias: HRCT findings that predict mortality. *Eur Radiol.* 2011;21(8):1586-93.
20. Rosenbloom J, Macarak E, Piera-Velazquez S, Jimenez SA. Human Fibrotic Diseases: Current Challenges in Fibrosis Research. *Methods Mol Biol.* 2017;1627:1-23.
21. Fernandez IE, Eickelberg O. The impact of TGF- β on lung fibrosis: from targeting to biomarkers. *Proc Am Thorac Soc.* 2012;9(3):111-6.
22. Yan Z, Kui Z, Ping Z. Reviews and prospectives of signaling pathway analysis in idiopathic pulmonary fibrosis. *Autoimmun Rev.* 2014;13(10):1020-5.
23. Bagnato G, Harari S. Cellular interactions in the pathogenesis of interstitial lung diseases. *Eur Respir Rev.* 2015;24(135):102-14.

24. Karsdal MA, Larsen L, Engsig MT, Lou H, Ferreras M, Lochter A, et al. Matrix metalloproteinase-dependent activation of latent transforming growth factor-beta controls the conversion of osteoblasts into osteocytes by blocking osteoblast apoptosis. *J Biol Chem.* 2002;277(46):44061-7.
25. Yu Q, Stamenkovic I. Cell surface-localized matrix metalloproteinase-9 proteolytically activates TGF-beta and promotes tumor invasion and angiogenesis. *Genes Dev.* 2000;14(2):163-76.
26. Lyons RM, Keski-Oja J, Moses HL. Proteolytic activation of latent transforming growth factor-beta from fibroblast-conditioned medium. *J Cell Biol.* 1988;106(5):1659-65.
27. Cui Y, Robertson J, Maharaj S, Waldhauser L, Niu J, Wang J, et al. Oxidative stress contributes to the induction and persistence of TGF- β 1 induced pulmonary fibrosis. *Int J Biochem Cell Biol.* 2011;43(8):1122-33.
28. Schultz-Cherry S, Murphy-Ullrich JE. Thrombospondin causes activation of latent transforming growth factor-beta secreted by endothelial cells by a novel mechanism. *J Cell Biol.* 1993;122(4):923-32.
29. Wipff PJ, Rifkin DB, Meister JJ, Hinz B. Myofibroblast contraction activates latent TGF-beta1 from the extracellular matrix. *J Cell Biol.* 2007;179(6):1311-23.
30. Munger JS, Huang X, Kawakatsu H, Griffiths MJ, Dalton SL, Wu J, et al. The integrin α v β 6 binds and activates latent TGF beta 1: a mechanism for regulating pulmonary inflammation and fibrosis. *Cell.* 1999;96(3):319-28.
31. Goumans MJ, Valdimarsdottir G, Itoh S, Lebrin F, Larsson J, Mummery C, et al. Activin receptor-like kinase (ALK)1 is an antagonistic mediator of lateral TGFbeta/ALK5 signaling. *Mol Cell.* 2003;12(4):817-28.
32. Pardali E, Sanchez-Duffhues G, Gomez-Puerto MC, Ten Dijke P. TGF- β -Induced Endothelial-Mesenchymal Transition in Fibrotic Diseases. *Int J Mol Sci.* 2017;18(10).
33. ten Dijke P, Arthur HM. Extracellular control of TGFbeta signalling in vascular development and disease. *Nat Rev Mol Cell Biol.* 2007;8(11):857-69.
34. Wilkes MC, Leof EB. Transforming growth factor beta activation of c-Abl is independent of receptor internalization and regulated by phosphatidylinositol 3-kinase and PAK2 in mesenchymal cultures. *J Biol Chem.* 2006;281(38):27846-54.
35. Hocevar BA, Brown TL, Howe PH. TGF-beta induces fibronectin synthesis through a c-Jun N-terminal kinase-dependent, Smad4-independent pathway. *EMBO J.* 1999;18(5):1345-56.
36. Derynck R, Zhang YE. Smad-dependent and Smad-independent pathways in TGF-beta family signalling. *Nature.* 2003;425(6958):577-84.

37. Moustakas A, Heldin CH. Non-Smad TGF-beta signals. *J Cell Sci.* 2005;118(Pt 16):3573-84.
38. Caraci F, Gili E, Calafiore M, Failla M, La Rosa C, Crimi N, et al. TGF-beta1 targets the GSK-3beta/beta-catenin pathway via ERK activation in the transition of human lung fibroblasts into myofibroblasts. *Pharmacol Res.* 2008;57(4):274-82.
39. Guo X, Wang XF. Signaling cross-talk between TGF-beta/BMP and other pathways. *Cell Res.* 2009;19(1):71-88.
40. White ES, Atrasz RG, Hu B, Phan SH, Stambolic V, Mak TW, et al. Negative regulation of myofibroblast differentiation by PTEN (Phosphatase and Tensin Homolog Deleted on chromosome 10). *Am J Respir Crit Care Med.* 2006;173(1):112-21.
41. Xia H, Diebold D, Nho R, Perlman D, Kleidon J, Kahm J, et al. Pathological integrin signaling enhances proliferation of primary lung fibroblasts from patients with idiopathic pulmonary fibrosis. *J Exp Med.* 2008;205(7):1659-72.
42. Xia H, Khalil W, Kahm J, Jessurun J, Kleidon J, Henke CA. Pathologic caveolin-1 regulation of PTEN in idiopathic pulmonary fibrosis. *Am J Pathol.* 2010;176(6):2626-37.
43. Nho RS, Hergert P, Kahm J, Jessurun J, Henke C. Pathological alteration of FoxO3a activity promotes idiopathic pulmonary fibrosis fibroblast proliferation on type I collagen matrix. *Am J Pathol.* 2011;179(5):2420-30.
44. Nho RS, Peterson M, Hergert P, Henke CA. FoxO3a (Forkhead Box O3a) deficiency protects Idiopathic Pulmonary Fibrosis (IPF) fibroblasts from type I polymerized collagen matrix-induced apoptosis via caveolin-1 (cav-1) and Fas. *PLoS One.* 2013;8(4):e61017.
45. Sun Z, Gong X, Zhu H, Wang C, Xu X, Cui D, et al. Inhibition of Wnt/ β -catenin signaling promotes engraftment of mesenchymal stem cells to repair lung injury. *J Cell Physiol.* 2014;229(2):213-24.
46. Akhmetshina A, Palumbo K, Dees C, Bergmann C, Venalis P, Zerr P, et al. Activation of canonical Wnt signalling is required for TGF- β -mediated fibrosis. *Nat Commun.* 2012;3:735.
47. Lagares D, Busnadiego O, García-Fernández RA, Kapoor M, Liu S, Carter DE, et al. Inhibition of focal adhesion kinase prevents experimental lung fibrosis and myofibroblast formation. *Arthritis Rheum.* 2012;64(5):1653-64.
48. Ding Q, Cai GQ, Hu M, Yang Y, Zheng A, Tang Q, et al. FAK-related nonkinase is a multifunctional negative regulator of pulmonary fibrosis. *Am J Pathol.* 2013;182(5):1572-84.

49. Sisson TH, Mendez M, Choi K, Subbotina N, Courey A, Cunningham A, et al. Targeted injury of type II alveolar epithelial cells induces pulmonary fibrosis. *Am J Respir Crit Care Med*. 2010;181(3):254-63.
50. Rock JR, Barkauskas CE, Crouce MJ, Xue Y, Harris JR, Liang J, et al. Multiple stromal populations contribute to pulmonary fibrosis without evidence for epithelial to mesenchymal transition. *Proc Natl Acad Sci U S A*. 2011;108(52):E1475-83.
51. Marmai C, Sutherland RE, Kim KK, Dolganov GM, Fang X, Kim SS, et al. Alveolar epithelial cells express mesenchymal proteins in patients with idiopathic pulmonary fibrosis. *Am J Physiol Lung Cell Mol Physiol*. 2011;301(1):L71-8.
52. Willis BC, Liebler JM, Luby-Phelps K, Nicholson AG, Crandall ED, du Bois RM, et al. Induction of epithelial-mesenchymal transition in alveolar epithelial cells by transforming growth factor-beta1: potential role in idiopathic pulmonary fibrosis. *Am J Pathol*. 2005;166(5):1321-32.
53. Kim KK, Kugler MC, Wolters PJ, Robillard L, Galvez MG, Brumwell AN, et al. Alveolar epithelial cell mesenchymal transition develops in vivo during pulmonary fibrosis and is regulated by the extracellular matrix. *Proc Natl Acad Sci U S A*. 2006;103(35):13180-5.
54. Kim KK, Wei Y, Szekeres C, Kugler MC, Wolters PJ, Hill ML, et al. Epithelial cell alpha3beta1 integrin links beta-catenin and Smad signaling to promote myofibroblast formation and pulmonary fibrosis. *J Clin Invest*. 2009;119(1):213-24.
55. Bauman KA, Wettlaufer SH, Okunishi K, Vannella KM, Stoolman JS, Huang SK, et al. The antifibrotic effects of plasminogen activation occur via prostaglandin E2 synthesis in humans and mice. *J Clin Invest*. 2010;120(6):1950-60.
56. Xie L, Law BK, Chytil AM, Brown KA, Aakre ME, Moses HL. Activation of the Erk pathway is required for TGF-beta1-induced EMT in vitro. *Neoplasia*. 2004;6(5):603-10.
57. Santibañez JF. JNK mediates TGF-beta1-induced epithelial mesenchymal transdifferentiation of mouse transformed keratinocytes. *FEBS Lett*. 2006;580(22):5385-91.
58. Bakin AV, Tomlinson AK, Bhowmick NA, Moses HL, Arteaga CL. Phosphatidylinositol 3-kinase function is required for transforming growth factor beta-mediated epithelial to mesenchymal transition and cell migration. *J Biol Chem*. 2000;275(47):36803-10.
59. Gonzalez DM, Medici D. Signaling mechanisms of the epithelial-mesenchymal transition. *Sci Signal*. 2014;7(344):re8.

60. Epa AP, Thatcher TH, Pollock SJ, Wahl LA, Lyda E, Kottmann RM, et al. Normal Human Lung Epithelial Cells Inhibit Transforming Growth Factor- β Induced Myofibroblast Differentiation via Prostaglandin E2. *PLoS One*. 2015;10(8):e0135266.
61. Hagimoto N, Kuwano K, Inoshima I, Yoshimi M, Nakamura N, Fujita M, et al. TGF-beta 1 as an enhancer of Fas-mediated apoptosis of lung epithelial cells. *J Immunol*. 2002;168(12):6470-8.
62. Kinnula VL, Fattman CL, Tan RJ, Oury TD. Oxidative stress in pulmonary fibrosis: a possible role for redox modulatory therapy. *Am J Respir Crit Care Med*. 2005;172(4):417-22.
63. Torres-González E, Bueno M, Tanaka A, Krug LT, Cheng DS, Polosukhin VV, et al. Role of endoplasmic reticulum stress in age-related susceptibility to lung fibrosis. *Am J Respir Cell Mol Biol*. 2012;46(6):748-56.
64. Andersson-Sjöland A, de Alba CG, Nihlberg K, Becerril C, Ramírez R, Pardo A, et al. Fibrocytes are a potential source of lung fibroblasts in idiopathic pulmonary fibrosis. *Int J Biochem Cell Biol*. 2008;40(10):2129-40.
65. Hong KM, Belperio JA, Keane MP, Burdick MD, Strieter RM. Differentiation of human circulating fibrocytes as mediated by transforming growth factor-beta and peroxisome proliferator-activated receptor gamma. *J Biol Chem*. 2007;282(31):22910-20.
66. Moore BB, Kolodnick JE, Thannickal VJ, Cooke K, Moore TA, Hogaboam C, et al. CCR2-mediated recruitment of fibrocytes to the alveolar space after fibrotic injury. *Am J Pathol*. 2005;166(3):675-84.
67. Moore BB, Murray L, Das A, Wilke CA, Herrygers AB, Toews GB. The role of CCL12 in the recruitment of fibrocytes and lung fibrosis. *Am J Respir Cell Mol Biol*. 2006;35(2):175-81.
68. Phillips RJ, Burdick MD, Hong K, Lutz MA, Murray LA, Xue YY, et al. Circulating fibrocytes traffic to the lungs in response to CXCL12 and mediate fibrosis. *J Clin Invest*. 2004;114(3):438-46.
69. Renzoni EA, Walsh DA, Salmon M, Wells AU, Sestini P, Nicholson AG, et al. Interstitial vascularity in fibrosing alveolitis. *Am J Respir Crit Care Med*. 2003;167(3):438-43.
70. Ebina M, Shimizukawa M, Shibata N, Kimura Y, Suzuki T, Endo M, et al. Heterogeneous increase in CD34-positive alveolar capillaries in idiopathic pulmonary fibrosis. *Am J Respir Crit Care Med*. 2004;169(11):1203-8.
71. Yin Q, Nan HY, Zhang WH, Yan LF, Cui GB, Huang XF, et al. Pulmonary microvascular endothelial cells from bleomycin-induced rats promote the transformation and collagen synthesis of fibroblasts. *J Cell Physiol*. 2011;226(8):2091-102.

72. Cao Z, Lis R, Ginsberg M, Chavez D, Shido K, Rabbany SY, et al. Targeting of the pulmonary capillary vascular niche promotes lung alveolar repair and ameliorates fibrosis. *Nat Med.* 2016;22(2):154-62.
73. Cipriani P, Di Benedetto P, Ruscitti P, Capece D, Zazzeroni F, Liakouli V, et al. The Endothelial-mesenchymal Transition in Systemic Sclerosis Is Induced by Endothelin-1 and Transforming Growth Factor- β and May Be Blocked by Macitentan, a Dual Endothelin-1 Receptor Antagonist. *J Rheumatol.* 2015;42(10):1808-16.
74. Wermuth PJ, Li Z, Mendoza FA, Jimenez SA. Stimulation of Transforming Growth Factor- β 1-Induced Endothelial-To-Mesenchymal Transition and Tissue Fibrosis by Endothelin-1 (ET-1): A Novel Profibrotic Effect of ET-1. *PLoS One.* 2016;11(9):e0161988.
75. Fu Y, Chang A, Chang L, Niessen K, Eapen S, Setiadi A, et al. Differential regulation of transforming growth factor beta signaling pathways by Notch in human endothelial cells. *J Biol Chem.* 2009;284(29):19452-62.
76. Niessen K, Fu Y, Chang L, Hoodless PA, McFadden D, Karsan A. Slug is a direct Notch target required for initiation of cardiac cushion cellularization. *J Cell Biol.* 2008;182(2):315-25.
77. Hashimoto N, Phan SH, Imaizumi K, Matsuo M, Nakashima H, Kawabe T, et al. Endothelial-mesenchymal transition in bleomycin-induced pulmonary fibrosis. *Am J Respir Cell Mol Biol.* 2010;43(2):161-72.
78. Ozkaynak E, Schnegelsberg PN, Jin DF, Clifford GM, Warren FD, Drier EA, et al. Osteogenic protein-2. A new member of the transforming growth factor-beta superfamily expressed early in embryogenesis. *J Biol Chem.* 1992;267(35):25220-7.
79. Kokabu S, Gamer L, Cox K, Lowery J, Tsuji K, Raz R, et al. BMP3 suppresses osteoblast differentiation of bone marrow stromal cells via interaction with Acvr2b. *Mol Endocrinol.* 2012;26(1):87-94.
80. Bidart M, Ricard N, Levet S, Samson M, Mallet C, David L, et al. BMP9 is produced by hepatocytes and circulates mainly in an active mature form complexed to its prodomain. *Cell Mol Life Sci.* 2012;69(2):313-24.
81. Xiao YT, Xiang LX, Shao JZ. Bone morphogenetic protein. *Biochem Biophys Res Commun.* 2007;362(3):550-3.
82. Katagiri T, Watabe T. Bone Morphogenetic Proteins. *Cold Spring Harb Perspect Biol.* 2016;8(6).
83. Daluiski A, Engstrand T, Bahamonde ME, Gamer LW, Agius E, Stevenson SL, et al. Bone morphogenetic protein-3 is a negative regulator of bone density. *Nat Genet.* 2001;27(1):84-8.

84. Mazerbourg S, Klein C, Roh J, Kaivo-Oja N, Mottershead DG, Korchynskiy O, et al. Growth differentiation factor-9 signaling is mediated by the type I receptor, activin receptor-like kinase 5. *Mol Endocrinol*. 2004;18(3):653-65.
85. Lin J, Patel SR, Cheng X, Cho EA, Levitan I, Ullenbruch M, et al. Kielin/chordin-like protein, a novel enhancer of BMP signaling, attenuates renal fibrotic disease. *Nat Med*. 2005;11(4):387-93.
86. Onichtchouk D, Chen YG, Dosch R, Gawantka V, Delius H, Massagué J, et al. Silencing of TGF-beta signalling by the pseudoreceptor BAMBI. *Nature*. 1999;401(6752):480-5.
87. Kirkbride KC, Townsend TA, Bruinsma MW, Barnett JV, Blobe GC. Bone morphogenetic proteins signal through the transforming growth factor-beta type III receptor. *J Biol Chem*. 2008;283(12):7628-37.
88. Scherner O, Meurer SK, Tihaa L, Gressner AM, Weiskirchen R. Endoglin differentially modulates antagonistic transforming growth factor-beta1 and BMP-7 signaling. *J Biol Chem*. 2007;282(19):13934-43.
89. Yoshida Y, Tanaka S, Umemori H, Minowa O, Usui M, Ikematsu N, et al. Negative regulation of BMP/Smad signaling by Tob in osteoblasts. *Cell*. 2000;103(7):1085-97.
90. Akiyoshi S, Inoue H, Hanai J, Kusanagi K, Nemoto N, Miyazono K, et al. c-Ski acts as a transcriptional co-repressor in transforming growth factor-beta signaling through interaction with smads. *J Biol Chem*. 1999;274(49):35269-77.
91. Marqués G, Musacchio M, Shimell MJ, Wünnenberg-Stapleton K, Cho KW, O'Connor MB. Production of a DPP activity gradient in the early *Drosophila* embryo through the opposing actions of the SOG and TLD proteins. *Cell*. 1997;91(3):417-26.
92. Piccolo S, Agius E, Lu B, Goodman S, Dale L, De Robertis EM. Cleavage of Chordin by Xolloid metalloprotease suggests a role for proteolytic processing in the regulation of Spemann organizer activity. *Cell*. 1997;91(3):407-16.
93. Wang S, Hirschberg R. BMP7 antagonizes TGF-beta -dependent fibrogenesis in mesangial cells. *Am J Physiol Renal Physiol*. 2003;284(5):F1006-13.
94. Zeisberg M, Hanai J, Sugimoto H, Mammoto T, Charytan D, Strutz F, et al. BMP-7 counteracts TGF-beta1-induced epithelial-to-mesenchymal transition and reverses chronic renal injury. *Nat Med*. 2003;9(7):964-8.
95. Morrissey J, Hruska K, Guo G, Wang S, Chen Q, Klahr S. Bone morphogenetic protein-7 improves renal fibrosis and accelerates the return of renal function. *J Am Soc Nephrol*. 2002;13 Suppl 1:S14-21.
96. Sugimoto H, Grahovac G, Zeisberg M, Kalluri R. Renal fibrosis and glomerulosclerosis in a new mouse model of diabetic nephropathy and its regression by bone

- morphogenic protein-7 and advanced glycation end product inhibitors. *Diabetes*. 2007;56(7):1825-33.
97. Chen BL, Peng J, Li QF, Yang M, Wang Y, Chen W. Exogenous bone morphogenetic protein-7 reduces hepatic fibrosis in *Schistosoma japonicum*-infected mice via transforming growth factor- β /Smad signaling. *World J Gastroenterol*. 2013;19(9):1405-15.
 98. Zhong L, Wang X, Wang S, Yang L, Gao H, Yang C. The anti-fibrotic effect of bone morphogenic protein-7(BMP-7) on liver fibrosis. *Int J Med Sci*. 2013;10(4):441-50.
 99. Chung YH, Huang YH, Chu TH, Chen CL, Lin PR, Huang SC, et al. BMP-2 restoration aids in recovery from liver fibrosis by attenuating TGF- β 1 signaling. *Lab Invest*. 2018;98(8):999-1013.
 100. Tacke F, Gäbele E, Bataille F, Schwabe RF, Hellerbrand C, Klebl F, et al. Bone morphogenetic protein 7 is elevated in patients with chronic liver disease and exerts fibrogenic effects on human hepatic stellate cells. *Dig Dis Sci*. 2007;52(12):3404-15.
 101. Wang S, Sun A, Li L, Zhao G, Jia J, Wang K, et al. Up-regulation of BMP-2 antagonizes TGF- β 1/ROCK-enhanced cardiac fibrotic signalling through activation of Smurf1/Smad6 complex. *J Cell Mol Med*. 2012;16(10):2301-10.
 102. Chen X, Xu J, Jiang B, Liu D. Bone Morphogenetic Protein-7 Antagonizes Myocardial Fibrosis Induced by Atrial Fibrillation by Restraining Transforming Growth Factor- β (TGF- β)/Smads Signaling. *Med Sci Monit*. 2016;22:3457-68.
 103. Zeisberg EM, Tarnavski O, Zeisberg M, Dorfman AL, McMullen JR, Gustafsson E, et al. Endothelial-to-mesenchymal transition contributes to cardiac fibrosis. *Nat Med*. 2007;13(8):952-61.
 104. Jeffery TK, Upton PD, Trembath RC, Morrell NW. BMP4 inhibits proliferation and promotes myocyte differentiation of lung fibroblasts via Smad1 and JNK pathways. *Am J Physiol Lung Cell Mol Physiol*. 2005;288(2):L370-8.
 105. Pegorier S, Campbell GA, Kay AB, Lloyd CM. Bone morphogenetic protein (BMP)-4 and BMP-7 regulate differentially transforming growth factor (TGF)-beta1 in normal human lung fibroblasts (NHLF). *Respir Res*. 2010;11:85.
 106. Liang D, Wang Y, Zhu Z, Yang G, An G, Li X, et al. BMP-7 attenuated silica-induced pulmonary fibrosis through modulation of the balance between TGF- β /Smad and BMP-7/Smad signaling pathway. *Chem Biol Interact*. 2016;243:72-81.
 107. Izumi N, Mizuguchi S, Inagaki Y, Saika S, Kawada N, Nakajima Y, et al. BMP-7 opposes TGF-beta1-mediated collagen induction in mouse pulmonary myofibroblasts through Id2. *Am J Physiol Lung Cell Mol Physiol*. 2006;290(1):L120-6.

108. Murray LA, Hackett TL, Warner SM, Shaheen F, Argentieri RL, Dudas P, et al. BMP-7 does not protect against bleomycin-induced lung or skin fibrosis. *PLoS One*. 2008;3(12):e4039.
109. Yang G, Zhu Z, Wang Y, Gao A, Niu P, Tian L. Bone morphogenetic protein-7 inhibits silica-induced pulmonary fibrosis in rats. *Toxicol Lett*. 2013;220(2):103-8.
110. Li X, An G, Wang Y, Liang D, Zhu Z, Lian X, et al. Anti-fibrotic effects of bone morphogenetic protein-7-modified bone marrow mesenchymal stem cells on silica-induced pulmonary fibrosis. *Exp Mol Pathol*. 2017;102(1):70-7.
111. Leppäranta O, Tikkanen JM, Bernalov MM, Koli K, Myllärniemi M. Bone morphogenetic protein-inducer tilorone identified by high-throughput screening is antifibrotic in vivo. *Am J Respir Cell Mol Biol*. 2013;48(4):448-55.
112. Kadoya K, Togo S, Tulafu M, Namba Y, Iwai M, Watanabe J, et al. Specific Features of Fibrotic Lung Fibroblasts Highly Sensitive to Fibrotic Processes Mediated via TGF- β -ERK5 Interaction. *Cell Physiol Biochem*. 2019;52(4):822-37.
113. Yu X, Gu P, Huang Z, Fang X, Jiang Y, Luo Q, et al. Reduced expression of BMP3 contributes to the development of pulmonary fibrosis and predicts the unfavorable prognosis in IIP patients. *Oncotarget*. 2017;8(46):80531-44.
114. Murphy N, Gaynor KU, Rowan SC, Walsh SM, Fabre A, Boylan J, et al. Altered Expression of Bone Morphogenetic Protein Accessory Proteins in Murine and Human Pulmonary Fibrosis. *Am J Pathol*. 2016;186(3):600-15.
115. De Langhe E, Cailotto F, De Vooght V, Aznar-Lopez C, Vanoirbeek JA, Luyten FP, et al. Enhanced endogenous bone morphogenetic protein signaling protects against bleomycin induced pulmonary fibrosis. *Respir Res*. 2015;16:38.
116. Dong Y, Geng Y, Li L, Li X, Yan X, Fang Y, et al. Blocking follistatin-like 1 attenuates bleomycin-induced pulmonary fibrosis in mice. *J Exp Med*. 2015;212(2):235-52.
117. Fang Y, Zhang S, Li X, Jiang F, Ye Q, Ning W. Follistatin like-1 aggravates silica-induced mouse lung injury. *Sci Rep*. 2017;7(1):399.
118. Chen Z, Fang Y, Zhang S, Li L, Wang L, Zhang A, et al. Haplodeletion of Follistatin-Like 1 Attenuates Radiation-Induced Pulmonary Fibrosis in Mice. *Int J Radiat Oncol Biol Phys*. 2019;103(1):208-16.
119. Jin YK, Li XH, Wang W, Liu J, Zhang W, Fang YS, et al. Follistatin-Like 1 Promotes Bleomycin-Induced Pulmonary Fibrosis through the Transforming Growth Factor Beta 1/Mitogen-Activated Protein Kinase Signaling Pathway. *Chin Med J (Engl)*. 2018;131(16):1917-25.

120. Koli K, Myllärniemi M, Vuorinen K, Salmenkivi K, Ryyänänen MJ, Kinnula VL, et al. Bone morphogenetic protein-4 inhibitor gremlin is overexpressed in idiopathic pulmonary fibrosis. *Am J Pathol.* 2006;169(1):61-71.
121. Myllärniemi M, Lindholm P, Ryyänänen MJ, Kliment CR, Salmenkivi K, Keski-Oja J, et al. Gremlin-mediated decrease in bone morphogenetic protein signaling promotes pulmonary fibrosis. *Am J Respir Crit Care Med.* 2008;177(3):321-9.
122. Farkas L, Farkas D, Gauldie J, Warburton D, Shi W, Kolb M. Transient overexpression of Gremlin results in epithelial activation and reversible fibrosis in rat lungs. *Am J Respir Cell Mol Biol.* 2011;44(6):870-8.
123. Chen NY, D Collum S, Luo F, Weng T, Le TT, M Hernandez A, et al. Macrophage bone morphogenic protein receptor 2 depletion in idiopathic pulmonary fibrosis and Group III pulmonary hypertension. *Am J Physiol Lung Cell Mol Physiol.* 2016;311(2):L238-54.
124. Bryant AJ, Robinson LJ, Moore CS, Blackwell TR, Gladson S, Penner NL, et al. Expression of mutant bone morphogenetic protein receptor II worsens pulmonary hypertension secondary to pulmonary fibrosis. *Pulm Circ.* 2015;5(4):681-90.
125. Asahara T, Murohara T, Sullivan A, Silver M, van der Zee R, Li T, et al. Isolation of putative progenitor endothelial cells for angiogenesis. *Science.* 1997;275(5302):964-7.
126. Asahara T, Masuda H, Takahashi T, Kalka C, Pastore C, Silver M, et al. Bone marrow origin of endothelial progenitor cells responsible for postnatal vasculogenesis in physiological and pathological neovascularization. *Circ Res.* 1999;85(3):221-8.
127. Medina RJ, Barber CL, Sabatier F, Dignat-George F, Melero-Martin JM, Khosrotehrani K, et al. Endothelial Progenitors: A Consensus Statement on Nomenclature. *Stem Cells Transl Med.* 2017;6(5):1316-20.
128. Medina RJ, O'Neill CL, Sweeney M, Guduric-Fuchs J, Gardiner TA, Simpson DA, et al. Molecular analysis of endothelial progenitor cell (EPC) subtypes reveals two distinct cell populations with different identities. *BMC Med Genomics.* 2010;3:18.
129. Hur J, Yoon CH, Kim HS, Choi JH, Kang HJ, Hwang KK, et al. Characterization of two types of endothelial progenitor cells and their different contributions to neovascularization. *Arterioscler Thromb Vasc Biol.* 2004;24(2):288-93.
130. Sieveking DP, Buckle A, Celermajer DS, Ng MK. Strikingly different angiogenic properties of endothelial progenitor cell subpopulations: insights from a novel human angiogenesis assay. *J Am Coll Cardiol.* 2008;51(6):660-8.

131. Heeschen C, Aicher A, Lehmann R, Fichtlscherer S, Vasa M, Urbich C, et al. Erythropoietin is a potent physiologic stimulus for endothelial progenitor cell mobilization. *Blood*. 2003;102(4):1340-6.
132. Ceradini DJ, Kulkarni AR, Callaghan MJ, Tepper OM, Bastidas N, Kleinman ME, et al. Progenitor cell trafficking is regulated by hypoxic gradients through HIF-1 induction of SDF-1. *Nat Med*. 2004;10(8):858-64.
133. Rabelink TJ, de Boer HC, de Koning EJ, van Zonneveld AJ. Endothelial progenitor cells: more than an inflammatory response? *Arterioscler Thromb Vasc Biol*. 2004;24(5):834-8.
134. de Boer HC, Verseyden C, Ulfman LH, Zwaginga JJ, Bot I, Biessen EA, et al. Fibrin and activated platelets cooperatively guide stem cells to a vascular injury and promote differentiation towards an endothelial cell phenotype. *Arterioscler Thromb Vasc Biol*. 2006;26(7):1653-9.
135. Valgimigli M, Rigolin GM, Fucili A, Porta MD, Soukhomovskaia O, Malagutti P, et al. CD34+ and endothelial progenitor cells in patients with various degrees of congestive heart failure. *Circulation*. 2004;110(10):1209-12.
136. Ghani U, Shuaib A, Salam A, Nasir A, Shuaib U, Jeerakathil T, et al. Endothelial progenitor cells during cerebrovascular disease. *Stroke*. 2005;36(1):151-3.
137. Tepper OM, Galiano RD, Capla JM, Kalka C, Gagne PJ, Jacobowitz GR, et al. Human endothelial progenitor cells from type II diabetics exhibit impaired proliferation, adhesion, and incorporation into vascular structures. *Circulation*. 2002;106(22):2781-6.
138. Loomans CJ, de Koning EJ, Staal FJ, Rookmaaker MB, Verseyden C, de Boer HC, et al. Endothelial progenitor cell dysfunction: a novel concept in the pathogenesis of vascular complications of type 1 diabetes. *Diabetes*. 2004;53(1):195-9.
139. Grisar J, Aletaha D, Steiner CW, Kapral T, Steiner S, Seidinger D, et al. Depletion of endothelial progenitor cells in the peripheral blood of patients with rheumatoid arthritis. *Circulation*. 2005;111(2):204-11.
140. de Groot K, Bahlmann FH, Sowa J, Koenig J, Menne J, Haller H, et al. Uremia causes endothelial progenitor cell deficiency. *Kidney Int*. 2004;66(2):641-6.
141. Choi JH, Kim KL, Huh W, Kim B, Byun J, Suh W, et al. Decreased number and impaired angiogenic function of endothelial progenitor cells in patients with chronic renal failure. *Arterioscler Thromb Vasc Biol*. 2004;24(7):1246-52.
142. Fadini GP, Schiavon M, Rea F, Avogaro A, Agostini C. Depletion of endothelial progenitor cells may link pulmonary fibrosis and pulmonary hypertension. *Am J Respir Crit Care Med*. 2007;176(7):724-5; author reply 5.

143. Diller GP, van Eijl S, Okonko DO, Howard LS, Ali O, Thum T, et al. Circulating endothelial progenitor cells in patients with Eisenmenger syndrome and idiopathic pulmonary arterial hypertension. *Circulation*. 2008;117(23):3020-30.
144. Smadja DM, Mauge L, Nunes H, d'Audigier C, Juvin K, Borie R, et al. Imbalance of circulating endothelial cells and progenitors in idiopathic pulmonary fibrosis. *Angiogenesis*. 2013;16(1):147-57.
145. Shintani S, Murohara T, Ikeda H, Ueno T, Honma T, Katoh A, et al. Mobilization of endothelial progenitor cells in patients with acute myocardial infarction. *Circulation*. 2001;103(23):2776-9.
146. Massa M, Rosti V, Ferrario M, Campanelli R, Ramajoli I, Rosso R, et al. Increased circulating hematopoietic and endothelial progenitor cells in the early phase of acute myocardial infarction. *Blood*. 2005;105(1):199-206.
147. Vasa M, Fichtlscherer S, Aicher A, Adler K, Urbich C, Martin H, et al. Number and migratory activity of circulating endothelial progenitor cells inversely correlate with risk factors for coronary artery disease. *Circ Res*. 2001;89(1):E1-7.
148. Hill JM, Zalos G, Halcox JP, Schenke WH, Waclawiw MA, Quyyumi AA, et al. Circulating endothelial progenitor cells, vascular function, and cardiovascular risk. *N Engl J Med*. 2003;348(7):593-600.
149. Werner N, Kosiol S, Schiegl T, Ahlers P, Walenta K, Link A, et al. Circulating endothelial progenitor cells and cardiovascular outcomes. *N Engl J Med*. 2005;353(10):999-1007.
150. Au P, Daheron LM, Duda DG, Cohen KS, Tyrrell JA, Lanning RM, et al. Differential in vivo potential of endothelial progenitor cells from human umbilical cord blood and adult peripheral blood to form functional long-lasting vessels. *Blood*. 2008;111(3):1302-5.
151. Schwarz TM, Leicht SF, Radic T, Rodriguez-Arabaolaza I, Hermann PC, Berger F, et al. Vascular incorporation of endothelial colony-forming cells is essential for functional recovery of murine ischemic tissue following cell therapy. *Arterioscler Thromb Vasc Biol*. 2012;32(2):e13-21.
152. Baker CD, Seedorf GJ, Wisniewski BL, Black CP, Ryan SL, Balasubramaniam V, et al. Endothelial colony-forming cell conditioned media promote angiogenesis in vitro and prevent pulmonary hypertension in experimental bronchopulmonary dysplasia. *Am J Physiol Lung Cell Mol Physiol*. 2013;305(1):L73-81.
153. Viñas JL, Burger D, Zimpelmann J, Haneef R, Knoll W, Campbell P, et al. Transfer of microRNA-486-5p from human endothelial colony forming cell-derived exosomes reduces ischemic kidney injury. *Kidney Int*. 2016;90(6):1238-50.

154. Au P, Tam J, Fukumura D, Jain RK. Bone marrow-derived mesenchymal stem cells facilitate engineering of long-lasting functional vasculature. *Blood*. 2008;111(9):4551-8.
155. Lin RZ, Moreno-Luna R, Li D, Jaminet SC, Greene AK, Melero-Martin JM. Human endothelial colony-forming cells serve as trophic mediators for mesenchymal stem cell engraftment via paracrine signaling. *Proc Natl Acad Sci U S A*. 2014;111(28):10137-42.
156. Traktuev DO, Prater DN, Merfeld-Clauss S, Sanjeevaiah AR, Saadatzadeh MR, Murphy M, et al. Robust functional vascular network formation in vivo by cooperation of adipose progenitor and endothelial cells. *Circ Res*. 2009;104(12):1410-20.
157. Kalka C, Masuda H, Takahashi T, Kalka-Moll WM, Silver M, Kearney M, et al. Transplantation of ex vivo expanded endothelial progenitor cells for therapeutic neovascularization. *Proc Natl Acad Sci U S A*. 2000;97(7):3422-7.
158. Kocher AA, Schuster MD, Szabolcs MJ, Takuma S, Burkhoff D, Wang J, et al. Neovascularization of ischemic myocardium by human bone-marrow-derived angioblasts prevents cardiomyocyte apoptosis, reduces remodeling and improves cardiac function. *Nat Med*. 2001;7(4):430-6.
159. Dellett M, Brown ED, Guduric-Fuchs J, O'Connor A, Stitt AW, Medina RJ, et al. MicroRNA-containing extracellular vesicles released from endothelial colony-forming cells modulate angiogenesis during ischaemic retinopathy. *J Cell Mol Med*. 2017;21(12):3405-19.
160. Moubarik C, Guillet B, Youssef B, Codaccioni JL, Piercecchi MD, Sabatier F, et al. Transplanted late outgrowth endothelial progenitor cells as cell therapy product for stroke. *Stem Cell Rev Rep*. 2011;7(1):208-20.
161. Huang XT, Zhang YQ, Li SJ, Li SH, Tang Q, Wang ZT, et al. Intracerebroventricular transplantation of ex vivo expanded endothelial colony-forming cells restores blood-brain barrier integrity and promotes angiogenesis of mice with traumatic brain injury. *J Neurotrauma*. 2013;30(24):2080-8.
162. Alphonse RS, Vadivel A, Fung M, Shelley WC, Critser PJ, Ionescu L, et al. Existence, functional impairment, and lung repair potential of endothelial colony-forming cells in oxygen-induced arrested alveolar growth. *Circulation*. 2014;129(21):2144-57.
163. Burger D, Viñas JL, Akbari S, Dehak H, Knoll W, Gutsol A, et al. Human endothelial colony-forming cells protect against acute kidney injury: role of exosomes. *Am J Pathol*. 2015;185(8):2309-23.

164. Lara-Hernandez R, Lozano-Villardell P, Blanes P, Torreguitart-Mirada N, Galmés A, Besalduch J. Safety and efficacy of therapeutic angiogenesis as a novel treatment in patients with critical limb ischemia. *Ann Vasc Surg.* 2010;24(2):287-94.
165. Tanaka R, Masuda H, Kato S, Imagawa K, Kanabuchi K, Nakashioya C, et al. Autologous G-CSF-mobilized peripheral blood CD34+ cell therapy for diabetic patients with chronic nonhealing ulcer. *Cell Transplant.* 2014;23(2):167-79.
166. Liotta F, Annunziato F, Castellani S, Boddi M, Alterini B, Castellini G, et al. Therapeutic Efficacy of Autologous Non-Mobilized Enriched Circulating Endothelial Progenitors in Patients With Critical Limb Ischemia - The SCELTA Trial. *Circ J.* 2018;82(6):1688-98.
167. Wang XX, Zhang FR, Shang YP, Zhu JH, Xie XD, Tao QM, et al. Transplantation of autologous endothelial progenitor cells may be beneficial in patients with idiopathic pulmonary arterial hypertension: a pilot randomized controlled trial. *J Am Coll Cardiol.* 2007;49(14):1566-71.
168. Zhu JH, Wang XX, Zhang FR, Shang YP, Tao QM, Chen JZ. Safety and efficacy of autologous endothelial progenitor cells transplantation in children with idiopathic pulmonary arterial hypertension: open-label pilot study. *Pediatr Transplant.* 2008;12(6):650-5.
169. Zhu J, Song J, Yu L, Zheng H, Zhou B, Weng S, et al. Safety and efficacy of autologous thymosin β 4 pre-treated endothelial progenitor cell transplantation in patients with acute ST segment elevation myocardial infarction: A pilot study. *Cytotherapy.* 2016;18(8):1037-42.
170. Granton J, Langleben D, Kutryk MB, Camack N, Galipeau J, Courtman DW, et al. Endothelial NO-Synthase Gene-Enhanced Progenitor Cell Therapy for Pulmonary Arterial Hypertension: The PHACeT Trial. *Circ Res.* 2015;117(7):645-54.
171. Lin Y, Chang L, Solovey A, Healey JF, Lollar P, Hebbel RP. Use of blood outgrowth endothelial cells for gene therapy for hemophilia A. *Blood.* 2002;99(2):457-62.
172. Ozelo MC, Vidal B, Brown C, Notley C, Hegadorn C, Webster S, et al. Omental implantation of BOECs in hemophilia dogs results in circulating FVIII antigen and a complex immune response. *Blood.* 2014;123(26):4045-53.
173. Lin RZ, Dreyzin A, Aamodt K, Li D, Jaminet SC, Dudley AC, et al. Induction of erythropoiesis using human vascular networks genetically engineered for controlled erythropoietin release. *Blood.* 2011;118(20):5420-8.
174. Dudek AZ, Bodempudi V, Welsh BW, Jasinski P, Griffin RJ, Milbauer L, et al. Systemic inhibition of tumour angiogenesis by endothelial cell-based gene therapy. *Br J Cancer.* 2007;97(4):513-22.

175. Bodempudi V, Ohlfest JR, Terai K, Zamora EA, Vogel RI, Gupta K, et al. Blood outgrowth endothelial cell-based systemic delivery of antiangiogenic gene therapy for solid tumors. *Cancer Gene Ther*. 2010;17(12):855-63.
176. Machado RD, Aldred MA, James V, Harrison RE, Patel B, Schwalbe EC, et al. Mutations of the TGF-beta type II receptor BMPR2 in pulmonary arterial hypertension. *Hum Mutat*. 2006;27(2):121-32.
177. Long L, Crosby A, Yang X, Southwood M, Upton PD, Kim DK, et al. Altered bone morphogenetic protein and transforming growth factor-beta signaling in rat models of pulmonary hypertension: potential for activin receptor-like kinase-5 inhibition in prevention and progression of disease. *Circulation*. 2009;119(4):566-76.
178. Reynolds PN, Zinn KR, Gavriilyuk VD, Balyasnikova IV, Rogers BE, Buchsbaum DJ, et al. A targetable, injectable adenoviral vector for selective gene delivery to pulmonary endothelium in vivo. *Mol Ther*. 2000;2(6):562-78.
179. Reynolds PN, Nicklin SA, Kaliberova L, Boatman BG, Grizzle WE, Balyasnikova IV, et al. Combined transductional and transcriptional targeting improves the specificity of transgene expression in vivo. *Nat Biotechnol*. 2001;19(9):838-42.
180. Reynolds AM, Xia W, Holmes MD, Hodge SJ, Danilov S, Curiel DT, et al. Bone morphogenetic protein type 2 receptor gene therapy attenuates hypoxic pulmonary hypertension. *Am J Physiol Lung Cell Mol Physiol*. 2007;292(5):L1182-92.
181. Reynolds AM, Holmes MD, Danilov SM, Reynolds PN. Targeted gene delivery of BMPR2 attenuates pulmonary hypertension. *Eur Respir J*. 2012;39(2):329-43.
182. Harper RL, Reynolds AM, Bonder CS, Reynolds PN. BMPR2 gene therapy for PAH acts via Smad and non-Smad signalling. *Respirology*. 2016;21(4):727-33.
183. Feng F, Harper RL, Reynolds PN. BMPR2 gene delivery reduces mutation-related PAH and counteracts TGF- β -mediated pulmonary cell signalling. *Respirology*. 2016;21(3):526-32.
184. Harper RL, Maiolo S, Ward RJ, Seyfang J, Cockshell MP, Bonder CS, et al. BMPR2-expressing bone marrow-derived endothelial-like progenitor cells alleviate pulmonary arterial hypertension in vivo. *Respirology*. 2019;24(11):1095-103.
185. Fadini GP, Schiavon M, Cantini M, Baesso I, Facco M, Miorin M, et al. Circulating progenitor cells are reduced in patients with severe lung disease. *Stem Cells*. 2006;24(7):1806-13.
186. Akita T, Murohara T, Ikeda H, Sasaki K, Shimada T, Egami K, et al. Hypoxic preconditioning augments efficacy of human endothelial progenitor cells for therapeutic neovascularization. *Lab Invest*. 2003;83(1):65-73.

187. Bacha NC, Blandinieres A, Rossi E, Gendron N, Nevo N, Lecourt S, et al. Endothelial Microparticles are Associated to Pathogenesis of Idiopathic Pulmonary Fibrosis. *Stem Cell Rev Rep*. 2018;14(2):223-35.
188. Blandinières A, Gendron N, Bacha N, Bièche I, Chocron R, Nunes H, et al. Interleukin-8 release by endothelial colony-forming cells isolated from idiopathic pulmonary fibrosis patients might contribute to their pathogenicity. *Angiogenesis*. 2019;22(2):325-39.
189. Smadja DM, Dorfmüller P, Guerin CL, Bieche I, Badoual C, Boscolo E, et al. Cooperation between human fibrocytes and endothelial colony-forming cells increases angiogenesis via the CXCR4 pathway. *Thromb Haemost*. 2014;112(5):1002-13.
190. Díez M, Musri MM, Ferrer E, Barberà JA, Peinado VI. Endothelial progenitor cells undergo an endothelial-to-mesenchymal transition-like process mediated by TGFbetaRI. *Cardiovasc Res*. 2010;88(3):502-11.
191. Moonen JR, Krenning G, Brinker MG, Koerts JA, van Luyn MJ, Harmsen MC. Endothelial progenitor cells give rise to pro-angiogenic smooth muscle-like progeny. *Cardiovasc Res*. 2010;86(3):506-15.
192. Blandinières A, Gille T, Sadoine J, Bièche I, Slimani L, Dizier B, et al. Endothelial Colony-Forming Cells Do Not Participate to Fibrogenesis in a Bleomycin-Induced Pulmonary Fibrosis Model in Nude Mice. *Stem Cell Rev Rep*. 2018;14(6):812-22.
193. Demedts M, Behr J, Buhl R, Costabel U, Dekhuijzen R, Jansen HM, et al. High-dose acetylcysteine in idiopathic pulmonary fibrosis. *N Engl J Med*. 2005;353(21):2229-42.
194. Raghu G, Brown KK, Costabel U, Cottin V, du Bois RM, Lasky JA, et al. Treatment of idiopathic pulmonary fibrosis with etanercept: an exploratory, placebo-controlled trial. *Am J Respir Crit Care Med*. 2008;178(9):948-55.
195. King TE, Albera C, Bradford WZ, Costabel U, Hormel P, Lancaster L, et al. Effect of interferon gamma-1b on survival in patients with idiopathic pulmonary fibrosis (INSPIRE): a multicentre, randomised, placebo-controlled trial. *Lancet*. 2009;374(9685):222-8.
196. Daniels CE, Lasky JA, Limper AH, Mieras K, Gabor E, Schroeder DR, et al. Imatinib treatment for idiopathic pulmonary fibrosis: Randomized placebo-controlled trial results. *Am J Respir Crit Care Med*. 2010;181(6):604-10.
197. King TE, Behr J, Brown KK, du Bois RM, Lancaster L, de Andrade JA, et al. BUILD-1: a randomized placebo-controlled trial of bosentan in idiopathic pulmonary fibrosis. *Am J Respir Crit Care Med*. 2008;177(1):75-81.

198. King TE, Brown KK, Raghu G, du Bois RM, Lynch DA, Martinez F, et al. BUILD-3: a randomized, controlled trial of bosentan in idiopathic pulmonary fibrosis. *Am J Respir Crit Care Med*. 2011;184(1):92-9.
199. Raghu G, Million-Rousseau R, Morganti A, Perchenet L, Behr J, Group MS. Macitentan for the treatment of idiopathic pulmonary fibrosis: the randomised controlled MUSIC trial. *Eur Respir J*. 2013;42(6):1622-32.
200. Martinez FJ, de Andrade JA, Anstrom KJ, King TE, Raghu G, Network IPFCR. Randomized trial of acetylcysteine in idiopathic pulmonary fibrosis. *N Engl J Med*. 2014;370(22):2093-101.
201. Parker JM, Glaspole IN, Lancaster LH, Haddad TJ, She D, Roseti SL, et al. A Phase 2 Randomized Controlled Study of Tralokinumab in Subjects with Idiopathic Pulmonary Fibrosis. *Am J Respir Crit Care Med*. 2018;197(1):94-103.
202. Raghu G, Rochweg B, Zhang Y, Garcia CA, Azuma A, Behr J, et al. An Official ATS/ERS/JRS/ALAT Clinical Practice Guideline: Treatment of Idiopathic Pulmonary Fibrosis. An Update of the 2011 Clinical Practice Guideline. *Am J Respir Crit Care Med*. 2015;192(2):e3-19.
203. Nakazato H, Oku H, Yamane S, Tsuruta Y, Suzuki R. A novel anti-fibrotic agent pirfenidone suppresses tumor necrosis factor-alpha at the translational level. *Eur J Pharmacol*. 2002;446(1-3):177-85.
204. Iyer SN, Gurujeyalakshmi G, Giri SN. Effects of pirfenidone on procollagen gene expression at the transcriptional level in bleomycin hamster model of lung fibrosis. *J Pharmacol Exp Ther*. 1999;289(1):211-8.
205. Iyer SN, Gurujeyalakshmi G, Giri SN. Effects of pirfenidone on transforming growth factor-beta gene expression at the transcriptional level in bleomycin hamster model of lung fibrosis. *J Pharmacol Exp Ther*. 1999;291(1):367-73.
206. Oku H, Shimizu T, Kawabata T, Nagira M, Hikita I, Ueyama A, et al. Antifibrotic action of pirfenidone and prednisolone: different effects on pulmonary cytokines and growth factors in bleomycin-induced murine pulmonary fibrosis. *Eur J Pharmacol*. 2008;590(1-3):400-8.
207. Azuma A, Nukiwa T, Tsuboi E, Suga M, Abe S, Nakata K, et al. Double-blind, placebo-controlled trial of pirfenidone in patients with idiopathic pulmonary fibrosis. *Am J Respir Crit Care Med*. 2005;171(9):1040-7.
208. Taniguchi H, Ebina M, Kondoh Y, Ogura T, Azuma A, Suga M, et al. Pirfenidone in idiopathic pulmonary fibrosis. *Eur Respir J*. 2010;35(4):821-9.

209. Noble PW, Albera C, Bradford WZ, Costabel U, Glassberg MK, Kardatzke D, et al. Pirfenidone in patients with idiopathic pulmonary fibrosis (CAPACITY): two randomised trials. *Lancet*. 2011;377(9779):1760-9.
210. Nathan SD, Albera C, Bradford WZ, Costabel U, Glaspole I, Glassberg MK, et al. Effect of pirfenidone on mortality: pooled analyses and meta-analyses of clinical trials in idiopathic pulmonary fibrosis. *Lancet Respir Med*. 2017;5(1):33-41.
211. Richeldi L, Cottin V, du Bois RM, Selman M, Kimura T, Bailes Z, et al. Nintedanib in patients with idiopathic pulmonary fibrosis: Combined evidence from the TOMORROW and INPULSIS(®) trials. *Respir Med*. 2016;113:74-9.
212. Flaherty KR, Wells AU, Cottin V, Devaraj A, Walsh SLF, Inoue Y, et al. Nintedanib in Progressive Fibrosing Interstitial Lung Diseases. *N Engl J Med*. 2019;381(18):1718-27.
213. Serrano-Mollar A, Nacher M, Gay-Jordi G, Closa D, Xaubet A, Bulbena O. Intratracheal transplantation of alveolar type II cells reverses bleomycin-induced lung fibrosis. *Am J Respir Crit Care Med*. 2007;176(12):1261-8.
214. Zhou Q, Ye X, Sun R, Matsumoto Y, Moriyama M, Asano Y, et al. Differentiation of mouse induced pluripotent stem cells into alveolar epithelial cells in vitro for use in vivo. *Stem Cells Transl Med*. 2014;3(6):675-85.
215. Wang D, Morales JE, Calame DG, Alcorn JL, Wetsel RA. Transplantation of human embryonic stem cell-derived alveolar epithelial type II cells abrogates acute lung injury in mice. *Mol Ther*. 2010;18(3):625-34.
216. Tanaka K, Fujita T, Umezawa H, Namiki K, Yoshioka K, Hagihara M, et al. Therapeutic effect of lung mixed culture-derived epithelial cells on lung fibrosis. *Lab Invest*. 2014;94(11):1247-59.
217. Ortiz LA, Gambelli F, McBride C, Gaupp D, Baddoo M, Kaminski N, et al. Mesenchymal stem cell engraftment in lung is enhanced in response to bleomycin exposure and ameliorates its fibrotic effects. *Proc Natl Acad Sci U S A*. 2003;100(14):8407-11.
218. Rojas M, Xu J, Woods CR, Mora AL, Spears W, Roman J, et al. Bone marrow-derived mesenchymal stem cells in repair of the injured lung. *Am J Respir Cell Mol Biol*. 2005;33(2):145-52.
219. Kumamoto M, Nishiwaki T, Matsuo N, Kimura H, Matsushima K. Minimally cultured bone marrow mesenchymal stem cells ameliorate fibrotic lung injury. *Eur Respir J*. 2009;34(3):740-8.
220. Moodley Y, Atienza D, Manuelpillai U, Samuel CS, Tchongue J, Ilancheran S, et al. Human umbilical cord mesenchymal stem cells reduce fibrosis of bleomycin-induced lung injury. *Am J Pathol*. 2009;175(1):303-13.

221. Cargnoni A, Gibelli L, Tosini A, Signoroni PB, Nassuato C, Arienti D, et al. Transplantation of allogeneic and xenogeneic placenta-derived cells reduces bleomycin-induced lung fibrosis. *Cell Transplant*. 2009;18(4):405-22.
222. Yan X, Liu Y, Han Q, Jia M, Liao L, Qi M, et al. Injured microenvironment directly guides the differentiation of engrafted Flk-1(+) mesenchymal stem cell in lung. *Exp Hematol*. 2007;35(9):1466-75.
223. Lee SH, Lee EJ, Lee SY, Kim JH, Shim JJ, Shin C, et al. The effect of adipose stem cell therapy on pulmonary fibrosis induced by repetitive intratracheal bleomycin in mice. *Exp Lung Res*. 2014;40(3):117-25.
224. Moodley Y, Ilancheran S, Samuel C, Vaghjiani V, Atienza D, Williams ED, et al. Human amnion epithelial cell transplantation abrogates lung fibrosis and augments repair. *Am J Respir Crit Care Med*. 2010;182(5):643-51.
225. Murphy S, Lim R, Dickinson H, Acharya R, Rosli S, Jenkin G, et al. Human amnion epithelial cells prevent bleomycin-induced lung injury and preserve lung function. *Cell Transplant*. 2011;20(6):909-23.
226. Tzouvelekis A, Paspaliaris V, Koliakos G, Ntoliou P, Bouros E, Oikonomou A, et al. A prospective, non-randomized, no placebo-controlled, phase Ib clinical trial to study the safety of the adipose derived stromal cells-stromal vascular fraction in idiopathic pulmonary fibrosis. *J Transl Med*. 2013;11:171.
227. Ntoliou P, Manoloudi E, Tzouvelekis A, Bouros E, Steiropoulos P, Anevlavis S, et al. Longitudinal outcomes of patients enrolled in a phase Ib clinical trial of the adipose-derived stromal cells-stromal vascular fraction in idiopathic pulmonary fibrosis. *Clin Respir J*. 2018;12(6):2084-9.
228. Chambers DC, Enever D, Ilic N, Sparks L, Whitelaw K, Ayres J, et al. A phase 1b study of placenta-derived mesenchymal stromal cells in patients with idiopathic pulmonary fibrosis. *Respirology*. 2014;19(7):1013-8.
229. Averyanov A, Koroleva I, Konoplyannikov M, Revkova V, Lesnyak V, Kalsin V, et al. First-in-human high-cumulative-dose stem cell therapy in idiopathic pulmonary fibrosis with rapid lung function decline. *Stem Cells Transl Med*. 2020;9(1):6-16.
230. Aguilar S, Scotton CJ, McNulty K, Nye E, Stamp G, Laurent G, et al. Bone marrow stem cells expressing keratinocyte growth factor via an inducible lentivirus protects against bleomycin-induced pulmonary fibrosis. *PLoS One*. 2009;4(11):e8013.
231. Richeldi L, Costabel U, Selman M, Kim DS, Hansell DM, Nicholson AG, et al. Efficacy of a tyrosine kinase inhibitor in idiopathic pulmonary fibrosis. *N Engl J Med*. 2011;365(12):1079-87.

232. Kadota T, Yoshioka Y, Fujita Y, Araya J, Minagawa S, Hara H, et al. Extracellular Vesicles from Fibroblasts Induce Epithelial-Cell Senescence in Pulmonary Fibrosis. *Am J Respir Cell Mol Biol.* 2020;63(5):623-36.
233. Makiguchi T, Yamada M, Yoshioka Y, Sugiura H, Koarai A, Chiba S, et al. Serum extracellular vesicular miR-21-5p is a predictor of the prognosis in idiopathic pulmonary fibrosis. *Respir Res.* 2016;17(1):110.
234. Njock MS, Guiot J, Henket MA, Nivelles O, Thiry M, Dequiedt F, et al. Sputum exosomes: promising biomarkers for idiopathic pulmonary fibrosis. *Thorax.* 2019;74(3):309-12.
235. Wan X, Chen S, Fang Y, Zuo W, Cui J, Xie S. Mesenchymal stem cell-derived extracellular vesicles suppress the fibroblast proliferation by downregulating FZD6 expression in fibroblasts via miRNA-29b-3p in idiopathic pulmonary fibrosis. *J Cell Physiol.* 2020;235(11):8613-25.
236. Lei X, He N, Zhu L, Zhou M, Zhang K, Wang C, et al. Mesenchymal Stem Cell-Derived Extracellular Vesicles Attenuate Radiation-Induced Lung Injury. *Antioxid Redox Signal.* 2021;35(11):849-62.
237. Dinh PC, Paudel D, Brochu H, Popowski KD, Gracieux MC, Cores J, et al. Inhalation of lung spheroid cell secretome and exosomes promotes lung repair in pulmonary fibrosis. *Nat Commun.* 2020;11(1):1064.
238. Gao Y, Sun J, Dong C, Zhao M, Hu Y, Jin F. Extracellular Vesicles Derived from Adipose Mesenchymal Stem Cells Alleviate PM2.5-Induced Lung Injury and Pulmonary Fibrosis. *Med Sci Monit.* 2020;26:e922782.
239. Bandeira E, Oliveira H, Silva JD, Menna-Barreto RFS, Takyia CM, Suk JS, et al. Therapeutic effects of adipose-tissue-derived mesenchymal stromal cells and their extracellular vesicles in experimental silicosis. *Respir Res.* 2018;19(1):104.
240. Hübner RH, Gitter W, El Mokhtari NE, Mathiak M, Both M, Bolte H, et al. Standardized quantification of pulmonary fibrosis in histological samples. *Biotechniques.* 2008;44(4):507-11, 14-7.
241. Holtzhausen A, Golzio C, How T, Lee YH, Schiemann WP, Katsanis N, et al. Novel bone morphogenetic protein signaling through Smad2 and Smad3 to regulate cancer progression and development. *FASEB J.* 2014;28(3):1248-67.
242. Zhang H, Tian S, Klausen C, Zhu H, Liu R, Leung PC. Differential activation of noncanonical SMAD2/SMAD3 signaling by bone morphogenetic proteins causes disproportionate induction of hyaluronan production in immortalized human granulosa cells. *Mol Cell Endocrinol.* 2016;428:17-27.

243. B Moore B, Lawson WE, Oury TD, Sisson TH, Raghavendran K, Hogaboam CM. Animal models of fibrotic lung disease. *Am J Respir Cell Mol Biol.* 2013;49(2):167-79.
244. Lynch DA, Sverzellati N, Travis WD, Brown KK, Colby TV, Galvin JR, et al. Diagnostic criteria for idiopathic pulmonary fibrosis: a Fleischner Society White Paper. *Lancet Respir Med.* 2018;6(2):138-53.
245. Raghu G, Remy-Jardin M, Myers J, Richeldi L, Wilson KC. The 2018 Diagnosis of Idiopathic Pulmonary Fibrosis Guidelines: Surgical Lung Biopsy for Radiological Pattern of Probable Usual Interstitial Pneumonia Is Not Mandatory. *Am J Respir Crit Care Med.* 2019;200(9):1089-92.
246. Oldham JM, Lee CT, Wu Z, Bowman WS, Vu Pugashetti J, Dao N, et al. Lung function trajectory in progressive fibrosing interstitial lung disease. *Eur Respir J.* 2021.